

An Examination of the Role of Cytosolic Superoxide Dismutase (SOD1) on C-X-C
Chemokine Receptor Type 4 (CXCR4)-Mediated Signal Transduction in Prostate Cancer
Cells

by

Jaime Wertman

Submitted in partial fulfilment of the requirements
for the degree of Master of Science

at

Dalhousie University
Halifax, Nova Scotia
July 2013

© Copyright by Jaime Wertman, 2013

DEDICATION

This thesis is dedicated to Dr. Arunika Gunawardena.

Although she is technically not involved directly in this degree, I like to think that with the phenomenal training she gave me, Arunika is, and will continue to be, an important part of all science that I do.

Thank you for being an amazing role model and teacher Arunika.

TABLE OF CONTENTS

LIST OF TABLES	vii
LIST OF FIGURES	viii
ABSTRACT	x
LIST OF ABBREVIATIONS AND SYMBOLS USED	xi
ACKNOWLEDGEMENTS	xvi
CHAPTER 1: INTRODUCTION	1
1.1 Cancer	1
1.2 Prostate Cancer	1
1.2.1 Significance and Risk Factors	1
1.2.2 Testing, Diagnosis and Treatment	3
1.3 Prostate Cancer Metastasis	5
1.4 G Protein-Coupled Receptors	8
1.4.1 Overview and Significance	8
1.4.2 Discovery	9
1.4.3 Structure	9
1.4.4 Classification	10
1.4.5 Signal Transduction	12
1.5 Chemokine Receptors and their Role in Cancer	14
1.6 C-X-C Chemokine Receptor Type 4 (CXCR4)	17
1.6.1 Overview and Role in Normal Cell Signaling	17
1.6.2 CXCR4 in Other Disease States	18
1.6.3 CXCR4 Signal Transduction	19

1.6.4	Role in Cancer	20
1.6.5	Regulation of CXCR4 Expression	22
1.7	Reactive Oxygen Species, Antioxidants, and their Role in Cancer	23
1.8	Cytosolic Superoxide Dismutase (SOD1)	26
1.9	SOD1 in Prostate Cancer	27
1.10	The Project	28
1.11	The Hypothesis	28
CHAPTER 2: MATERIALS AND METHODS		38
2.1	Materials	38
2.2	Molecular Constructs	39
2.3	Cell Culture	39
2.4	Transient Transfection	39
2.5	Protein Collection	40
2.6	Cell Counting and Bradford Assays	41
2.7	Polyacrylamide Gel Electrophoresis and Western Blotting	41
2.8	Co-Immunoprecipitations	42
2.9	Annexin V Staining	42
2.10	Transwell Migration Assays	43
2.11	Bioluminescence Resonance Energy Transfer (BRET) Assays	44
2.12	Statistical Analysis	45
CHAPTER 3: RESULTS		50
3.1	Expression of Endogenous and Transfected CXCR4 and SOD1 in PC3 cells	50

3.2 Interaction of CXCR4 with SOD1 in PC3 cells in Normal and Hypoxic Conditions	51
3.3 Modulation of CXCR4 Signal Transduction by SOD1 and Hypoxia	52
3.3.1 Extracellular Signal-Regulated Kinase (ERK) Activation	52
3.3.1 AKT (Protein Kinase B) Activation	53
3.4 Role of SOD1 and Hypoxia in the Modulation of Apoptosis Levels	55
3.5 Effects of SOD1 on CXCR4-Mediated Cell Migration	56
3.6 Modulation of G Protein Coupling by SOD1 and Hypoxia	58
CHAPTER 4: DISCUSSION	69
4.1 Overview and Preliminary Findings	69
4.2 SOD1 May Modulate CXCR4-Induced ERK and AKT Activation	72
4.3 SOD1 Protects Against Apoptosis in Normoxic, but not in Hypoxic Conditions	77
4.4 SOD1 Inhibits Migration in Normoxic, but not Hypoxic Environments	79
4.5 G Protein Coupling with CXCR4 Appears to Change in Hypoxia	83
4.6 Future Directions	84
CHAPTER 5: CONCLUSION	87
REFERENCES	90
APPENDIX i: American Joint Committee on Cancer (AJCC) Prostate Cancer Staging	100
APPENDIX ii: License for Figure 1.2	101
APPENDIX iii: License for Table 1.1	102
APPENDIX iv: License for Figure 1.3A	103
APPENDIX v: License for Figure 1.3B	104
APPENDIX vi: License for Figure 1.5	105

APPENDIX vii: License for Figure 1.6	106
APPENDIX viii: SOD1 siRNA-Mediated Knockdown	107

LIST OF TABLES

Table 1.1 Overview of Chemokine Receptor Expression on Normal and Cancerous Cells.....	16
--	----

LIST OF FIGURES

Figure 1.1 Schematic of the Metastatic Transition	30
Figure 1.2 G Protein Activation Cycle	31
Figure 1.3 CXCR4 Structure	32
Figure 1.4 Overview of CXCR4 Signal Transduction	33
Figure 1.5 The Effects of the Hypoxic Microenvironment in a Tumor	34
Figure 1.6 The Structure of SOD1	35
Figure 1.7 Overview of SOD1 Activity	36
Figure 1.8 Working Hypothesis	37
Figure 2.1 Annexin V Staining Schematic	47
Figure 2.2 Schematic of Transwell Migration Assays	48
Figure 2.3 Bioluminescence Resonance Energy Transfer (BRET) Technique Schematic	49
Figure 3.1 Endogenous Levels of CXCR4 and SOD1 in Normal and Hypoxic Conditions in PC3 Cells	60
Figure 3.2 Endogenous Interaction between CXCR4 and SOD1 in PC3 Cells	61
Figure 3.3 Exogenous Interaction Levels between CXCR4 and SOD1 in PC3 cells in both Normal and Hypoxic Conditions	62
Figure 3.4 Effects of both SOD1 and Hypoxia on CXCR4-Mediated Extracellular Signal-Regulated Kinase Activation in PC3 Cells	63
Figure 3.5 Effects of both SOD1 and Hypoxia on CXCR4-Mediated AKT/ Protein Kinase B (PKB) Activation in PC3 Cells	64
Figure 3.6 Effect of SOD1 and CXCR4 on Apoptosis Levels in PC3 Cells in Normoxic Conditions	65
Figure 3.7 Effect of SOD1 and CXCR4 on Apoptosis Levels in PC3 Cells in Hypoxic Conditions	66

Figure 3.8 Effect of SOD1 and Pertussis Toxin (PTX) on CXCR4-Mediated Migration in Response to CXCL12 in both Normoxic and Hypoxic Conditions	67
Figure 3.9 Effect of SOD1 on G Protein Coupling, Assessed Using Bioluminescence Resonance Energy Transfer (BRET), with CXCR4 in both Normoxic and Hypoxic Conditions.....	68
Figure 5.1 Updated Hypothesis	89

ABSTRACT

Prostate cancer (PCa) is associated with high rates of cancer spread, or metastasis, the process that accounts for up to 90% of cancer-related deaths. CXCR4, a chemokine G protein-coupled receptor (GPCR), and its ligand CXCL12, are highly expressed in both PCa tissue, and common locations of metastasis, including the lymph nodes, lungs and bone. Multiple studies have demonstrated the importance of the CXCR4/CXCL12 signaling axis in cancer progression, specifically due to its role in cell survival, proliferation and migration. In addition, antioxidants are implicated in modulating cell survival through the scavenging of free oxygen radicals. Our lab has shown that the antioxidant superoxide dismutase (SOD1) interacts with CXCR4. The goal of this project was to determine to what extent this interaction modulates PCa metastasis. We have shown that the level of interaction between CXCR4 and SOD1 in PC3 prostate cancer cells is increased by CXCL12 stimulation in normoxic, but not in hypoxic conditions. Our work suggests that SOD1 can prevent apoptosis in normoxic, but not in hypoxic conditions. We also found that, unexpectedly, CXCR4 signaling seems to switch from coupling with both $G\alpha_i$ and $G\alpha_q$ in normal conditions to favouring $G\alpha_q$ coupling in hypoxia, regardless of SOD1 expression level. This result was corroborated by the fact that the $G\alpha_i$ inhibitor pertussis toxin (PTX) was able to ablate CXCR4-mediated chemotaxis in normal, but not in hypoxic conditions. Overall, this project was able to characterize the effects of the interaction between SOD1 and CXCR4 on the regulation of certain pathways involved in the metastatic transition. Future work involves investigating second messenger levels to confirm the G protein switch that occurs in hypoxia and the use of animal models for *in vivo* work. The eventual aim of this project is to exploit this protein interaction to develop a therapeutic that can help prevent cancer-related deaths.

LIST OF ABBREVIATIONS AND SYMBOLS USED

7TMR	7-transmembrane receptor
AV	Annexin V
AIDS	Acquired immunodeficiency syndrome
AJCC	American Joint Committee on Cancer
ALS	Amyotrophic lateral sclerosis
ANOVA	Analysis of variance
ATP	Adenosine triphosphate
BF	Bright field
B-NHL	B-cell Non-Hodgkin's Lymphoma
BMI	Body mass index
BPH	Benign prostatic hyperplasia
BRET	Bioluminescence resonance energy transfer
BSA	Bovine serum albumin
C-terminus	Carboxy(l)-terminus
cAMP	3',5'-cyclic AMP
CCL21	C-C chemokine ligand type 21
CCR5	C-C chemokine receptor type 5
CCR7	C-C chemokine receptor type 7
CCR8	C-C chemokine receptor type 8
CD4	Cluster of differentiation 4
CD184	Cluster of differentiation 184
CICR	Calcium-induced calcium release

CO-IP	Co-immunoprecipitation
CREB	cAMP response element-binding protein
Cu,Zn-SOD	Cytosolic superoxide dismutase
CXCL12	C-X-C chemokine ligand type 12
CXCR2	C-X-C chemokine receptor type 2
CXCR4	C-X-C chemokine receptor type 4
dH ₂ O	Distilled water
DAG	Diacylglycerol
DMEM	Dulbecco's Modified Eagle's Medium
DNA	Deoxyribonucleic Acid
EGFR	Epidermal growth factor receptor
EMT	Epithelial-mesenchymal transition
ER	Endoplasmic reticulum
ERK	Extracellular signal-related kinase
FBS	Fetal bovine serum
GDP	Guanosine diphosphate
GPCR	G protein coupled receptor
gp120	Envelope glycoprotein GP120
GTP	Guanosine triphosphate
H ₂ O ₂	Hydrogen peroxide
HCP	Hematopoietic CD34+ progenitor cells
HEK293A	Human embryonic kidney cells
HIF-1	Hypoxia-inducible factor 1

HIV	Human immunodeficiency virus
HRE	Hypoxia-responsive elements
HRP	Horseradish peroxidase
HA	Human influenza agglutinin
IP ₃	Inositol triphosphate
InsP ₃ R	Inositol triphosphate receptor
IT1t	Isothiourea derivative
MAPK	Mitogen-activated protein kinase
mRNA	Messenger ribonucleic acid
MSR1	Macrophage scavenger receptor 1
N-terminus	Amino-terminus
NF-κB	Nuclear factor kappa-light-chain-enhancer of activated B cells
NK	Natural killer cells
O ₂ ⁻	Superoxide
OH ⁻	Hydroxyl ions
PBS	Phosphate-buffered saline
PGCs	Primordial germ cells
PI	Protease inhibitor cocktail tablets
PI	Propidium iodide
PI3K	Phosphoinositide 3-kinase
PIP ₂	Phosphatidylinositol 4,5-biphosphate
PLCβ	Phospholipase C β
PS	Penicillin-Streptomycin

PSA	Prostate-specific antigen
PKA	Protein kinase A
PTEN	Phosphatase and tensin homolog
PTX	Pertussis toxin
RGS	Regulators of G protein signaling
RIPA	Radioimmunoprecipitation assay
<i>RlucII</i>	<i>Renilla</i> luciferase
ROS	Reactive oxygen species
RTK	Receptor tyrosine kinase
RyR	Ryanodine receptors
SCID	Severe combined immunodeficiency
SDF1 α	Stromal cell-derived factor 1
SDS-PAGE	Sodium Dodecyl Sulfate Polyacrylamide Gel Electrophoresis
SFM	Serum-free media
shRNA	Short-hairpin ribonucleic acid
siRNA	Short-interfering ribonucleic acid
SOD1	Cytosolic superoxide dismutase
SOD2	Mitochondrial superoxide dismutase
SOD3	Extracellular superoxide dismutase
TBS	Tris-buffered saline
TBST	Tris-buffered saline with 0.1% Tween-20
TM	Transmembrane
TNM	Tumor, lymph nodes, metastasis staging system

TRAMP	Transgene adenocarcinoma mouse prostate
UV	Ultraviolet
VEGF	Vascular endothelial growth factor
VFTM	Venus flytrap mechanism
WT	Wild-type
X-tremeGENE	X-tremeGENE HP DNA Transfection Reagent
YFP	Yellow fluorescent protein

ACKNOWLEDGEMENTS

I would like to extend my most grateful thanks and utmost appreciation to my supervisor Dr. Denis Dupré. As I have mentioned before, the only thing that I do not like about being one of Dr. Dupré's students is that having a French accent in his name makes it difficult to fill out certain application forms. Dr. Dupré has been an excellent supervisor. He has taught me techniques that I will remember and use for the rest of my science career and more importantly, has reminded me to think critically about science, no matter where or who it comes from. Not only is he always there to answer my incessant stream of questions, but he also tolerates my quirks with humour and grace. For all of these things and many more that I could never fit in a page, I would like to thank him for having me in the lab.

To my present lab mates, Kelsie Gillies and Brent Young, I do not know what I would do without you. Thank you for answering my questions, helping me both technically and emotionally, and most importantly, for picking up my slack on the lab chore front for the past couple months. Kelsie – our coffee dates are the best part of my school day. Brent – you make me laugh so hard I sometimes forget I'm working. To the past lab mates, thank you so much for your lab books, teaching me techniques and setting everything up so well. Importantly, I want to thank Chad Purcell, Nicholle Charette and Dr. Yi-Qun Kuang for the preliminary data to get me started on this project.

To the rest of the students in the Pharmacology department, thank you for being there for me. I am certain that I have asked each and every one of you at least one question during my degree and I truly appreciate the friendships and collegial relationships I have formed. To my Scientific Advisory Committee, Dr. Susan Howlett, Dr. Kerry Goralski, and Dr. Eileen Denovan-Wright, thank you for your support and suggestions throughout my degree. To the rest of the faculty and technicians in the department, thank you for letting me use your labs, equipment and brains over the last year and a half. Finally, to the administrative staff, Luisa Vaughan, Sandi Leaf and Cheryl Bailey, I don't know where I would be without you. To think of it, I probably do know where I would be, I'd be lost somewhere in Wayne's world without funding, without scholarships, without candy, with stains on my shirt and with a misbehaved dog. Thank you ladies for making me smile daily.

Last but not least, I need to thank my amazing personal network of family and friends. Justin – thank you for listening to me practice my talks, keeping me company in lab after hours, racking tips, and most importantly for supporting me no matter what I do or how much I complain while doing it. Debra – thank you for your advice, for listening to me complain about my failed experiments and for the countless hours of laughter over the phone. Mom and Dad – thank you for supporting me emotionally, for sending me money if I can't afford food, and most importantly, for understanding and standing by my decision to become something other than a medical doctor. To my friends, you all know who you are, thank you for supporting me, hugging me, and reminding me that there will be an end to my life as a student. To my furry babies, Olive, Peanut and Jean-Jacques, thanks for not caring when I am late or tired or smelly.

CHAPTER 1: INTRODUCTION

1.1 Cancer

Broadly speaking, cancer is a disease involving uncontrolled cell growth and division. Cancer can affect any area of the body and is a leading cause of death worldwide (The World Health Organization [WHO], 2013). The burden of cancer is increasing globally over time; however, this increase can be partly attributed to an aging population and a longer lifespan, resulting from improved medical care (Jemal, Bray, & Ferlay, 2011). Although cancer clearly has a genetic component, increases in cancer rates have been linked to physical inactivity, tobacco use and an unhealthy diet (Jemal et al., 2011). According to Canadian Cancer Society and Statistics Canada in the Canadian Cancer Statistics Report 2012, the top four types of cancer diagnosed in this country are lung, breast, colorectal and prostate cancer. In total, an estimated 75,700 deaths in Canada will occur in 2012 due to cancer. These statistics are of acute concern to those in Nova Scotia, as Atlantic Canada and Quebec have the highest cancer incidence and mortality rates in Canada (Canadian Cancer Society's Steering Committee on Cancer Statistics, 2012).

1.2 Prostate cancer

1.2.1 Significance and Risk Factors

Cancer of the prostate gland is common and can be deadly. The prostate is a gland in the male reproductive system that surrounds the upper portion of the urethra. The role of the prostate is to excrete an alkaline solution that accounts for 50-75% of the volume of semen. In a normal state, the prostate gland is defined into two separate lobes and is approximately

the size of a walnut. The growth of this gland, both regular and cancerous, is normally stimulated by androgens secreted by the testes, including testosterone. An important distinction to make is that not all prostate enlargement is cancerous. The condition known as benign prostatic hyperplasia (BPH), affecting approximately 3 of 4 men in the United States, is a non-cancerous growth in both the size and number of prostate cells (Litwin & Saigal, 2004). This condition may be accompanied by some of the symptoms of prostate cancer, but is not a known risk factor for the disease.

Globally in 2008, there were an estimated 903,500 new cases of prostate cancer and 258,400 deaths resulting from this disease (Jemal et al., 2011). According to Prostate Cancer Canada, this translates into roughly 1 in 7 men Canadian men being diagnosed with prostate cancer at some point in their life. Prostate Cancer Canada cites the following characteristics as the main risk factors for developing prostate cancer: increasing age (>50), a diet low in fiber and high in saturated fats, family history of the disease, high body mass index (BMI) and either a Caribbean or African descent. However, there does seem to be a complex genetic component in the probability in developing prostate cancer that is only beginning to be elucidated.

There are several locations in the genome that have been of particular interest in both molecular genetic and epidemiological studies; it has been suggested that the short arm of chromosome 8 is the location of some of the genes that may be important for prostate cancer development (Gibbs et al., 2000; Miller et al., 2003). For example, a rare Asp174Tyr missense mutation on the macrophage scavenger receptor 1 (*MSR1*) gene was found twice as frequently in African-Americans with prostate cancer than in those without (Miller et al., 2003). While there are many studies available demonstrating a link between genome

differences and susceptibility to prostate cancer, all of the above analyses highlight the difficulty in examining risk factors for such a common and diverse disease. Looking forward, studies suggest analyzing the genomes of specimens from localized disease separately from samples taken from metastatic disease to further enhance our comprehension of prostate cancer (Zhang et al., 2003).

1.2.2 Testing, Diagnosis and Treatment

Owing to the fact that symptoms of prostate cancer typically do not appear until advanced stages of the disease, early detection of this cancer is imperative. Prior to a biopsy, the two main preliminary tests for prostate cancer involve both a digital rectal exam to detect an enlarged prostate and a prostate-specific antigen (PSA) test (Freedland, 2011). Reports stress the importance of supplementing the digital rectal exam with other test types due to the highly subjective nature of this assessment (Cooner et al., 2002). The reduction in prostate cancer-related mortality in developed countries has been partially attributed to the adoption of PSA testing (Jemal et al., 2011; Yousef & Diamandis, 2001).

PSA is a member of the tissue kallikrein gene family and acts as a serine protease (Balk, Ko, & Bubley, 2003; Yousef & Diamandis, 2001). Although elevated PSA levels can indicate prostate cancer, they can also arise from other circumstances and conditions, including, but not limited to: urinary tract infection, BPH and recent ejaculation. Early guidelines suggested that levels of 4.0 ng/ml could be indicative of prostate cancer (Cooner et al., 2002); however, more recent studies suggest that physicians should perform biopsies at a lower threshold than 4.0 ng/ml to increase detection rates (Thompson et al., 2004). Importantly, up to 15% of patients with prostate cancer will not display elevated PSA levels

(Thompson et al., 2004). Thus, the literature recommends combining screening mechanisms in order to effectively diagnose the disease, as it is a heterogeneous disease that may exhibit different characteristics at different disease stages and in different individuals (Balk et al., 2003; Cooner et al., 2002; Freedland, 2011).

Determining the stage and severity of prostate cancer is an integral and early part of effective treatment. The American Joint Committee on Cancer (AJCC) provides the most widely used staging system for prostate cancer (AJCC, 2009; Appendix i). The system is a “stage grouping” system, based on the TNM acronym, which stands for: tumor, lymph nodes and metastases. Briefly, this system bases the stage of the disease on 5 pieces of information including: the size of the primary tumor, the presence of cancer at neighboring lymph nodes, the presence or absence of metastases, the PSA levels of the patient and the Gleason score of the biopsy. The Gleason score is based on the microscopic appearance of the prostate biopsy; a higher score is indicative of more irregular-looking tissue and is normally associated with heightened disease aggression.

The treatment of prostate cancer depends on a variety of factors, including the age of the patient, family history and the severity of the disease. Generally, specialists recommend treatment for localized disease when the patient has a life expectancy of 10 years or greater, without considering cancer stage (Fowler et al., 2001). In the case of patients with a survival outlook of <10 years or select low-risk cancer types, most clinicians recommend watchful waiting or active surveillance, where the patient is followed closely and may or may not be treated (Fowler et al., 2001; Freedland, 2011). A study following 769 men that was conducted for over 15 years by a group at John Hopkins University School of Medicine supported the idea of active surveillance with eventual curative intent as a safe alternative to

immediate therapy; this study also suggested that this approach may help reduce overtreatment and adverse reactions (Tosoian et al., 2011). The vast majority of cases that are diagnosed in the Western world involve patients with localized disease. The three main therapies that men with localized disease would choose from include radical prostatectomy, brachytherapy and external beam radiation (Fowler et al., 2001). However, when the disease is metastatic, chemotherapy using docetaxel or mitoxantrone seems to be most effective (Freedland, 2011).

1.3 Prostate cancer metastasis

Metastasis has been defined as the spread of cancer cells from the primary tumor to a non-adjacent location in the body, resulting in the formation of a secondary tumor (Coghlin & Murray, 2010). A schematic of the metastatic process is shown in Figure 1.1. Metastasis is a multi-step process, in which cancer cells must escape their tumor, travel through the blood or lymph vessels, and invade and colonize a new area. Metastasis is an important area for prostate cancer research, as the majority of prostate cancer-related deaths do not occur due to primary tumor burden, but due to the metastatic disease. Studies estimate that in all cancer types, up to 90% of deaths due to solid tumors are a result of metastasis (Gupta & Massagué, 2006). Prostate cancer metastasis is a highly regulated process, and seems to result in secondary tumors in characteristic places, including the bone, lymph nodes and lungs (Gladson & Welch, 2008). The directed metastasis of cancer cells provides insight into the notion that molecular pathways closely regulate this process. As a corollary, researchers hope to learn enough about the metastatic transition to intervene and prevent the process.

There are many types of molecules involved in the development cancer and the subsequent metastatic transition. Importantly, not all types of cancer or even all cells within a single tumor are capable of metastasizing. This begs the question: what are the requirements for a cancer cell to metastasize? Early on, researchers found a link between increased genomic mutability and metastatic potential. This suggested that as cancer cells acquire mutations, a population of cells from a heterogeneous tumor may have mutations that allow them to survive conditions that metastatic cells are exposed to, conferring a selective advantage (Gupta & Massagué, 2006).

One of the major steps in the change from a defined tumor to metastatic cancer is called the epithelial-mesenchymal transition (EMT). Epithelial cells make up the epithelium, one of the four basic types of tissue found in animals. Epithelial cells have several important characteristics including their close association with each other, lack of vascularization, and close association with the basement membrane. In contrast, mesenchymal cells are normally found in loose connective tissue and are normally more mobile and rely less on cell-cell adhesion. The EMT occurs when cancerous epithelial tissues exhibit a loss in structural integrity and a loss of cell-cell adhesions, largely mediated by production of matrix metalloproteinases (MMPs) that can break down the extracellular matrix and an increase in TGF β signaling (Kalluri & Weinberg, 2009). These changes can result in cancer cells that are more invasive and rely less on cell contact, thus making it more likely that they will be capable of moving through the endothelial cell layer into the bloodstream.

Two main categories of molecules that are involved in cancer development, the EMT, and subsequent cancer spread are tumor suppressor genes and oncogenes. Tumor suppressor genes are genes that encode proteins that help prevent cancer. However, when these genes

are mutated, the protection that once existed is gone and this can lead to cancer development or progression. A well-characterized example of a tumor suppressor gene is the protective p53 protein encoded by the TP53 gene. Normally, p53 acts to induce apoptosis in cells with accumulations of DNA mutations. As a result, when p53 is non-functional, the cells with damaged DNA remain alive and can divide and produce more mutant cells (Vivanco & Sawyers, 2002). Another example of a tumor suppressor gene that is implicated in prostate cancer development and metastasis is phosphatase and tensin homolog (PTEN). When PTEN is working properly, its protein product acts to inhibit the AKT/Protein Kinase B pathway that is involved in cell growth, survival and migration (Croce, 2008). Thus, when PTEN is non-functional, aberrant activation of the AKT pathway can lead to irregular growth resulting ultimately in cancer.

In contrast, oncogenes encode proteins that are mainly involved in the cell cycle, or proliferation (Croce, 2008). When these important regulatory genes are mutated, the lack of control over cell death and growth can allow tumors to form. A well-known group of oncogenes encode a variety of growth factor receptors that are commonly receptor-tyrosine kinases (RTKs). The epidermal growth factor receptor (EGFR) is a common example of an RTK that is mutated in some cancer types. Deletion of the ligand-binding domain of this receptor renders it constitutively active and as a result, constantly signals the cell to grow, proliferate and differentiate even in the absence of ligand (Croce, 2008). Cells that either have a malfunctioning EGFR or overexpress this receptor are characteristic of many types of cancers.

There are several extrinsic factors that influence the propensity of tumor cells to migrate. One integral aspect is hypoxia, or low oxygen. Low levels of oxygen lead to

stabilization of the hypoxia-inducible factor (HIF-1), a transcriptional complex that is known to promote angiogenesis, cell migration and survival. Therefore, the low levels of oxygen present in the center of a tumor can itself be a signal for cancer cells to migrate (Brahimmi-Horn, Chiche, & Pouyssegur, 2007; Gupta & Massagué, 2006). Another important extrinsic factor involved in prostate cancer metastasis is the involvement of cell-surface chemokine receptors and their respective chemokine ligands. Specifically, some organs have been found to express high levels of signaling chemokines that may attract the cancer cells that express the corresponding receptor. The involvement of chemokine receptors and hypoxia in prostate cancer development and metastasis will be discussed in further detail later.

Knowledge of oncogenes and tumor suppressor genes, in addition to the microenvironment that can favour metastasis, is imperative to the comprehension of cancer development and spread. Although more work needs to be done to better understand known oncogenes and tumor suppressor genes, additional efforts should be directed at the discovery of new molecules and factors that regulate cancer growth. Chemokine G protein-coupled receptors (GPCRs) are an example of a group of signaling molecules that have attracted the interest of cancer researchers.

1.4 G Protein-Coupled Receptors

1.4.1 Overview and Significance

G protein-coupled receptors (GPCRs), otherwise known as seven transmembrane receptors (7TMRs) or serpentine receptors, are a group of structurally related receptors that are found in the plasma membrane of eukaryotic cells. These receptors have been an important and active area of research since their discovery. The most convincing evidence of

the importance of GPCR research is that according to recent estimates, this receptor family represents the target for between 30% and 40% of modern pharmaceuticals (Filmore, 2004; Hopkins & Groom, 2002; Overington, Al-Lazikani, & Hopkins, 2006).

1.4.2 Discovery

Arguably, the discovery of GPCRs began downstream of the receptors themselves; although the signaling cascade moves from receptor activation, through G protein activation, to effector activation and second messenger production, the discovery of these components was in the opposite order. In a series of publications in the mid-1950s, E. Sutherland and T. Rall identified and isolated a “heat stable” factor now known as cyclic 3’5-AMP (cAMP), the first identified second messenger molecule (Rall, Sutherland, & Berther, 1957; Sutherland & Rall, 1957). The discovery of G proteins soon followed, with the realization that different hormones acted on distinct receptors, but activate a single adenylyl cyclase (Rodbell, Birnbaumer, & Pohl, 1970). This research ignited the scientific community’s interest in the receptors that were governing these basic biochemical processes and set the stage for GPCR research.

1.4.3 Structure

G protein coupled receptors are a group of morphologically distinct cell-surface proteins. These proteins have an amino-, or N-terminus that is outside of the cell and a carboxy-, or C-terminus, inside the cell. The middle portion of the protein consists of 7 hydrophobic α -helices, that span the plasma membrane (PM) 7 times, hence their pseudonyms – serpentine receptors, or 7TMRs (Gurevich & Gurevich, 2009). While the

transmembrane loops are relatively well conserved among the GPCRs, the carboxy- and amino termini, in addition to the intracellular loop spanning between the TM5 and TM6 segments display sequence diversity (Kobilka, 2007). The vast array of ligands that can bind to, and activate the GPCRs provides insight into the amount of diversity that must exist within this relatively similar superfamily of receptors. The ligands include, but are not restricted to: peptides, proteins, nucleotides, ions, photons, organic odorants, and hormones (Fredriksson, Lagerström, Lundin, & Schiöth, 2003; Gurevich & Gurevich, 2009; Kobilka, 2007). As mentioned, despite the similar gross structure, these receptors are variable in their amino acid sequences. Based on sequence similarity, this receptor family has been grouped into 5 families (Kobilka, 2007).

1.4.4 Classification

The classification of GPCRs has evolved alongside the understanding of the diversity of these receptors. The current arrangement is based mostly on sequence homology and divides the receptors into 5 families: class A, or Rhodopsin-like receptors, class B, which includes the Secretin receptor and the Adhesion families of receptors, class C, the Glutamate family, and the Frizzled/Tas2 family (Fredriksson et al., 2003; Gloriam, Fredriksson, & Schiöth, 2007; Kobilka, 2007).

The Rhodopsin group is the largest family of 7TMR, with over ~ 670 full length receptors in the human genome (Gloriam et al., 2007). This group of GPCRs includes the rhodopsin receptor, the first GPCR to have its primary structure determined (Hargrave et al., 1983; Nathans & Hogness, 1984). The diversity among these receptors is mostly restricted to the TM portions of the receptor, as the N-termini are relatively well conserved (Lagerström

& Schiöth, 2008). Examples of Rhodopsin receptors targeted pharmaceutically include the histamine receptors 1 and 2, the dopamine receptors 1 and 2, a subset of the serotonin receptors and the cannabinoid 1 receptor (Lagerström & Schiöth, 2008).

The Secretin family of GPCRs contains 15 members, all of which have known ligands (Gloriam et al., 2007; Lagerström & Schiöth, 2008). All of these receptors have a peptide hormone-binding domain in their N-termini. The Adhesion receptors, also in family B, exhibit similarities to the Secretin receptors in their TM domains. However, in contrast with the Secretin receptors, the Adhesion GPCRs have long N-termini. There are 33 known Adhesion GPCRs, however, none of these receptors are the known target of clinically used drugs (Kobilka, 2007; Lagerström & Schiöth, 2008).

The Glutamate family of receptors contains 22 full-length GPCRs that are characterized by the “Venus flytrap mechanism” (VFTM) of ligand binding, where two portions of the extended N-terminus fold to create a cavity, in which the ligand can be engulfed (Fredriksson et al., 2003; Kobilka, 2007; Lagerström & Schiöth, 2008). This group of receptors was the first GPCRs that were recognized to form functional dimers. It was discovered that the GABA_B receptors in isoforms GABA_BR1 (GBR1) and GABA_BR2 (GBR2) function as a heterodimer (Sullivan et al., 2000). When the proteins are expressed alone, the GBR1 receptor stays within the cell, while the GBR2 receptor moves to the cell surface but cannot signal. When the receptors are co-expressed, the GBR2 receptor is capable of blocking the ER-retention motif on GBR1, thus allowing the heterodimer to reach the cell surface and signal through ligand binding to the GBR1 receptor. The phenomenon of dimerization is now well established and is known to occur in all GPCR families (Gurevich & Gurevich, 2009).

1.4.5 Signal Transduction

Although there is recognized diversity among the GPCR families, the receptors seem to follow similar signal transduction pathways, beginning with activation and ending with a cellular response. Although there are some GPCRs that are constitutively active, most signaling occurs when the ligand binds to the receptor. Ligands of variable chemical nature bind to different regions of the receptor. Peptide ligands normally bind in the transmembrane region of the helix or on the extracellular portions of the loops. In contrast, small ligands that interact with Type I receptors usually bind at sites buried within the transmembrane regions of the helices (Kristiansen, 2004; Oldham & Hamm, 2008).

When a ligand binds, there is a change in conformation of the receptor that seems to be common to most GPCRs, as it was observed in the bovine rhodopsin receptor, thyrotropin-releasing-hormone receptor, the M₃-muscarinic receptor and the β_2 -adrenergic receptor (Jensen et al., 2001). Specifically, studies have demonstrated that agonist binding causes a rearrangement of the cytoplasmic side of TMVI (Jensen et al., 2001; Oldham & Hamm, 2008). In addition, this study concerning the β_2 -adrenergic receptor suggests a decrease in the polarity of the environment of labeled amino acids in the TMVI; this suggests a movement of TMVI away from the receptor (Jensen et al., 2001). This opening is then thought to allow for the C-terminus of the G protein to bind at the cytoplasmic side of the GPCR (Oldham & Hamm, 2008).

When the receptor is inactive, the G protein also remains in the inactive guanosine diphosphate (GDP) bound conformation. Ligand binding to the GPCR causes a conformational change in the structure of the G α subunit, causing the release of GDP

(Oldham and Hamm, 2008). Cellular guanosine triphosphate (GTP) then binds with the $G\alpha$ subunit, rendering the active conformation of the G protein. Binding of GTP causes conformational changes in $G\alpha$, allowing for the functional dissociation of the $G\beta\gamma$ subunit (Kristiansen, 2004). This active G protein then exerts its' effects on downstream effectors. It was originally assumed the $G\beta\gamma$ subunits simply served as a negative regulator of G protein function and that it physically dissociated from the $G\alpha$ subunit. However, evidence now suggests that this apparent separation may be explained by a conformational change within the G protein subunits, and that the $G\beta\gamma$ itself can modulate the activity of many downstream effectors (Dupré, Robitaille, Rebois, & Hébert, 2009). Intrinsic enzymatic activity of the $G\alpha$ subunit, regulated by other factors such as regulators of G protein signaling (RGS), catalyzes hydrolysis of GTP to GDP- P_i , re-setting the G protein to its inactive state (Oldham & Hamm, 2008). An overview of GPCR ligand binding, conformational change and G protein activation can be found in Figure 1.2.

Due to the vast array of effectors that can be activated by GPCRs, only the most common effectors will be discussed here. Adenylyl cyclase is an effector protein that is activated by $G\alpha_s$ and inhibited by $G\alpha_i$ (Gilman, 1995). Upon activation of adenylyl cyclase, the catalytic domains of this enzyme convert adenosine triphosphate (ATP) to 3',5'-cyclic AMP (cAMP) and pyrophosphate. cAMP can move freely in the cytosol and can allosterically bind to cAMP-dependent protein kinase, otherwise known as protein kinase A (PKA). Some activated PKA enzymes can translocate into the nucleus, where they phosphorylate the transcription factor cAMP response element-binding protein (CREB). Final effects of adenylyl cyclase activation normally include gluconeogenesis, glycogen

breakdown, inhibition of glycogen synthesis, increased contractility of cardiac muscle, and water reuptake in the kidney (Oldham & Hamm, 2008).

The G_q subunits function mainly in the increase in active phosphatidyl-inositol-specific (PLCβ), and can initiate a reaction that will create the second messengers inositol triphosphate (IP₃) and diacylglycerol (DAG) from PI 4,5-biphosphate (PIP₂). DAG is able to attract and activate protein kinase C (PKC), an enzyme that can phosphorylate a multitude of proteins. Generally, PKC plays a role in metabolism, transcriptional regulation, cell growth, and differentiation. IP₃ moves to the surface of organelles containing calcium stores (usually the smooth endoplasmic reticulum), and binds to an IP₃ receptor (InsP₃R); these receptors are also calcium channels and they allow Ca²⁺ ions to move into the cytosol. Here, calcium ions are capable of interacting with ryanodine receptors (RyRs), and cause more calcium to be released in a process known as calcium-induced-calcium-release (CICR; Berridge, Lipp, & Bootman, 2000).

Signal transduction cascades that are downstream of GPCR activation are diverse. Some of the cell responses to GPCR activation include, but are not limited to: cell growth, differentiation, migration or chemotaxis, division and cell survival.

1.5 Chemokine receptors and their role in cancer

Chemokines are small cytokine proteins (8-10 kDa) that have been classified into four groups based on the two cysteine residues closest to the N-terminus of the protein (Balkwill, 2004a). These proteins bind to chemokine GPCRs to elicit their effects that are normally linked to the immune response. Chemokine receptor expression varies based on cell lineage, environment and exposure to chemokines. Chemokine signaling that can result

in the migration of white blood cells can be activated by a number of factors including: pathogen invasion, inflammation and certain growth factors (Rossi & Zlotnik, 2000).

Chemokine receptors were initially identified on the surface of leukocytes, but have since been discovered on the surface of some endothelial and epithelial cells that have undergone malignant transformation (Balkwill, 2004a; Gupta & Massagué, 2006; Müller et al., 2001).

Numerous studies have demonstrated high levels of expression of chemokine receptors on cancer cells (Balkwill, 2004a). Table 1 shows a summary of the chemokine receptor-expressing cancer cells types. This table highlights the fact that chemokine receptors are often hijacked from their original immune function to participate in the progression of cancer. In a landmark study published in 2001, Müller et al. report three main expression patterns of chemokine receptors in breast cancer. The receptors are either present in normal tissue and down-regulated in malignant tissue (CXCR2), present at high levels in both tissue types (CCR7 and CCR8) or absent in control tissue and upregulated in cancerous tissue (CXCR4; Müller et al., 2001). For example, CCR7 expression has been linked with poor patient survival and exhibits elevated levels in many cancer types (Mashino, Sadanaga, & Yamaguchi, 2002). Additionally, CCL21, the ligand for CCR7, is found in high levels of the lymph nodes, a common metastasis destination (Mashino, Sadanaga, & Yamaguchi, 2002; Müller et al., 2001). Recently, both CCR7 and CXCR4 have been demonstrated to prevent anoikis, the process of apoptosis resulting from loss of cell-cell interaction, highlighting a role for these receptors in the spread of cancer cells (Kochetkova, Kumar, & McColl, 2009).

Table 1 Overview of Chemokine Receptor Expression on Normal and Cancerous cells. Table reproduced, with minor alterations, with permission (Appendix iii), from Balkwill, F. (2004). Cancer and the chemokine network. *Nat Rev Cancer*. 4(7):540-550.

Chemokine Receptor	Normal Expression	Cancer Cell/Tissue Expression
CCR3	T cells, eosinophils, basophils and plasma cells	T-cell leukemia, renal cell carcinoma, skin cancer
CCR4	Natural Killer (NK) cells, immature dendritic cells, some T-cells	T-cell leukemia, breast cancer cell lines
CCR5	B-lymphocytes, immature and mature dendritic cells, macrophages	B-cell Non-Hodgkin's lymphoma (B-NHL), breast cancer cell lines
CCR7	T-cells, B-cells, mature dendritic cells	B-NHL, breast cancer, gastric cancer, non-small-cell lung cancer, oesophageal cancer
CCR10	Plasma cells, skin-homing T-cells	Melanoma
CXCR2	Macrophages, eosinophils, neutrophils	Melanoma
CXCR7	Embryonic cardiac and neural tissue, hematopoietic cells	Breast cancer, lung cancer, prostate cancer
CXCR4	Immature and mature dendritic cells, B-cells, T-cells, hematopoietic stem cells, macrophages, neutrophils, thymocytes	B-NHL, prostate cancer, breast cancer, ovarian cancer, pancreatic cancer, intraocular lymphoma, renal cancer, neuroblastoma, thyroid cancer, colorectal cancer, squamous cell carcinoma, rhabdomyosarcoma, small-cell lung cancer, melanoma, cervical cancer, astrocytoma

1.6 C-X-C Chemokine Receptor Type 4 (CXCR4)

1.6.1 Overview and Role in Normal Cell Signaling

C-X-C chemokine receptor type 4 (CXCR4) is a chemokine GPCR that is otherwise known as fusin or cluster of differentiation 184 (CD184). This receptor is 352 amino acids in length and exhibits a typical 7TM GPCR conformation. The structure and amino acid sequence of this receptor can be found in Figure 1.3. The only known ligand for CXCR4 is CXCL12 (Stromal Cell-Derived Factor-1; SDF1 α).

The essential role for CXCR4 in early normal development is exemplified by the fact that mice that do not express normal CXCR4 or CXCL12 have an embryonic lethal phenotype (Balkwill, 2004b; Zou, Kottmann, Kuroda, Taniuchi, & Littman, 1998). The few homozygous mutant CXCR4 mice that were born died within several hours of birth (Zou et al., 1998). This study of CXCR4 mutants suggested that the mice had hematopoietic, cardiac and fetal cerebellar development defects and that the cardiac effects are similar to those seen in CXCL12 deficient mice (Nagasawa et al., 1996; Zou et al., 1998). Additionally, at early embryonic stages, high levels of CXCR4 mRNA have been found in the brain and in the spinal cord, a pattern also seen in rats (Zou et al., 1998). An additional defect in zebrafish lacking CXCR4 or CXCL12 is that they have a reduced number of primordial germ cells (PGCs) arriving at the gonads, suggesting that this signaling axis is needed for sexual development (Knaut, Werz, Geisler, & Nüsslein-Volhard, 2003). These and other studies have demonstrated the importance of CXCR4 in normal development; however, they also note that the embryonic lethal phenotype makes studying the role of CXCR4 in development difficult (Balkwill, 2004b).

CXCR4 has also been identified in some human adult cells, including a wide array of white blood cells, neurons, intestinal epithelial cells and in the bone marrow (Balkwill, 2004b; Rossi & Zlotnik, 2000). This receptor has been demonstrated to play a role in normal immune responses. For instance, CXCR4 is involved in the migration of antibody-secreting plasmablasts in the memory immune response in mice (Hauser et al., 2002). The CXCR4/CXCL12 signaling axis has also been implicated in the retention, survival (due to anti-apoptotic effects) and homing of primitive hematopoietic CD34+ progenitor cells (HCP) in the bone marrow both *in vitro* and *in vivo* (Balkwill, 2004b; Broxmeyer et al., 2003). The importance of the CXCR4/CXCL12 signaling axis in both embryonic development and adult homeostatic and immune responses is best exemplified by the role of this receptor in various disease states.

1.6.2 CXCR4 in Other Disease States

Although the receptor is best known for its role in cancer progression and metastasis, CXCR4 is implicated in a myriad of diseases. Only several of these diseases will be included here, with the aim of supporting the notion of CXCR4 as a viable drug target.

Due to the homeostatic role that chemokine GPCRs play in inflammation and immunity, it is not surprising that CXCR4 is involved in several inflammatory diseases including arthritis and airway inflammation (Balkwill, 2004b). An example of the importance of CXCR4 in arthritis is that treatment of arthritis-induced joints in rodents with CXCL12 increased the inflammatory response and the majority of cells harvested from this area were CXCR4+. Additionally, pretreatment of these mice with AMD3100, a CXCR4 antagonist, reduced the severity of their symptoms (Matthys et al., 2001). However, CXCR4

has not yet been a specific target for any clinically used drugs treating inflammation due to either adverse effects or ineffectiveness.

Acquired immunodeficiency syndrome (AIDS) is a worldwide pandemic that is caused by a virus called the human immunodeficiency virus (HIV). The HIV virus possesses an envelope with a surface glycoprotein gp120 (envelope glycoprotein GP120). This glycoprotein attaches to the cluster of differentiation 4 (CD4) immunoglobulin receptor (O'Hara & Olson, 2002; Pierson & Doms, 2003). When this interaction takes place, a change in the conformation of gp120 allows for a required interaction with a co-receptor, usually CCR5 (C-C chemokine receptor type 5) or CXCR4 (O'Hara and Olson 2002; Pierson and Doms 2003). The formation of this complex allows for the fusion of the viral membrane with the cell plasma membrane (O'Hara and Olson 2002). Once the membranes have fused, the virus has access to the intracellular machinery of the immune cell, and infection has occurred. AMD3100, the CXCR4 antagonist, was effective in clinical trials, and 8 of 19 patients displayed complete loss of CXCR4-dependent viruses. Although this drug has demonstrated promising clinical results, it has some debilitating side effects, including tachycardia and premature ventricular contractions (O'Hara and Olson 2002). However, a CCR5 inhibitor called Maraviroc is currently in use for the treatment of HIV, supporting the concept of these co-receptors as a viable drug target.

1.6.3 CXCR4 Signal Transduction

Upon stimulation with CXCL12, CXCR4 is capable of stimulating G protein activity. CXCR4 has been demonstrated to couple to both $G\alpha_i$ and $G\alpha_q$ G proteins (Ngai, Inngjerdigen, Berge, & Taskén, 2009; Shi et al., 2007). This means that this receptor can

both inhibit adenylyl cyclase (decreasing cAMP production) and activate PLC β , increasing the creation of DAG and IP $_3$. The downstream signaling events following CXCR4 stimulation are diverse, and include activation of various extracellular signal-related kinases (ERKs), including ERK1 and ERK2, that are examined in the current study, increased nuclear factor kappa-light-chain-enhancer of activated B cells (NF- κ B) activity, and increased calcium flux (Ganju et al., 1998). Due to the array of signaling pathways activated by CXCR4 activation, downstream effects are also variable. Some of the main effects of CXCR4 activation include protection from apoptosis, cell migration (normally towards CXCL12), cell proliferation, and cell growth (Balkwill, 2004b; Ganju et al., 1998). An overview of the cellular effects of CXCR4 activation is provided in Figure 1.4. Given the effects of CXCR4 activation listed above, it is not surprising that CXCR4 has been implicated in the progression and metastasis of cancer.

1.6.4 Role in Cancer

CXCR4 has been implicated in over 24 cancer types. The first strong evidence suggesting that CXCR4 is involved in cancer metastasis came from Müller et al., 2001. They found that CXCR4 was highly expressed in breast cancer cells, malignant tumors and metastatic cancer cells. Further, they demonstrated that high levels of CXCL12 were found in common metastatic locations for this disease, including the lymph nodes, bone marrow and lungs. Lastly, they demonstrated *in vivo* that treatment of mice with an anti-CXCR4 antibody that blocked the interaction between CXCR4 and CXCL12 inhibited migration of breast cancer cells to the lymph nodes and lungs (Müller et al., 2001).

Importantly, levels of CXCR4 were found to be higher in prostate cancer than in other cancer types, supporting the further examination of this receptors role in prostate cancer (Fischer, Nagel, Jacobs, Stumm, & Schulz, 2008). Several researchers hypothesized that the role that CXCR4 plays in hematopoiesis indicated a possible role for the receptor in prostate cancer metastasis to the bone (Taichman et al., 2002; J. Wang, Loberg, & Taichman, 2006). These studies found that prostate cancer cells lines (PC3, C4-2B, LNCaP) expressed CXCR4, and that this receptor was functional, as it could activate ERK1 and ERK2 in a CXCL12-dependent manner (Taichman et al., 2002). Furthermore, CXCL12 increased invasion and migration potential of these cells, in addition to increasing their binding to human osteosarcoma cells, supporting a role for CXCR4 in the process of metastasis to bone (Taichman et al., 2002). Other studies have shown that overexpression of CXCR4 in PC3 cells prior to injection into a severe combined immunodeficiency (SCID) mouse significantly increases size, weight and vascularization of the tumors formed (Darash-Yahana et al., 2004). These observations are important, as tumors that do not form their own network of blood vessels are limited in their size. In humans, biopsies have demonstrated that CXCR4 expression levels correlated with the metastatic propensity of the disease and the probability of patient survival (Akashi et al., 2008; Sun et al., 2003). Overall, these studies provided sufficient evidence to warrant close examination of the CXCR4/CXCL12 signaling axis in prostate cancer metastasis.

While the aforementioned investigations demonstrated that CXCR4 signaling increases metastatic potential of prostate cancer, several studies have demonstrated that the inhibition of CXCR4 signaling can reduce metastasis of these cancers. For example, treatment with an anti-CXCL12 antibody significantly decreases the proliferation of prostate

cancer cell lines (Sun et al., 2003). Additional studies have used the CXCR4 antagonist AMD3100 in cancer studies. Zhang et al., 2008 demonstrated that AMD3100 decreased the invasiveness of prostate cancer cells and CXCL12 enhanced invasiveness, as measured by a transwell migration assay (Zhang et al., 2008). This report also found that *in vivo* treatment with AMD3100 significantly decreased the perineural invasiveness of prostate tumors (Zhang et al., 2008). Recently, Domanska et al., 2012 have demonstrated that treatment of mice with AMD3100 increases their sensitivity to docetaxil chemotherapy; this suggests that the coadministration of these drugs may help to reduce cancer growth (Domanska et al., 2012). Other studies showed that short-hairpin ribonuclease nucleic acid (shRNA)-mediated CXCR4 knockdown resulted in a decrease in bone marrow metastasis (Xing et al., 2008). The findings mentioned above are key, as they represent the therapeutic potential of the CXCR4/CXCL12 signaling axis.

Although it is clear that CXCR4 plays a role in prostate cancer metastasis, it is important to note that this chemokine receptor is not the only factor regulating the process. While the CXCR4 antagonist AMD3100 prevented prostate cancer metastasis in animal models, it is not currently used to treat prostate cancer in humans (Wong & Korz, 2008). The clear role that CXCR4 plays in the progression of prostate cancer, but absence of effective treatment options necessitates continued investigations into CXCR4 signaling in cancer.

1.6.5 Regulation of CXCR4 Expression

The regulation of CXCR4 expression is affected by a multitude of factors, only several of which will be discussed here. Activation of vascular endothelial growth factor (VEGF), a known oncogenic molecule, can induce the expression of CXCR4 in breast cancer

(Balkwill, 2004b; Dewan et al., 2006). Additionally, Kukreja et al., 2005 have demonstrated that there was upregulation of CXCR4 expression on PC3 cells in response to CXCL12 treatment that was mediated by ERK1/2 and NF- κ B signaling (Kukreja, Abdel-Mageed, Mondal, Liu, & Agrawal, 2005). Importantly, CXCR4 expression seems to be increased by long-term exposure to hypoxic, or low oxygen conditions. This change was dependent on the activation of hypoxia inducible factor 1 (HIF-1 α , a transcription factor) that occurs in tumors due to relatively low levels of vascularization and low oxygen-carrying ability resulting from tumor-related anemia (Schioppa et al., 2003). Supporting this notion, Chetram et al., 2011 found that the addition of hydrogen peroxide to the media of human prostate cancer cells caused a significant increase in CXCR4 expression (Chetram, Don-Salu-Hewage, & Hinton, 2011).

1.7 Reactive Oxygen Species, Antioxidants, and their Role in Cancer

The tumor microenvironment has very low levels of oxygen. Due to both low levels of vascularization and low oxygen carrying capabilities, the mean oxygen tension in tumor tissues is approximately 1.5%, while in normal tissues it is approximately 7% (Kimbrow & Simons, 2006; Vaupel, Kelleher, & Höckel, 2001). Histologically, tumors normally have a center core of necrotic cells that have died due to lack of glucose and oxygen (Brahimmi-Horn et al., 2007). Additionally, the extracellular pH within hypoxic tumors is significantly lower than that found in normoxic tissue, largely due to the modulation of metabolism in these conditions (Brahimmi-Horn et al., 2007). Since oxygen is only able to diffuse approximately 150 μ m into tissues, in order to survive, tumor cells must adapt to low oxygen conditions and/or produce more blood vessels.

The selection for more hypoxic-resistant cells in tumors could partially explain the increased aggressiveness and poor prognosis associated with low-oxygen tumors (Gupta & Massagué, 2006; Kimbro & Simons, 2006). Many of the changes that occur in the cell in hypoxic conditions occur as a result of HIF-1 stabilization. HIF-1 is a dimeric protein with an α and a β subunit. While both subunits are constitutively expressed, HIF-1 α is rapidly degraded in normal conditions (Wang, Jiang, Rue, & Semenza, 1995). In hypoxic conditions, the subunits are bound together, stabilized, and capable of interacting with hypoxia-responsive elements (HRE); this in turn, increases transcription of certain genes that are important for the cell to survive the low oxygen environment. In prostate cancer, HIF-1 α expression correlates with clinical stage of the patient (Kimbrow & Simons, 2006). This transcription factor is demonstrated to be elevated in rat and human prostate cancer (Zhong et al., 1998). Zhong et al., 1998 also showed that PC3 cells express functional HIF-1 α in normoxic conditions, when plated at high density (Zhong et al., 1998).

In addition to inducing the expression of CXCR4, HIF-1 α stabilization is known to play several roles in cancer progression. HIF-1 α activation has been shown to play a role in angiogenesis, a process that is particularly important for cancer cells in hypoxic environments (Brahimmi-Horn et al., 2007; Hirota & Semenza, 2006). Additionally, in normal environments, inactive HIF-1 α is bound to p53, it stabilizes it and allows for p53-mediated apoptosis to occur (Suzuki, Tomida, & Tsuruo, 2001). However, in hypoxic environments, HIF-1 α is bound to HIF- β , preventing this pro-apoptotic interaction between HIF-1 α and p53. An overview of the effects of the oxidative stress that exists within a tumor is shown in Figure 1.5.

Antioxidants are enzymes that are responsible for the breakdown of reactive oxygen species (ROS) into less harmful substances (Johnson & Giulivi, 2005). ROS, such as superoxide (O_2^-), hydrogen peroxide (H_2O_2), hydroxyl ions (OH^-) and hydroxyl radicals (OH^\bullet), are created in cells as a byproduct of normal oxidative phosphorylation. The ROS can originate within the cell as a part of normal cell metabolism in the electron transport chain or as a response to stress such as ultraviolet (UV) light or inflammatory cytokines (Waris & Ahsan, 2006). Increased levels of these ROS have been implicated in the process of aging, DNA damage and declines in membrane integrity (Johnson & Giulivi, 2005). Perhaps as a result of increased levels of ROS found in cancers, there also seems to be an augmented expression of antioxidants in various cancer types as well (Hileman, Liu, Albitar, Keating, & Huang, 2004). The antioxidant system within cells consists of multiple enzymes and several steps that result in the breakdown of ROS less harmful molecules. Superoxide (O_2^-) is dismutated into hydrogen peroxide (H_2O_2) by superoxide dismutase (SOD). Then, the much less reactive H_2O_2 can be acted upon by both catalase and glutathione peroxidase, creating water in the process. However, when H_2O_2 is in the presence of ferrous iron the Fenton reaction results in the creation of the very reactive OH^\bullet (Halliwell, 1994; Salganik, 2001). Due to the multistep process of eliminating the ROS, it is essential that the antioxidant molecule expression levels be tightly regulated, as changes in the level of one enzyme can cause a backup in the system and accumulation of detrimental ROS can occur.

Paradoxically, depending on circumstance and possibly cell type, oxidative stress leading to increases in ROS represents the cause of some cancers and the treatment that is used to cure it. Specifically, exogenous carcinogens such as radiation and certain pathogens have been implicated in oxidative DNA damage and can lead to the development of cancer

(Hileman et al., 2004; Waris & Ahsan, 2006). However, many of the chemotherapeutic agents used in the treatment of cancer, such as tetrathiomolybdate (TM; superoxide dismutase inhibitor) and the taxane paclitaxel, are drugs that increase ROS to cause cell death (Hileman et al., 2004; Juarez et al., 2006; Watson, 2013). This dual role for ROS in cancer suggests that close control of the balance between ROS and antioxidants is necessary for the prevention and treatment of cancer.

1.8 Cytosolic Superoxide Dismutase (SOD1)

Cytosolic superoxide dismutase (SOD1, Cu,Zn-SOD) is a dimeric antioxidant enzyme that is the first line defense against ROS; it converts O_2^- to H_2O_2 in the cytosol of cells. An overview of the structure of this enzyme and is provided below in Figure 1.6. SOD1 is also known as copper, zinc superoxide dismutase because of the copper and zinc metal ions that are associated with the enzyme. Copper deficiency is sufficient to ablate the activity of SOD1 (Estrada-Carrasco et al., 2010; Vonk, Wijmenga, Berger, van de Sluis, & Klomp, 2010). This enzyme is one member of a group of SOD molecules that are mainly characterized by their cellular location: SOD1 is mostly cytoplasmic, although a small amount has been found inside mitochondria, SOD2 is mitochondrial and SOD3 is extracellular (Johnson & Giulivi, 2005). Like the other SOD molecules, SOD1 is initially present as an apo-enzyme prior to coupling with a copper ion (Johnson & Giulivi, 2005; Vonk et al., 2010). Generally, the transcription of SOD enzymes increases with cell stress. The importance of this enzyme is exemplified by the plethora of disorders that are associated with mutations in this enzyme, including amyotrophic lateral sclerosis (ALS, or Lou Gehrig's Disease; Abe et al., 2011; Johnson & Giulivi, 2005).

The chemical reaction involved in the dismutation of superoxide has two steps. First, the oxidized form of the enzyme, SOD1-Cu²⁺, binds to superoxide, acquires a proton, and releases molecular oxygen. Next, the reduced enzyme, SOD1-Cu⁺, binds to a proton and another superoxide anion, releasing H₂O₂ and returning to its original state (Johnson & Giulivi, 2005). It is important to note that although this enzyme is an integral part of the defense against oxidative stress, SOD1 is responsible for breaking down a detrimental antioxidant into another antioxidant. Thus, to avoid excess oxidative stress, it is imperative that the activity of SOD1 is coupled with H₂O₂-consuming molecules, such as catalase and glutathione peroxidase. An overview of the activity of SOD1 is provided in Figure 1.7.

1.9 SOD1 in Prostate Cancer

As previously mentioned, antioxidant inhibitors have been tested for the treatment of cancer. The rationale is that reducing the antioxidants will increase ROS levels and cause cell death. SOD1 inhibitors such as the second generation tetrathiomolybdate (ATN-224) have been used to demonstrate that inhibiting SOD1 can decrease ERK1/2 activation, angiogenesis, and cell proliferation (Juarez et al., 2006). This drug has also been used in a clinical trial of men with biochemically-recurrent prostate cancer. Results demonstrated that treatment with ATN-224 may decrease PSA-progression in these patients (Lin et al., 2011). Interestingly, as SOD1 inhibitors TM and 2-methoxyoestrodial have been used in the treatment of various cancers, Marikovsky et al., 2002 established a transgenic mouse that overexpresses human SOD to demonstrate that angiogenesis was higher in this mouse in comparison with control mice (Marikovsky, Nevo, Vadai, & Harris-Cerruti, 2002).

Although there have not been conclusive studies into the role of SOD1 in prostate cancer, Bostwick et al., 2000 show that there is trend towards decreased levels of SOD1 and SOD2 activity in prostate cancer specimens in comparison with benign controls (Bostwick et al., 2000). In contrast, Estrada-Carrasco et al., 2010 found significantly increased levels of SOD1 in prostate cancer specimens in comparison with benign prostatic hyperplasia (Estrada-Carrasco et al., 2010). Regardless of the expression levels of SOD in prostate cancer, the relative success of SOD1 inhibitors in the treatment of prostate cancer suggests that this enzyme plays a role in disease progression.

1.10 The Project

A yeast-two hybrid screen that was performed in the Dupré lab found an interaction between CXCR4 and SOD1. This preliminary finding was then confirmed by a co-immunoprecipitation (Co-IP) of these two proteins following their transfection into human embryonic kidney cells (HEK293A). Since both CXCR4 and SOD1 are known to play a role individually in the metastatic transition, the goal of this project is to further characterize and elucidate the implications of this interaction in prostate cancer cells.

1.11 The Hypothesis

We hypothesize that the protein-protein interaction between CXCR4 and SOD1 will have an effect on CXCR4 signal transduction. We know that CXCR4 is implicated in metastasis, so we believe that modulation of signaling through this GPCR will have an effect in the pathways activated in the metastatic transition. Due to the ability of SOD1 to scavenge ROS, we hypothesize that the interaction between CXCR4 and SOD1 may act as a sensor of

cellular environment. An overview of our hypothesis is displayed in a schematic in Figure 1.8. We believe that SOD1 physically interacts with CXCR4 in PC3 prostate cancer cells. We hypothesize that in normal conditions with low levels of ROS present in the cell, depicted in Figure 1.8A, SOD1 interacts with CXCR4 at a basal level. This would allow CXCR4 to signal at a normal level. We believe that following stimulation of CXCR4, this interaction will increase. However, with acute exposure to hypoxia, like the conditions that a cell may encounter within a tumor, depicted in Figure 1.8B, SOD1 will interact in the cytoplasm with the potentially detrimental superoxide that we hypothesize to have accumulated due to oxidative stress. This means that less SOD1 would be available to interact with CXCR4 at the membrane. We hypothesize that when SOD1 is not interacting with this GPCR, CXCR4-mediated signal transduction will be differentially modulated. This could result in amplification of CXCR4-mediated signaling, possibly increasing cell migration, proliferation and survival - all processes known to be integral to the metastatic transition.

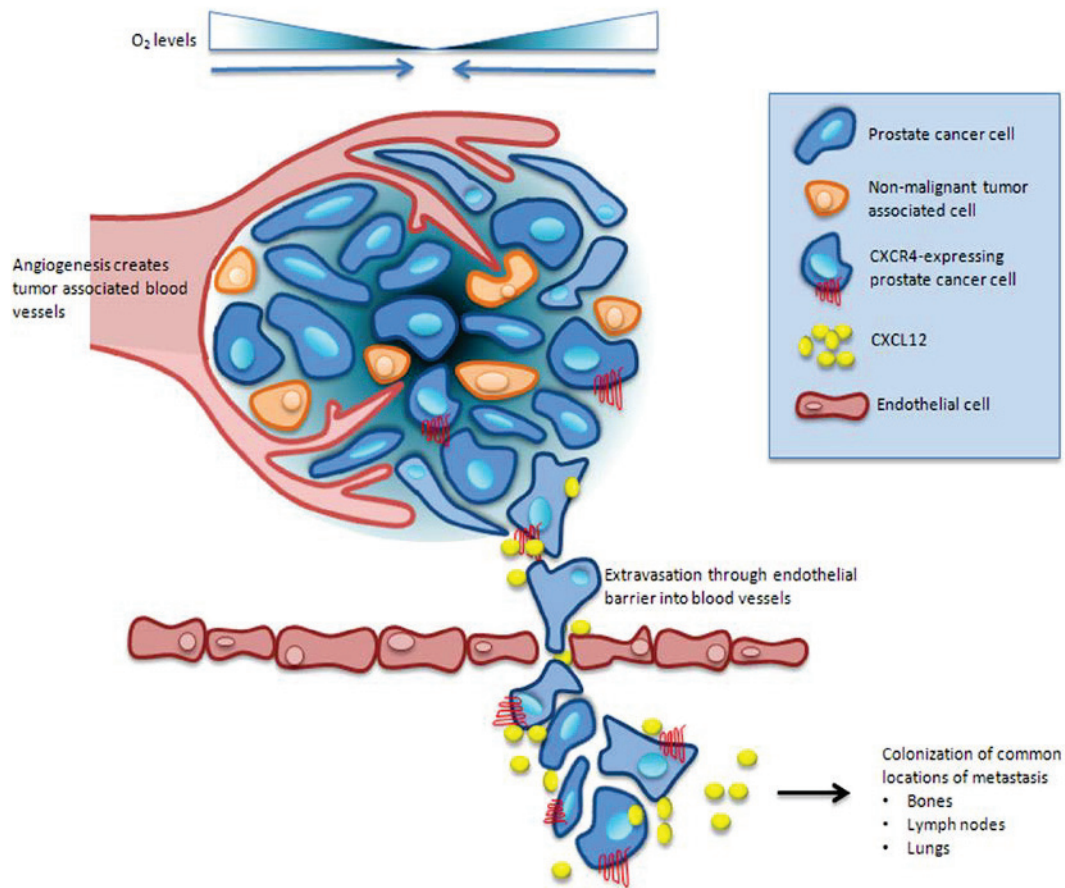
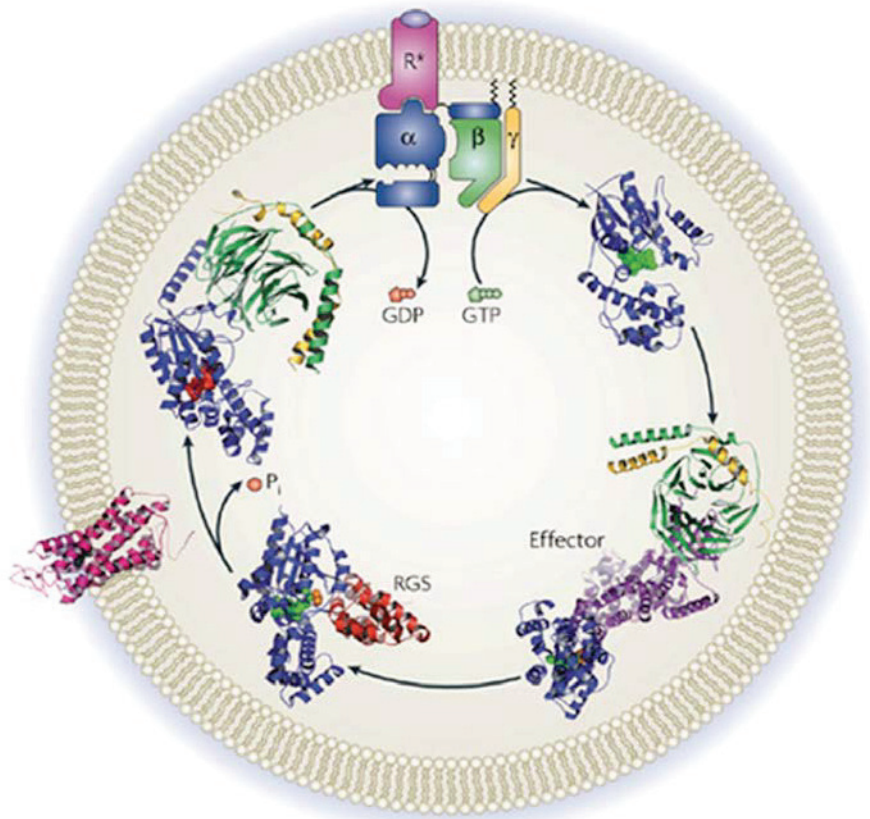


Figure 1.1 Schematic of the Metastatic Transition.

Primary prostate cancer tumor with associated blood vessels. A gradient of oxygen concentration exists within the tumor, from normal oxygenation at the exterior to an anoxic center. This is represented by the O_2 level gradient schematic at the top of the diagram. The tumor consists of cancer cells and non-cancerous tumor associated cells such as fibroblasts and white blood cells. Cancer cells expressing the chemokine GPCR CXCR4 can migrate through endothelial cell layers and travel through the blood along a gradient of CXCL12. CXCR4-expressing prostate cancer cells then colonize a new location, commonly in the bones, lymph nodes or lungs, forming a secondary tumor. A legend describing the cartoon schematic of the cell types can be found in the top right of the figure.



Nature Reviews | Molecular Cell Biology

Figure 1.2 G Protein Activation Cycle.

The general activation and return to resting state of a GPCR-associated G protein. While this image shows the structure of bovine rhodopsin and the G protein heterotrimer $G\alpha_{t_i}\beta_1\gamma_1$, this general process can be generalized across receptors. The GPCR is coloured magenta, the ligand is violet, GDP is orange, GTP is light green, effector is purple, the regulators of G protein signaling (RGS) are dark red, and the G protein subunits α , β , γ are blue, green and yellow, respectively. Upon ligand binding, a conformational change that occurs within the receptor causes release of the GDP from the G protein. This activated receptor (R^*) then binds with high affinity to the G protein, allowing GTP to bind. Following this, both $G\alpha$ -GTP and $G\beta\gamma$ functionally dissociate from the receptor and couple with their effector proteins. RGS can accelerate and catalyze this signal termination process, where GTP is hydrolyzed into GDP. This cycle can then continue again following activation by another ligand, or through constitutive receptor activation. Figure reproduced, with permission (Appendix ii), from Oldham, W., and Hamm, H. (2008). Heterotrimeric G protein activation by G-protein-coupled receptors. *Nat Rev Mol Cell Biol.* 9(1):60-71.

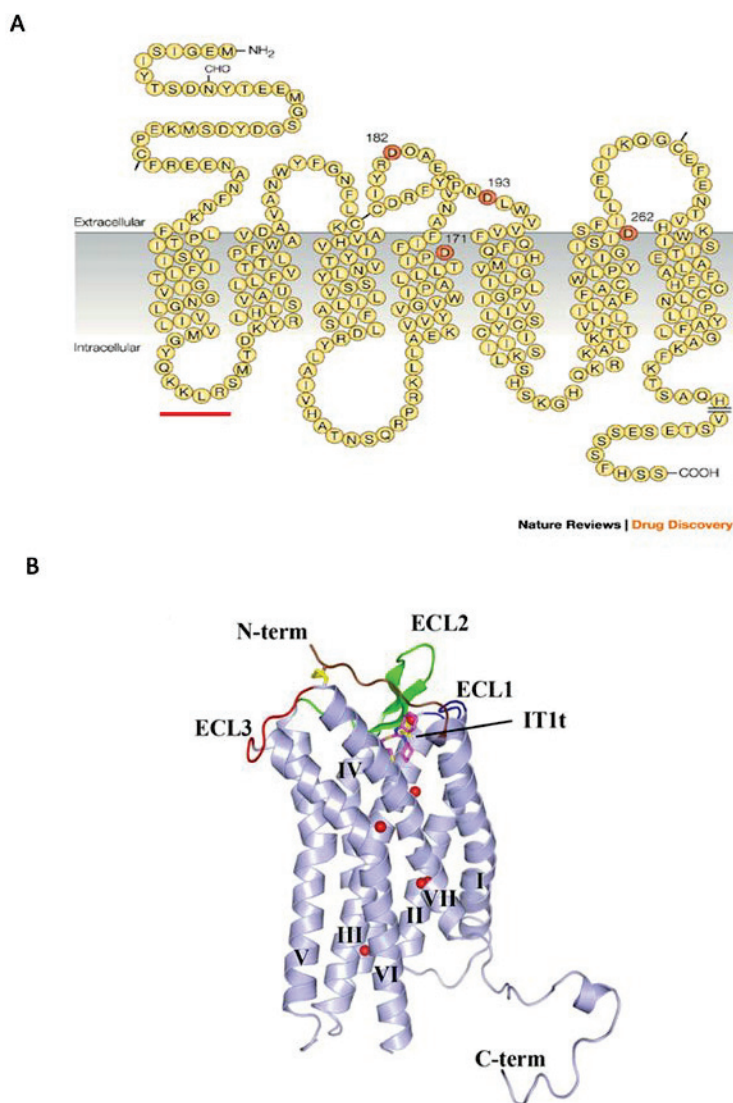


Figure 1.3 CXCR4 Structure.

A. Snake plot depicting amino acid sequence along with membrane orientation of the CXCR4 receptor. The aspartic acid residues highlighted in red, at position 171, 182, 193 and 262 are critical for the interaction between this GPCR and its small molecule inhibitor, AMD3100. The KKLRL motif in loop 1, highlighted with the red underline, is hypothesized to play a role in the novel interaction we discovered between CXCR4 and SOD1. Figure reproduced, with permission (Appendix iv), from De Clercq, E. (2008). The bicyclam AMD3100 story. *Nat Rev Drug Discov.* 2(7):581-587. B. Crystal structure of CXCR4 in complex with a small drug-like isothiourea derivative (IT1t). The receptor is blue, IT1t drug is magenta, N-terminus is brown, ECL1 is blue, ECL2 is green, ECL3 is red, and disulfide bonds are yellow. Figure reproduced, with permission (Appendix v), from Wu, B., Chien, E., Mol, C., et al. (2011). Structures of the CXCR4 chemokine receptor in complex with small molecule and cyclic peptide antagonists. *Science.* 330(6007):1066-1071.

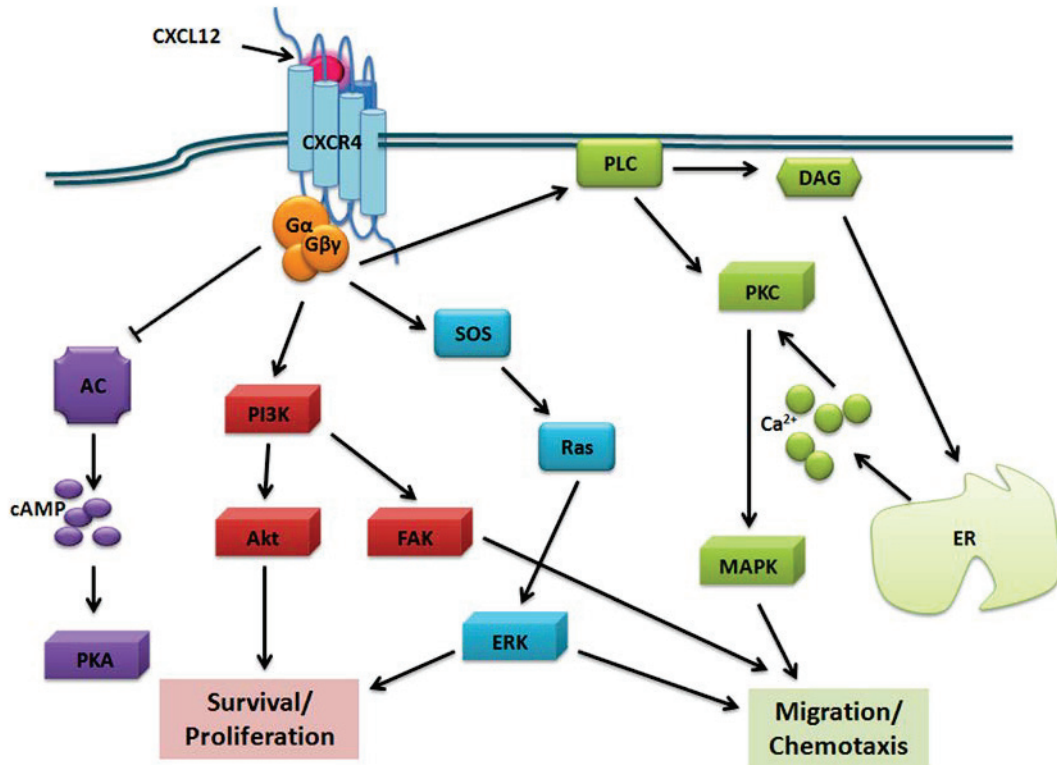


Figure 1.4 Overview of CXCR4 Signal Transduction.

Several of the intracellular signaling cascades activated by CXCR4 are highlighted in this figure. Following stimulation of CXCR4 by CXCL12, the G protein activates multiple effector proteins. Final results of CXCR4 activation can include cell migration, chemotaxis, survival and proliferation.

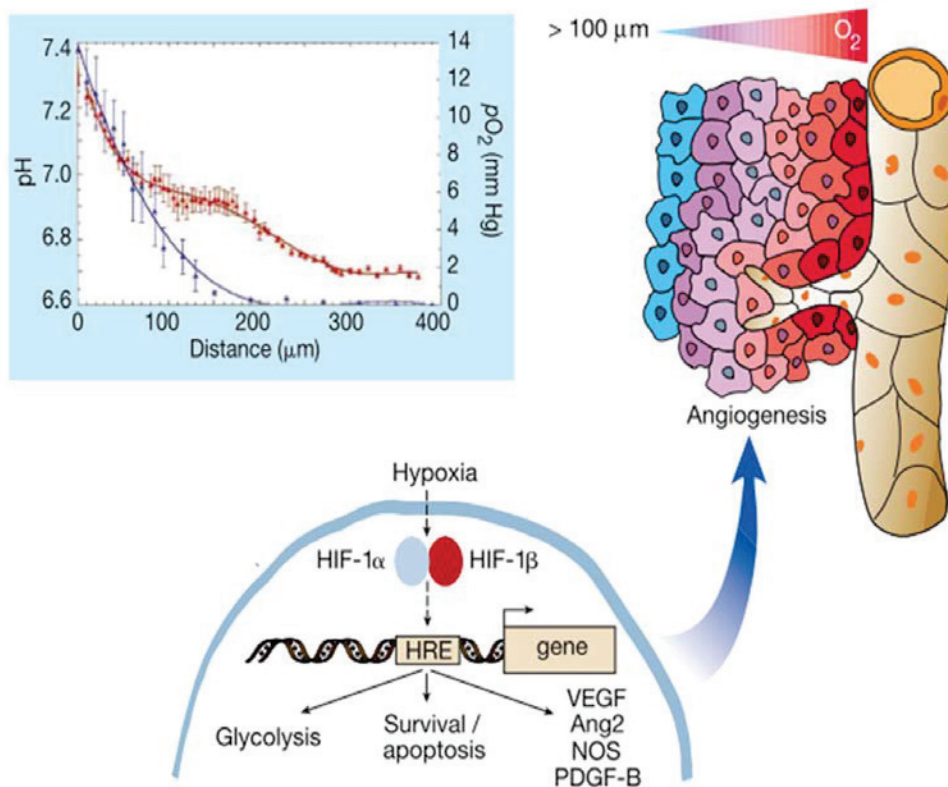


Figure 1.5 The Effects of the Hypoxic Microenvironment in a Tumor.

The top left image is a graph that displays the relationship between tissue pH (red symbols) and degree of hypoxia (blue symbols; measured as mm Hg, or pressure O_2) and distance of the area from a nearby vessel. As is evident in this figure, the further the tissue from a blood vessel, the more acidic and lower oxygen pressure. The top right image depicts the gradient of O_2 found within a tumor, with the gradient going from red to blue showing progressive hypoxia. This also shows the beginning of angiogenesis, the process where new blood vessels form to deliver oxygen to cancer cells. The image on the bottom shows a magnified image of a representative hypoxic cell and the signal transduction that occurs within this cell. Decreased levels of O_2 are associated with increased levels of stabilized hypoxia-inducible factors (HIF), which will bind to hypoxia responsive-elements (HRE) in the nucleus and increase transcription of genes associated with glycolysis, survival and angiogenesis. Image reproduced, with permission (Appendix iv), from Carmeliet, P. and Rakesh, K. (2000). Angiogenesis in cancer and other diseases. *Nature*. 407:249-257.

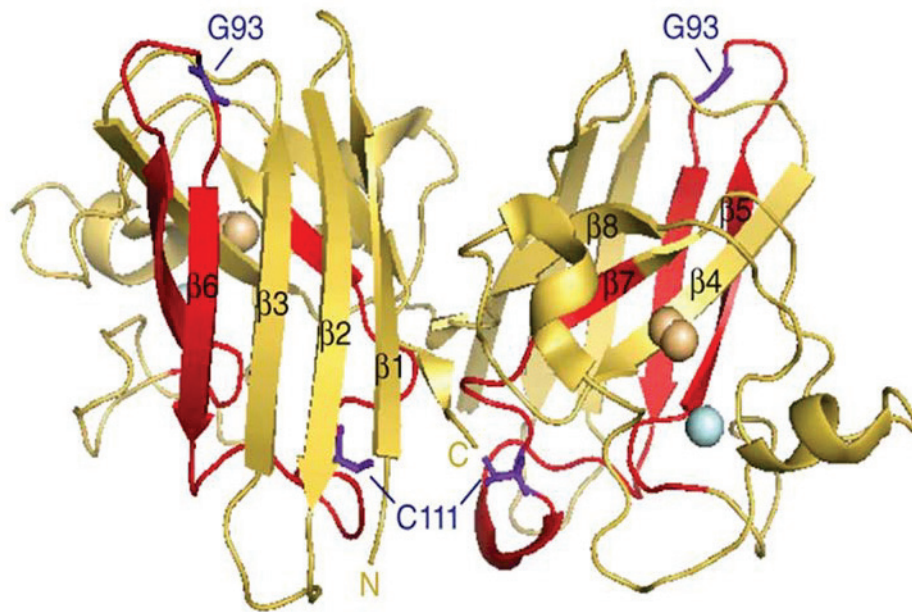


Figure 1.6 The Structure of SOD1.

X-ray crystallographic representation of the structure of wild-type (WT) SOD1, a dimeric protein. The G93 amino acid that is commonly mutated in SOD1, resulting in familial amyotrophic lateral sclerosis (FALS), is highlighted in purple. The zinc and copper atoms are depicted in cyan and orange, respectively. Amino acid Cys 111 is also highlighted in purple, showing the site of enzyme oxidation following addition of hydrogen peroxide (H_2O_2) to the system. Image reproduced, with permission (Appendix vii), from Bosco, D., Morfini, G., Murat Karabacak, N., Song, Y., Gros-Louis, F., Pasinelli, P., Goolsby, H., Fontaine, B., Lemay, N., McKenna-Yasek, D., Frosch, M., Agar, J., Julien, J., Brady, S. and Brown, R. (2010). *Wild-type and mutant SOD1 share an aberrant conformation and a common pathogenic pathway in ALS*. *Nat Neurosci.* 13(11):1396-1403.

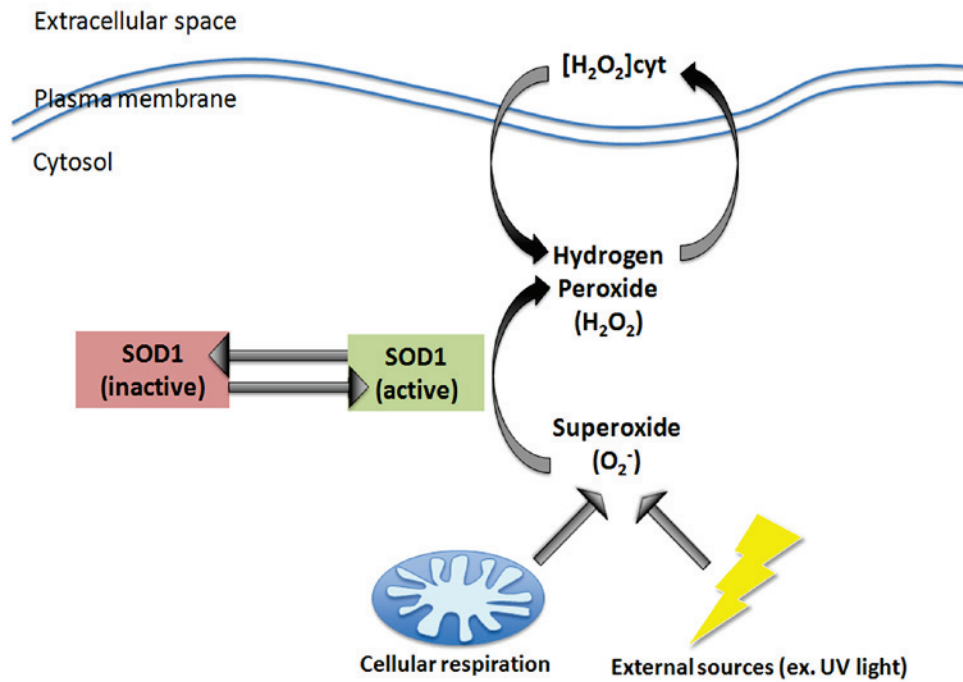


Figure 1.7 Overview of SOD1 Activity.

Normal cellular respiration and external sources including, but not limited to, UV light and pathogen invasion can increase intracellular levels of superoxide (O_2^-). SOD1 is found within the cytosol of the cell. The active enzyme dismutates the highly reactive O_2^- into the less detrimental hydrogen peroxide (H_2O_2). H_2O_2 can move into and out of the cell based on the concentration gradient that exists.

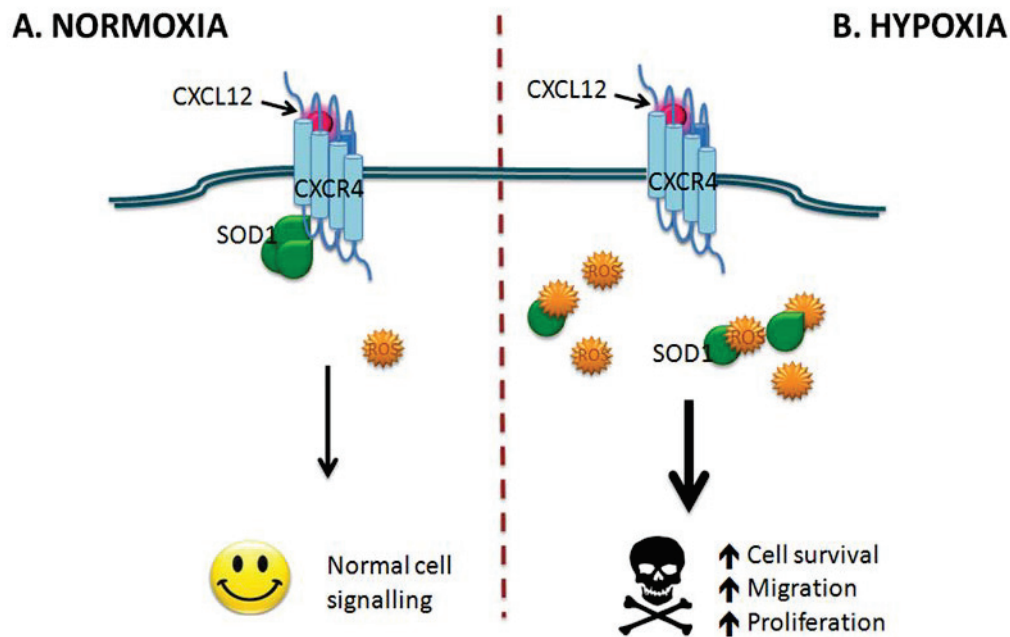


Figure 1.8 Working Hypothesis.

The schematic of our hypothesis is in two parts, with the cartoon cell in normoxic conditions on in Figure 1.8A and hypoxic conditions in Figure 1.8A. A. CXCL12 (SDF1 α) will bind to CXCR4 and initiate signaling. We believe that SOD1 is bound at intracellular loop 1 (loop 1) of CXCR4 at a basal level, but this interaction will increase following stimulation of CXCR4 with CXCL12. In normal conditions, the interaction between CXCR4 and SOD1 results in normal levels of CXCR4 signaling and healthy cells. B. Due to the accumulation of detrimental reactive oxygen species (ROS) that exist within the cell due to the hypoxic conditions, we believe that SOD1 will dissociate from CXCR4 to combat the ROS. Even following stimulation of CXCR4 with CXCL12, we believe that there will be decreased levels of interaction between SOD1 and CXCR4. We hypothesize that the decreased interaction between these two molecules could lead to modulation of CXCR4 signal transduction, possibly increasing cell survival, migration and proliferation, all processes known to be integral to the transition of the metastatic phenotype.

CHAPTER 2: MATERIALS AND METHODS

2.1 Materials

PC3 (CRL-1435) human prostate cancer cells were acquired from American Type Culture Collection (ATCC; Manassas, VA, USA). Heat Inactivated Fetal Bovine Serum (FBS) and Penicillin-Streptomycin (PS) were purchased from Invitrogen (Etobicoke, ON, Can). Complete, EDTA-free Protease Inhibitor Cocktail Tablets (PI) and X-tremeGENE HP DNA Transfection Reagent (X-tremeGENE) were acquired from Roche Applied Science (Laval, QC, Can). Dulbecco's Modified Eagle's Medium High Glucose (DMEM), Protein A-Sepharose, and all other chemicals, unless otherwise noted, were obtained from Sigma-Aldrich (Oakville, ON, Can). Supersignal West Femto Maximum Sensitivity Substrate was from Pierce Biotechnology (Rockford, IL, USA). Anti-SOD1, anti-CXCR4, anti-phospho-ERK, anti-phospho-AKT (ser-473), anti-c-myc, anti-HA primary antibodies and all horseradish peroxidase-conjugated secondary antibodies in addition to the Annexin V Apoptosis Assay Kit were purchased from Santa Cruz Biotechnologies, Inc. (Santa Cruz, CA, USA). Polyclonal anti-ERK1/2 antibody was acquired from Cell Signaling Technology (Beverly, MA, USA). BioTraceTM nitrocellulose transfer membrane was from Pall Corporation (Port Washington, NY, USA) and Laemmli sample buffer was from BioRad (Mississauga, ON, Can). Bovine Serum Albumin (BSA) was purchased from BioBasic Inc. (Markham, ON, Can). Cell culture dishes and other cell plates were purchased from VWR International (Mississauga, ON, Can). SOD1 siRNA (short-interfering ribonucleic acid), β -Actin primary antibody and CXCL12 (SDF1 α) were purchased from Abcam (Toronto, ON,

Can). Pertussis toxin (PTX) was purchased from List Biological Laboratories, Inc. (Campbell, CA, USA).

2.2 Molecular Constructs

The pcDNA3.1 HA-CXCR4 receptor was purchased from Missouri University of Science and Technology cDNA resource center (Rolla, MO, USA). pCMV6-myc-DDK-hSOD1 WT was purchased from Origene Technologies Inc. (Rockville, MD, USA).

CXCR4-YFP was a gift from Dr. Nikolaus Heveker, from Hôpital Ste-Justine (Montréal, QC, Canada). The $G\alpha_i$ and $G\alpha_q$ constructs were a gift from Dr. Michel Bouvier, from Université de Montréal (Montréal, QC, Canada).

2.3 Cell Culture

PC3 cells were maintained in 10 cm cell culture dishes a sterile culture chamber with 5% CO₂ at 37°C in Dulbecco's Modified Eagle's Medium (DMEM). PC3 cells were supplemented with 10% heat-inactivated FBS and 2% PS. Cells were routinely subcultured so that the cells never surpassed 90% confluence. For experiments, cells were plated in 6-well plates 24 hr prior to treatment.

For hypoxic cell treatment, the cells were place in a hypoxia chamber containing 0.2% O₂ at 37°C for variable lengths of time. The chamber was purged prior to usage to ensure that the chamber contained the correct oxygen concentrations.

2.4 Transient Transfection

The following quantities will be expressed in amount per well of a 6-well plate. 1 µg of each required DNA construct per well was mixed with 100 µl of FBS-free culture media and 3 µl of XtremeGENE. This mixture was incubated for 15 min before dispersing, drop wise, on cells that were 70-80% confluent. 24 hr following transfection, the media was replaced with fresh FBS-free culture media.

SOD1 Small-Interfering RNA (siRNA) was resuspended in 330 µl RNase-free water to make a 10 µM stock solution in a 10 µM Tris-HCl, pH 8.0, 20 mM NaCl, 1 mM EDTA buffered solution. siRNA transfection was accomplished using the same method as DNA transfection, except with 5 µl stock solution per well, creating a final concentration of 50 nM of the siRNA duplex resuspension in DMEM. Also, scrambled siRNA control and subsequent western blotting was done to ensure that the siRNA-mediated knockdown was specific to SOD1.

2.5 Protein Collection

Following all cell treatments, media was aspirated from cells and cells were collected in 1 ml ice-cold phospho-buffered saline (PBS). Cells were centrifuged at 16,000 g for 30 sec and supernatant was aspirated. The pellet was then lysed in 3 µl DNase, 100 µl radioimmunoprecipitation assay (RIPA) buffer (50 mM Tris (pH 7.4), 100 mM MgCl₂, 150 mM NaCl, 0.5% sodium deoxycholate, 1% Nonidet P-40, 0.1% SDS, Roche COMPLETE protease inhibitor tablet), 10 µl preclear beads and 2 µl 5 M EDTA. Samples were nutated for 30 min at 4°C. These samples were then centrifuged at 16,000 g for 10 min and the supernatant was collected.

2.6 Cell Counting and Bradford Assays

Prior to cell counting, cells were collected in 1 ml sterile PBS. 10 μ l of suspended cells were ejected onto a hemocytometer under a coverslip. 4 quadrants were counted and averaged to determine the number of cells per quadrant. Cells per ml were calculated as $10^4 \times$ average cells/quadrant.

Protein standard curves were constructed with BSA at concentrations varying from 0.01 to 10 μ g/ml. 1 μ l of each protein sample was loaded into a well of a 96-well plate. 119 μ l Bradford sample buffer was added to each well, pipetted up and down to mix, and incubated at room temperature for 5 min prior to reading absorbance on a plate reader at 595 nm.

2.7 Polyacrylamide Gel Electrophoresis and Western Blotting

Following cell treatment and protein collection, amount of protein to load was calculated using lysate Bradford values. Samples were nutated with 710 mM β -mercaptoethanol-Laemmli sample buffer at room temperature. Samples were then incubated in a 65°C dry bath for 5 min prior to being resolved using Sodium Dodecyl Sulfate Polyacrylamide Gel Electrophoresis (SDS-PAGE). Gels were then transferred to a nitrocellulose membrane. These membranes were then blocked with 5% milk powder in Tris-buffered saline (TBS) and nutated overnight at 4°C in milk containing a dilution of primary antibody ranging from 1:200-1:2000, depending on the experiment. The next day, membranes were washed with TBS containing 0.1% Tween-20 (TBST) and incubated with HRP-conjugated (horseradish peroxidase) secondary antibodies for 1 hr in TBS milk. Following another wash with TBST, these membranes were visualized with Western

Lightning Plus-ECL Chemiluminescence Substrate. ImageJ 4.3 software (NIH) was used to calculate band densities of the immunoblots. ERK1/2 bands were measured together, as close proximity of the bands complicated separation of each band for analysis.

2.8 Co-Immunoprecipitations

Following protein collection, samples were nutated for 30 min at 4°C with the necessary antibody to precipitate out the protein of choice. Following this, 50 µl of pre-washed protein-A sepharose beads were added and samples were nutated at 4°C overnight. The next day, samples were rinsed 3 times with 1 ml RIPA buffer. The RIPA was then aspirated and remaining beads were nutated for 20 min at room temperature in β-mercaptoethanol-Laemmli sample buffer prior to resolving using SDS-PAGE, the probed and visualized as above, for western blotting. The band density was representative of the amount of immunoblotted protein that was interacting with the immunoprecipitated protein. Part of the cell lysate was also treated as a western blot without immunoprecipitation, to use as a control of input protein levels.

2.9 Annexin V Staining

Annexin V binds with high affinity to exposed phosphatidylserine phospholipids on cell membranes. Early in apoptosis, this phospholipid switches from the inner to the outer plasma membrane of the cell. Therefore, Annexin V-FITC binds to and fluorescently labels apoptotic cells. For this assay, PC3 cells were transfected with CXCR4 and either the pcDNA control, SOD1 cDNA or SOD1 siRNA. Twenty-four hrs later, these cells were treated with etoposide (50 ng/ml) for 24 hrs. Etoposide, a common chemotherapeutic agent,

was used in this assay because it is a topoisomerase inhibitor known to cause apoptosis in mammalian cells. Six hrs following etoposide treatment, cells were either stimulated with 100 ng/ml CXCL12, or remained unstimulated. Incubations took place in either normal cell culture conditions or in hypoxic conditions beginning with stimulation. Cells were harvested and washed in PBS, then resuspended in 100 μ l Annexin V Assay Buffer per sample. The assay was conducted according to the manufacturer's instructions. Cells were nutated in the dark with propidium iodide (PI) and Annexin V-FITC conjugated stain for 20 min. Cells were then examined in the fluorescent microscope and at least 5 fields of view were recorded using an Olympus IX81 microscope equipped with a Photometrics coolSNAP HQ2 camera and an excite series 120Q light source. Annexin V stain was excited at 488 nm and images were captured at 525 nm. PI was excited at 535 nm. Rates of apoptosis were determined by dividing the number of cells that stained positive for Annexin V divided by the total number of cells. For reference, a sample image of cells and a schematic representation of staining are provided in Figure 2.1A and 2.1B, respectively.

2.10 Transwell Migration Assays

PC3 cells were transfected with CXCR4 HA and either the pcDNA control, SOD1 cDNA or SOD1 siRNA in 6 well plates. Twenty-four hrs post-transfection, the growth media was aspirated and replaced with SFM (serum-free media) to starve the cells. Forty-eight hrs post transfection, the cells were collected, rinsed with PBS and counted. Five hundred thousand cells per condition were resuspended in SFM and plated into the top portion of a transwell migration plate that contains a polycarbonate membrane, pore size 5.0 μ m (Costar, Corning, NY). In the bottom portion of the well, 600 μ l of either SFM or SFM

containing 100 ng/ml of CXCL12 was added. Cells were incubated for 24 hrs in normal culture conditions. For quantification, the membranes were rinsed with cold PBS and then fixed in 100% ice cold methanol for 15 min at room temperature. These fixed membranes were then stained with 0.5% crystal violet stain for 5 min to allow visualization of the cells. Non-migrated cells were then removed from the upper side of the membrane with a cotton bud. Membranes were then rinsed in dH₂O, dried, and then mounted on a slide. At least 3 areas of the membrane were viewed under 10X objective of an Olympus IX81 equipped with a photometrics coolSNAP HQ2 camera using MetaMorph software. The number of cells for each field of view were counted. Net migration was determined by comparing the number of cells that migrated with CXCL12 to the number of cell that migrated in the control conditions. For hypoxic migration experiments, the same protocol was followed, except cells were maintained in the hypoxia chamber following ligand exposure.

PTX was resuspended in 500 µl dH₂O, creating a stock solution of 100 µg/ ml PTX in a buffer containing 0.01 M sodium phosphate and 0.05 M sodium chloride, pH 7.0. PTX treatment included adding stock solution to each well, such that the final concentration was 0.1 µg/ml, treated for the full 24 hr duration of the experiment.

An overview of this experimental design is displayed in Figure 2.2, where an example of a well without CXCL12 is in Figure 2.2A and a well with it is in Figure 2.2B.

2.11 Bioluminescence Resonance Energy Transfer (BRET) Assays

Bioluminescence Resonance Energy Transfer (BRET) was used in order to determine the levels of interaction between CXCR4 and the G protein. PC3 cells were transfected with CXCR4 tagged with yellow fluorescent protein (CXCR4-YFP) and either Gα_i tagged with

Renilla luciferase ($G\alpha_i$ -Rluc II or $G\alpha_q$ -Rluc II) in addition to the SOD1 expression modulation, as described above. Twenty-four hrs post-transfection, the growth media was replaced with SFM. Forty-eight hrs post-transfection, the cells were either stimulated with 100 ng/ml CXCL12 for 15 min in normal culture conditions, or remained unstimulated. These cells were then collected, rinsed with PBS and resuspended in 100 μ l PBS/sample. When in the presence of oxygen, RlucII can catalyze the breakdown of coelenterazine, which releases energy at the wavelength 480 nm. When the molecule that is tagged with RlucII, and the energy emission is in close enough proximity (50-100 Å or 5-10 nm) to a suitable yellow fluorescent protein (YFP) variant, the YFP will be excited and will emit light at 527 nm. Therefore, a ratio of emissions measured as donor emission: acceptor emission (RlucII emission: YFP emission) provides information of the relative proximity of the molecules tagged with these proteins. The data is presented as the BRET¹ ratio, which is a direct measure of the ratio of emissions between the donor and acceptor. An overview of this technique is found in Figure 2.3. Figure 2.3A is the state of the proteins prior to coelenterazine or ligand addition. Figure 2.3B is when the ligand does not bring the proteins of interest in close enough proximity to emit a signal. Figure 2.3C represents the scenario when ligand stimulates a movement of the proteins towards each other, to be in close enough proximity to emit a BRET signal.

2.12 Statistical Analysis

All analysis was completed using GraphPrism software. All error bars are representative of mean +/-SEM (Standard error). Two-tailed unpaired Student's T-tests were performed for analysis of co-immunoprecipitation data. Annexin V raw apoptosis and

necrosis experimental data, the p-ERK and p-AKT western blot data, the BRET data and the migration data was analyzed with a two-way ANOVA and a Bonferroni post test. P values are reported as follows: * $p < 0.05$, ** $p < 0.01$, *** $p < 0.001$.

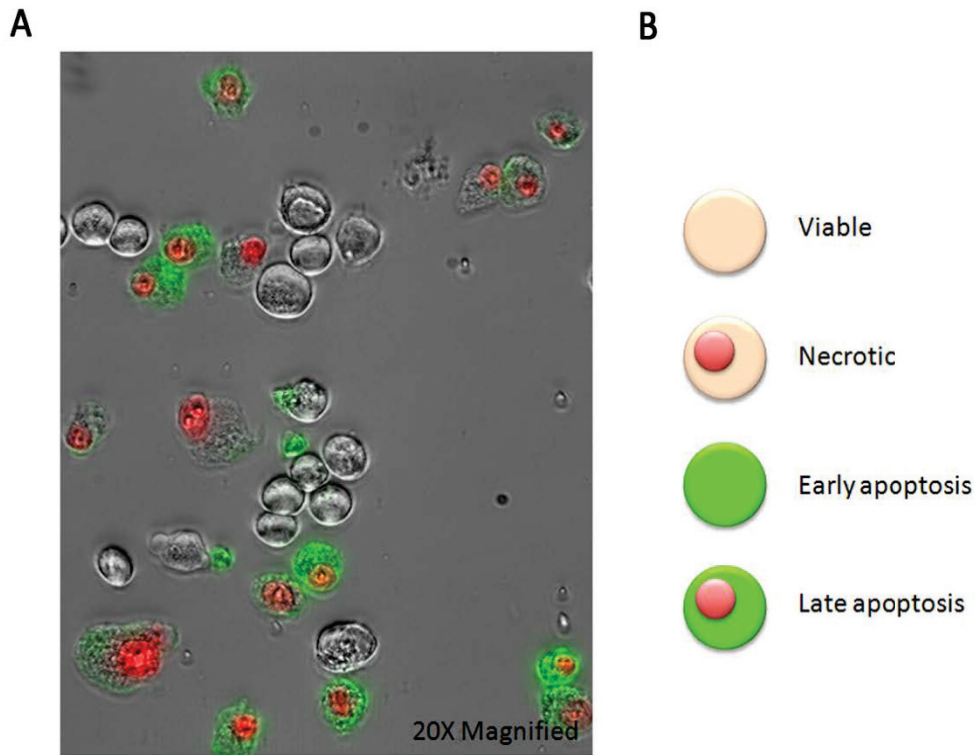


Figure 2.1 Annexin V Staining Schematic.

A. Representative micrograph of Annexin V staining experiment. Image is an overlay of bright field (BF), Annexin V staining and propidium iodide (PI) staining. Annexin V stain was excited at 488 nm and images were captured at 525 nm PI was excited at 535 nm. 20X magnification. B. Schematic of apoptotic status. From top to bottom: unstained cells are viable, cells with red nuclei are PI positive and are necrotic, cells that are stained green are Annexin V positive and apoptotic, cells that are stained green with red nuclei are PI and Annexin V positive and are in the late stages of apoptosis.

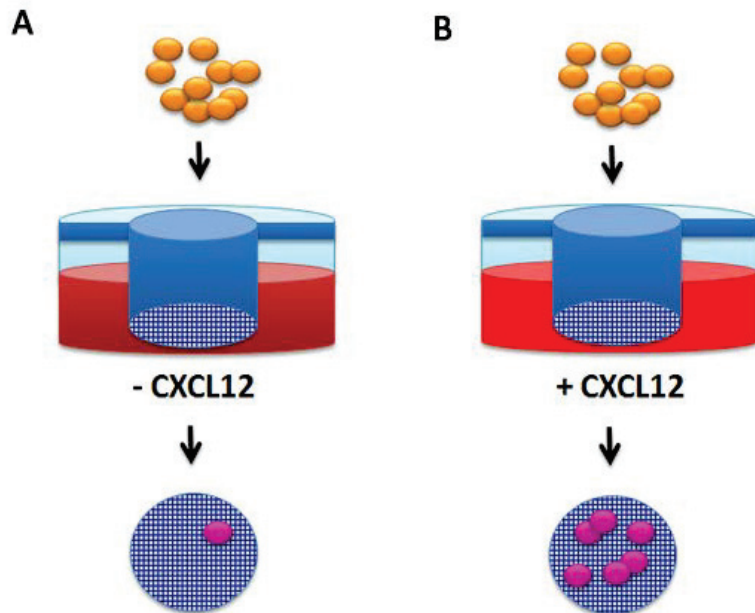


Figure 2.2 Schematic of Transwell Migration Assays.

A. PC3 cells were transfected with the pcDNA vector control, SOD1 WT cDNA or SOD1 siRNA. 500,000 cells were counted per well. 600 μ l of serum-free media (SFM) was added to the bottom of the well. The counted, transfected cells were added to the top of the transwell membrane insert. The cells were then incubated in either normal or hypoxic culture conditions for 24 hr. The inserts were then fixed with methanol, rinsed and stained with crystal violet to allow for easy visualization of the cells. Cells were then counted at 10X magnification with a light microscope. Net migration was calculated as number of migrated cells in the wells without chemoattractant subtracted from number of cells migrated in the wells with CXCL12. B. Same experiment as seen in A., except with CXCL12 added to the bottom of the well to promote chemotaxis.

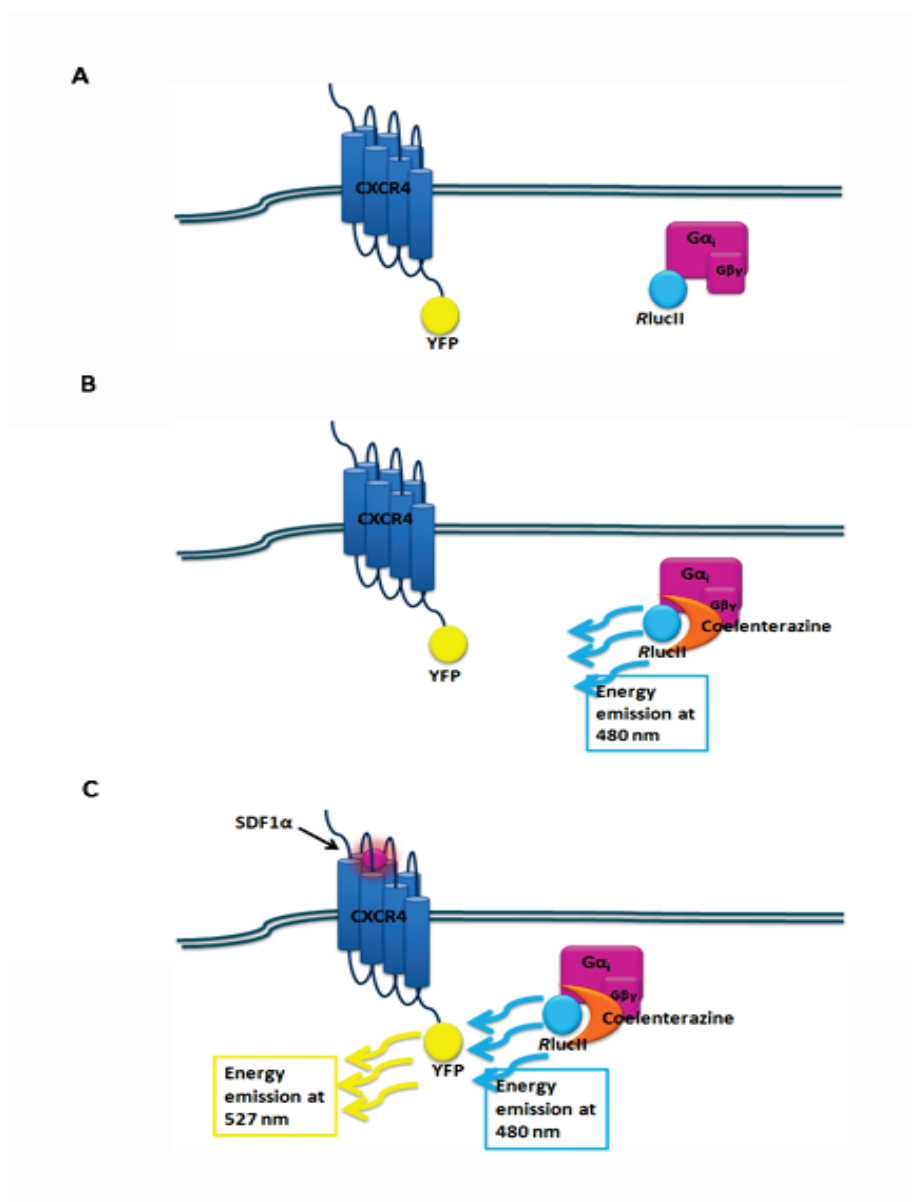


Figure 2.3 Bioluminescence Resonance Energy Transfer (BRET) Technique Schematic.

A. Schematic showing the CXCR4 receptor in the plasma membrane (PM) tagged with the yellow fluorescent protein (YFP) and the $G\alpha$ protein, here $G\alpha_i$, to *Renilla* luciferase (*RlucII*). B. This schematic shows the same proteins tagged as in A., but following the addition of coelenterazine. *RlucII* cleaves its substrate, coelenterazine, emitting energy at 480 nm. In this case, the *RlucII* and YFP-tagged proteins are not in close enough proximity (further than 50-100 Å or 5-10 nm apart) to allow the light emitted by *RlucII* to activate YFP. C. In this schematic, the ligand CXCL12 has been added. Addition of the ligand results in an increase in the proximity between the *RlucII* and YFP-tagged proteins; this results in the energy emitted by *RlucII* exciting the YFP molecule, allowing for energy emission at 527 nm. The ratio of energy emitted by the donor (*RlucII*): energy emitted by the acceptor (YFP) is measured as the BRET ratio.

CHAPTER 3: RESULTS

3.1 Expression of Endogenous and Transfected CXCR4 and SOD1 in PC3 cells

In order to evaluate the effects of the protein-protein interaction between CXCR4 and SOD1 in a prostate cancer cell line, we first needed to verify the presence of these molecules in prostate cancer cells. We chose to use the PC3 prostate cancer cell line for several reasons. Firstly, PC3 cells express endogenous levels of CXCR4 (Singh, Singh, Stiles, Grizzle, & Lillard, 2004). Secondly, PC3 cells are more metastatic in comparison with other prostate cancer cells lines such as LNCaP and DU145 cells as measured in an *in vitro* matrigel invasion assay (Muralikrishna et al., 2005). Lastly, PC3 cells are androgen-independent and are derived from bone marrow metastases, two features that are characteristic of the advanced metastatic stage of disease that we are looking to investigate (Sobel & Sadar, 2005).

In order to determine endogenous levels of CXCR4 and SOD1, PC3 cells were maintained in either normal or hypoxic cell culture conditions, lysed, and immunoblotted for the presence of both SOD1 and CXCR4. Results are shown in Figure 3.1. The results in Figure 3.1A and Figure 3.1B demonstrate that both SOD1 and CXCR4, respectively, are expressed endogenously in PC3 cells in both conditions. The histograms in Figure 3.1A and 3.1B show that that SOD1 levels increase approximately 1.7-fold following 8 hr hypoxic treatment and CXCR4 levels increase approximately 1.7-fold, with a higher degree of variability. To verify that the siRNA-mediated knockdown resulted in lower levels of SOD1 in the cells, we performed a western blot against SOD1 following addition of the siRNA.

Results show that there is approximately a 50% reduction in SOD1 protein following SOD1 siRNA transfection (Appendix viii).

3.2 Interaction of CXCR4 with SOD1 in PC3 cells in Normal and Hypoxic Conditions

Following the original indication obtained with a yeast-two hybrid screen that SOD1 was interacting with CXCR4 and subsequent verification that PC3 cells endogenously expressed these proteins, we wanted to confirm that CXCR4 and SOD1 were interacting in PC3 cells with a Co-IP assay. Briefly, PC3 cells were treated with CXCL12 or remained untreated as specified, lysed, and subjected to immunoprecipitation of CXCR4 and immunoblotting of SOD1. A summary of the results is provided in Figure 3.2, demonstrating that CXCR4 and SOD1 interacted endogenously. This figure also shows that this interaction was affected by CXCR4 stimulation, as 15 min stimulation with CXCL12 increased the interaction levels. The specificity and validity of this experiment was also confirmed with a reduction in the interaction between the two proteins following transfection of PC3 cells with SOD1 siRNA.

Next, we sought to assess our hypothesis that the protein-protein interaction between CXCR4 and SOD1 would be reduced in a hypoxic environment. Figure 3.3A demonstrates that both SOD1 tagged with c-myc and CXCR4 tagged with the human influenza agglutinin (HA) were detected following transient transfection in PC3 cells. As can be seen in the representative blots in Figure 3.3B and the histogram in Figure 3.3C, following transfection of CXCR4-HA and SOD1-c-myc, there is basal level of interaction between these proteins. Following stimulation with 100 ng/ml CXCL12 for 15 min in normoxic conditions, this interaction increased significantly ($p < 0.05$). However, when the cells were maintained in a

hypoxia for 8 hr prior to the experiment, CXCL12 stimulation no longer increased this interaction. Overall, these results suggest that CXCR4 and SOD1 interact at a basal level endogenously in PC3 cells, and that stimulation of CXCR4 in normoxic, but not hypoxic conditions increases this interaction.

3.3 Modulation of CXCR4 Signal Transduction by SOD1 and Hypoxia

Due to the importance of CXCR4-activated signaling pathways in the metastatic transition, we next decided to determine if SOD1 levels affected CXCR4 signal transduction pathways. Although there are many signaling pathways activated by CXCR4, we chose to assess both extracellular signal-regulated kinase 1 and 2 (ERK1/2) activation and AKT activation due to the role that these kinases play in cell survival and migration (Barbero et al., 2003).

3.3.1 Extracellular Signal-Regulated Kinase 1 and 2 (ERK1/2) Activation

Extracellular signal-regulated kinase 1 and 2 (ERK1/2) are heavily implicated in metastasis. ERK1/2 activation can lead to the proliferation, growth and survival of cells. Additionally, mutations in molecules in this pathway causing heightened ERK1/2 activation are associated with many cancer types (Roberts & Der, 2007). Some of the best evidence for the importance of ERK1/2 signaling in cancer is the mounting interest in ERK1/2 as a potential target for cancer therapeutics (Hilger, Scheulen, & Strumberg, 2002; Roberts & Der, 2007). As a corollary, we decided to use western blotting to analyze the levels of total ERK1/2 and the active phosphorylated ERK1/2 (p-ERK1/2) in PC3 cells overexpressing

SOD1 or with SOD1 knocked down using siRNA. The results from these experiments are shown in Figure 3.4, where Figure 3.4A and 3.4C are in normoxic conditions and Figures 3.4B and 3.4D are following 8 hr hypoxic treatment of cells prior to stimulation.

Figure 3.4A shows a representative western blot of p-ERK1/2 and total ERK1/2 in PC3 cell lysate. Figure 3.4C is a histogram that represents the data obtained from our experiments with PC3 cells in normoxic conditions. Data demonstrates that following activation of CXCR4 with CXCL12 treatment for 15 min, levels of p-ERK1/2 increase in cells transfected with SOD1 WT ($p < 0.05$). However, in cells that have been transfected with either the pcDNA vector control or SOD1 siRNA, there is no increase in levels of p-ERK1/2 following stimulation. Figure 3.4B is a representative blot of both p-ERK1/2 and total ERK1/2 levels in PC3 cell lysate following hypoxic pretreatment. Figure 3.4D summarizes the results of this western blot experiment. Results demonstrate that regardless of SOD1 WT transfection or SOD1 knockdown, there is not a significant increase in ERK1/2 phosphorylation. However, there is a trend towards significant increases in ERK1/2 activation regardless of SOD1 expression level. Therefore, according to these results, SOD1 knockdown inhibits ERK1/2 activation in normoxic, but not hypoxic conditions.

3.3.2 AKT (Protein Kinase B) Activation

AKT, or protein kinase B, is a molecule that is implicated in the development and progression of cancer, mainly due to its role in the inhibition of apoptosis (Vivanco & Sawyers, 2002). AKT is activated following activation of phosphoinositide 3-kinase (PI3K) by either RTKs or GPCRs at the cell surface. The active, phosphorylated AKT then goes on to inhibit apoptosis by inhibiting pro-apoptotic proteins such as BAD, or by activating anti-

apoptotic factors such as NF- κ B (Chetram, Don-Salu-Hewage, & Hinton, 2011b; Vivanco & Sawyers, 2002). As a result of the role AKT plays in preventing apoptosis, over activity of AKT caused by a mutation, such as a mutation in PTEN, can increase cancer risk (Chetram et al., 2011b; Vivanco & Sawyers, 2002). Therefore, we decided to measure the effects of SOD1 on AKT activation. We measured the levels of active AKT (p-AKT) in comparison to β -actin levels in PC3 cells following the activation of CXCR4 by 100 ng/ml CXCL12 for 15 min and the results are shown below in Figure 3.5. Figure 3.5A and 3.5C are results from cells maintained in normoxic conditions and Figures 3.5B and 3.5D are following 8 hr hypoxic pre-treatment of cells.

Representative western blots against p-AKT from the experiment conducted on cells maintained in normoxic conditions are shown in Figure 3.5A and a corresponding histogram showing the change in AKT activation is shown in Figure 3.5C. This experiment showed that cells overexpressing the pcDNA control vector or the SOD1 WT had a significant increase in AKT activation following stimulation with CXCL12 ($p < 0.01$ and $p < 0.05$, respectively). However, there was no significant change in AKT activation following stimulation in cells transfected with SOD1 siRNA. Figure 3.5B and 3.5D show a representative western blot and a histogram, respectively, from the same experiment conducted on cells maintained in hypoxic conditions. This experiment demonstrated that there did not seem to be a significant increase in AKT activation following CXCR4 stimulation, regardless of SOD1 expression levels. Taken together, these results suggest that SOD1 knockdown causes an inhibition of CXCR4-mediated AKT activation in normoxic, but not in hypoxic conditions.

3.4 Role of SOD1 and Hypoxia in the Modulation of Apoptosis Levels

Apoptosis is the process through which cells are either genetically or environmentally induced to commit suicide. It is well known that many types of cancer arise and progress due to dysregulation of apoptosis pathways, resulting in aberrant cell growth and survival. Therefore, we chose to measure the effects of SOD1 on CXCR4-mediated cell survival following apoptosis induction.

Results of the apoptosis assays in normoxic conditions are shown in Figure 3.6. Figures 3.6A and B show the levels of necrosis and apoptosis respectively. Figure 3.6A demonstrates that following treatment with etoposide, an apoptosis-inducing topoisomerase inhibitor, there is no difference in levels of necrosis, as measured by percentage of propidium iodide (PI) positive, Annexin V (AV) negative cells. This figure also demonstrates that there is no significant effect of CXCL12 stimulation or SOD1 expression level on necrosis levels. Figure 3.6B demonstrates that apoptosis levels increase significantly following etoposide treatment, as was expected ($p < 0.05$). Also, this figure shows that pcDNA transfected cells demonstrate a reduction in apoptosis following 18 hr stimulation with CXCL12, measured as percentage of AV positive stained cells ($p < 0.05$). This reduction in apoptosis following CXCL12 treatment was not seen in cells transfected with SOD1 WT or SOD1 siRNA following CXCL12 stimulation, although a trend towards decreased apoptosis is observed for SOD1 WT. Overall, these results suggest that knockdown of SOD1 with siRNA seems to ablate the reduction in apoptosis seen following stimulation seen in the pcDNA control cells, supporting the notion of a protective effect of SOD1 in the cell following CXCL12 stimulation.

We next repeated the same experiment in hypoxic conditions and the results are shown in Figure 3.7. Figure 3.7A demonstrates that none of the treatments caused significantly different levels of necrosis. Figure 3.7B shows the levels of apoptosis, measured as percentage AV staining. First, hypoxic conditions increase the overall basal apoptosis levels, without etoposide treatment, to approximately 20% of all cells. Results demonstrate that levels of apoptosis decrease following stimulation of pcDNA vector control-transfected cells pre-treated with etoposide ($p < 0.05$). However, there is no significant change in apoptosis levels following stimulation of either SOD1 WT or SOD1 siRNA transfected cells. This data suggests that in normal and hypoxic conditions, the pcDNA-expressing control cells are protected from apoptosis following CXCR4 stimulation. While SOD1 overexpression seems to have caused a trend towards a decrease in apoptosis following CXCR4 stimulation in normal conditions, this does not necessarily seem to be the case in hypoxic conditions. Additionally, in both normal and hypoxic conditions, SOD1 knockdown seems to have caused no significant change in levels of apoptosis following stimulation of CXCR4.

Overall, results from our apoptosis experiments suggest that in the PC3 cell model system, in normal and in hypoxic conditions, CXCR4 stimulation protects against apoptosis. However, in in hypoxia, SOD1 overexpression is not able to reduce levels of apoptosis following CXCR4 stimulation to the same extent as in normal conditions.

3.5 Effects of SOD1 on CXCR4-Mediated Cell Migration

In order to provide more insight into the downstream effects of the totality of the complex cell signaling events occurring inside the cell we performed transwell migration

experiments. Transwell migration assays are an excellent tool to study migration and an overview of this technique is provided in Figure 2.2. We measured the number of cells that migrated in control conditions and subtracted this from the number of cells migrated in the presence of CXCL12 as net migration. As an additional aspect of this experiment, we used Pertussis toxin (PTX) to inhibit $G\alpha_i$ in order to determine whether or not the CXCR4-mediated migration was dependent on $G\alpha_i$.

The results from the transwell migration experiments performed in normoxic conditions is provided in Figure 3.8A. This figure demonstrates that following exposure to the chemoattractant there is a significant increase in migration in cells transfected with pcDNA ($p<0.001$). However, there is not a significant increase in the cells transfected with either SOD1 WT or SOD1 siRNA although the siRNA trends towards rescuing the migration loss. Additionally, following the treatment with PTX, the $G\alpha_i$ inhibitor, there is no change in migration levels.

The results from the same experiment conducted in hypoxic conditions for 24 hr are displayed in Figure 3.8B. Results demonstrate that there is no significant increase in migration following stimulation of any SOD1 overexpressing or SOD1 knockdown cells. However, the pcDNA control transfected cells do show a significant increase in migration following stimulation ($p<0.05$). However, following treatment with PTX, there is a significant increase in the migration of PC3 cells following stimulation with CXCL12 ($p<0.001$). Taken together, the results obtained from the transwell migration assay suggest that overexpression of SOD1 WT ablates the migration of PC3 cells in both normal and hypoxic conditions. Also, these results indicate that in PC3 cells, PTX, a known inhibitor of $G\alpha_i$ proteins, inhibits migration in normoxic but not in hypoxic conditions.

3.6 Modulation of G Protein Coupling by SOD1 and Hypoxia

We next sought to investigate the possible mechanism through which SOD1 interaction with CXCR4 could modulate downstream signaling. It has been shown that, although both $G\alpha_i$ and $G\alpha_q$ can be activated by CXCR4, these G proteins may play differing roles in cell migration. We used the BRET technique in living cells to measure the coupling of CXCR4 with both $G\alpha_i$ and $G\alpha_q$ G proteins. An overview of the technique can be found in Figure 2.3. Basically, the higher the ratio between donor:acceptor (Rluc II:YFP) emission, the closer the proteins of interest are together.

Figure 3.9A demonstrates the results obtained with BRET analysis of PC3 cells maintained in normoxic conditions. Figure 3.9A shows that following stimulation with CXCL12, regardless of SOD1 transfection (pcDNA, SOD1 WT or SOD1 siRNA), there was a significant net BRET value between CXCR4 and $G\alpha_i$ ($p < 0.05$ for pcDNA and SOD1 siRNA, $p < 0.01$ for SOD1 WT). Interestingly, similar results were found with CXCR4 and $G\alpha_q$ coupling, regardless of SOD1 expression level ($p < 0.05$ for pcDNA and SOD1 WT, $p < 0.01$ for SOD1 siRNA). This indicates that in normoxic conditions, following a 2 min CXCL12 stimulation, CXCR4 comes in close enough proximity to be likely interacting with either $G\alpha_i$ or $G\alpha_q$.

Figure 3.9B displays the results of the same experiment conducted with cells that had been maintained in hypoxic conditions for 8 hr prior to the experiment start. Firstly, following CXCL12 stimulation, there was no significant increase in the BRET¹ ratio, regardless of SOD1 expression levels between CXCR4 and $G\alpha_i$. This indicates that stimulation does not increase the proximity of CXCR4 with $G\alpha_i$ when the cells had been

cultured in hypoxic conditions. Following stimulation, there was a significant increase in the BRET¹ ratio measured between CXCR4 and G α_q , regardless of whether the cells were transfected with pcDNA, SOD1 cDNA or SOD1 siRNA ($p < 0.05$ for pcDNA and SOD1 WT, $p < 0.01$ for SOD1 siRNA). Taken together, these results demonstrate that SOD1 expression level does not alter the physical coupling of CXCR4 with the G proteins in normal conditions. However, for cells cultured in hypoxic conditions a shift in G protein interaction from both G α_i and G α_q to just G α_q , regardless of SOD1 expression levels tested was noted, although more experiments are needed to validate this observation.

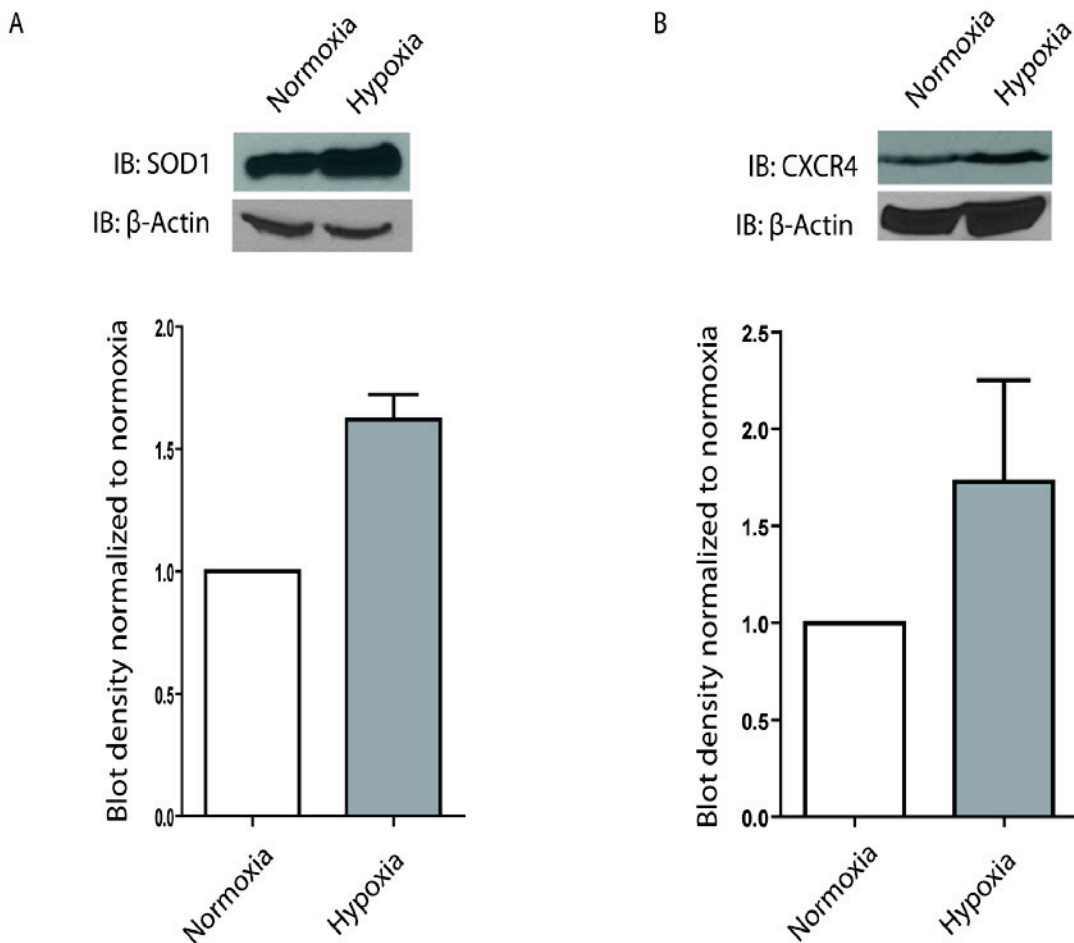


Figure 3.1 Endogenous Levels of CXCR4 and SOD1 in Normal and Hypoxic Conditions in PC3 Cells.

A. Top panel shows a representative western blot against SOD1 in normoxic and hypoxic conditions. The loading control was β -actin. Bottom panel is a histogram summarizing the results of the western blot experiment. B. Top panel shows a representative western blot against CXCR4 in normoxic and hypoxic conditions. The loading control was β -actin. Bottom panel shows the effect of hypoxic conditions on the endogenous expression of CXCR4. Results represent the means \pm SEM of 5 independent experiments.

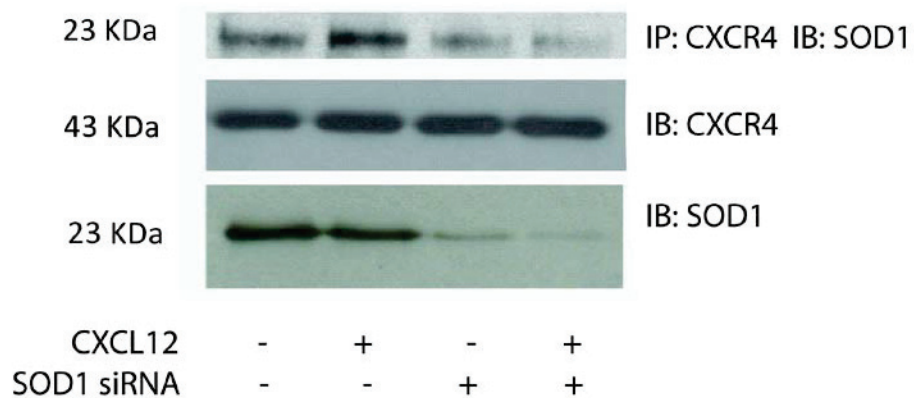


Figure 3.2 Endogenous Interaction between CXCR4 and SOD1 in PC3 Cells.

This image shows a co-immunoprecipitation (Co-IP) experiment performed on non-transfected PC3 cells. The first two lanes are non-transfected PC3 cells and the last two lanes are PC3 cells transfected with SOD1 siRNA to reduce SOD1 levels. The second and fourth lane display results of the experiment using PC3 cells that had been stimulated with 100 ng/ml CXCL12. Top panel shows the results of the Co-IP, where CXCR4 was precipitated with an anti-CXCR4 antibody, then run with SDS-PAGE and immunoblotted with an anti-SOD1 antibody. The middle and bottom panels show the lysate from the Co-IP experiment, run with SDS-PAGE and blotted against CXCR4 and SOD1, respectively. Results are representative of 3 independent experiments.

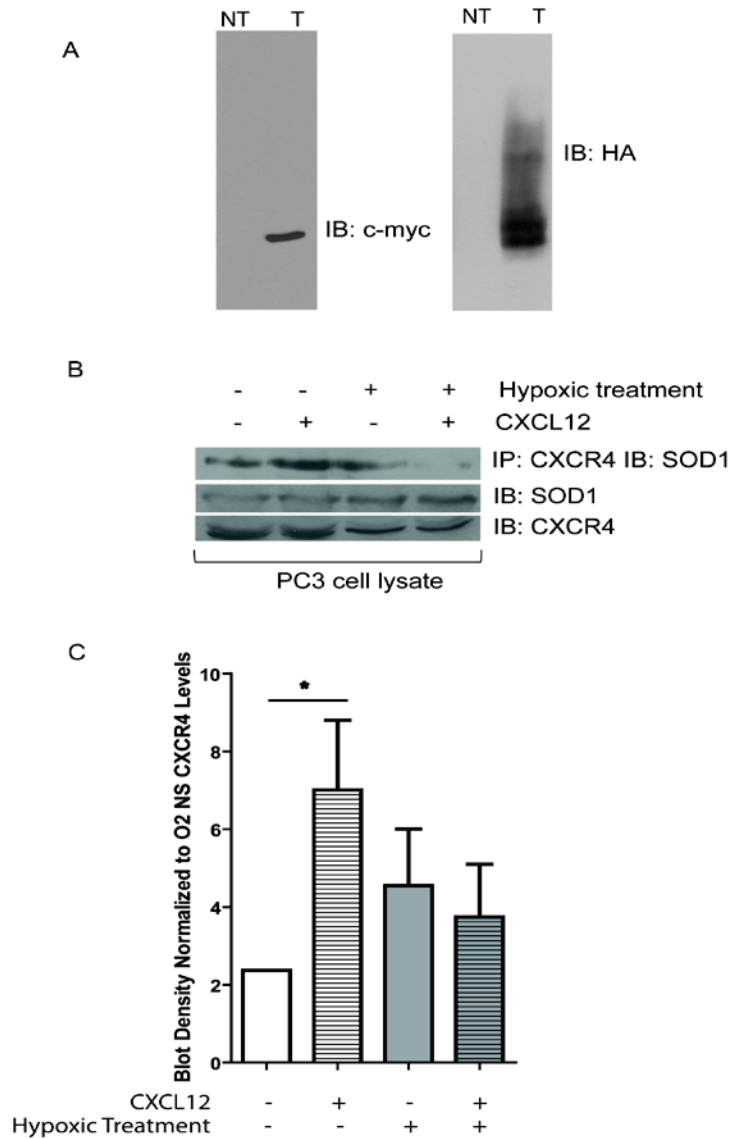


Figure 3.3 Exogenous Interaction Levels between CXCR4 and SOD1 in PC3 cells in both Normal and Hypoxic Conditions.

A. Western blots showing transient transfection of SOD1 and CXCR4. Each panel shows two lanes, lane 1 contains non-transfected PC3 cell lysate and lane 2 contains lysate of cells transfected with CXCR4-HA and SOD1-c-myc. First panel is blotted against c-myc and the second against HA. B. Representative results of a Co-IP experiment. PC3 cells were transfected with CXCR4 and SOD1. Lane 2 and 4 display results of the experiment using cells that were stimulated with 100 ng/ml CXCL12 for 15 min. Top panel shows results of the Co-IP, where CXCR4 was precipitated and SOD1 was immunoblotted. The middle and bottom panels show the lysate from the Co-IP experiment, blotted against SOD1 and CXCR4, respectively. C. Histogram summarizing the results of the Co-IP experiment. The Co-IP blot density was normalized to non-stimulated CXCR4 levels in normoxic conditions. Results represent the means \pm SEM of 4 independent experiments. * $p < 0.05$, using two-way ANOVA with a Bonferroni posttest.

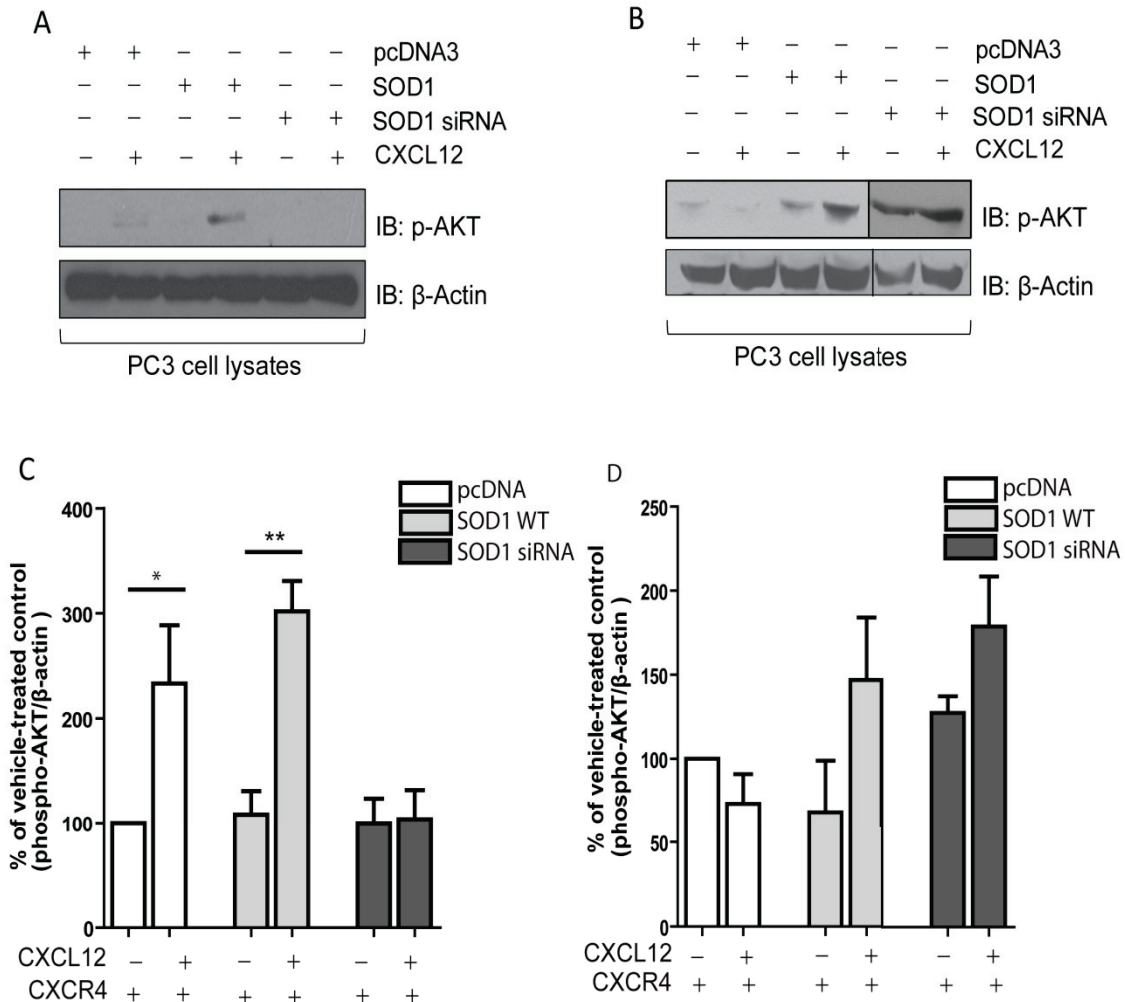


Figure 3.5 Effects of both SOD1 and Hypoxia on CXCR4-Mediated AKT/ Protein Kinase B (PKB) Activation in PC3 Cells.

A. Representative western blot against p-AKT (top panel) and β -actin (bottom panel). All cells were transfected with CXCR4. First two lanes show the results from PC3 cells co-transfected with pcDNA, the next two of cells co-transfected with SOD1 cDNA and the last two of cells co-transfected with SOD1 siRNA. Lanes 2, 4 and 6 display results of the experiment using PC3 cells that had been stimulated for 15 min with 100 ng/ml CXCL12 prior to experimentation. B. Same representative western blot against p-AKT and β -actin as found in A, using cell lysate from PC3 cells maintained in hypoxic conditions for 8 hr prior to experimentation. C. Histogram summarizing results found in A. The bars are in the same order as the lanes in image A. p-AKT blot density was normalized first to β -actin levels, then to blot density of non-stimulated cells co-expressing the pcDNA vector control. D. Histogram summarizing results found in B. Blot density values normalized as per image C. Results represent the means \pm SEM of 5 independent experiments in normoxic conditions, and 4 independent experiments in hypoxic conditions. * p <0.05, ** p <0.01, using two-way ANOVA with a Bonferroni posttest.

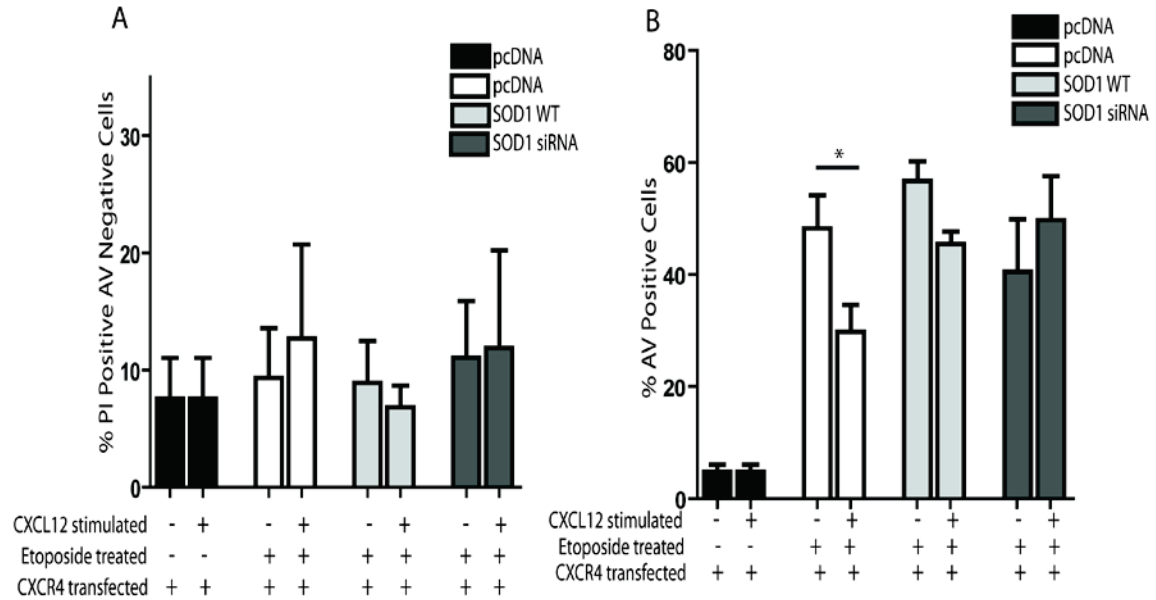


Figure 3.6 Effect of SOD1 and CXCR4 on Apoptosis Levels in PC3 Cells in Normoxic Conditions. Results of PC3 cells transfected with CXCR4 and maintained in normoxic conditions. A. Percent necrotic cells, identified as propidium iodide (PI) positive and Annexin V (AV) negative. First four bars, bars 5 and 6 and bars 7 and 8 represent results from cells co-transfected with pcDNA, SOD1 cDNA and SOD1 siRNA, respectively. The first two bars represent results from cells that were not treated with etoposide, while the remaining bars were all pre-treated with etoposide. Bars 2, 4, 6 and 8 display results of the experiment using PC3 cells that had been stimulated with 100 ng/ml CXCL12 for 18 hr. B. Percent apoptotic cells, identified as positive for AV staining. Bar layout is the same as seen in image A. Results represent the means \pm SEM of 5 independent experiments. * $p < 0.05$, *** $p < 0.001$, using two-way ANOVA with a Bonferroni posttest.

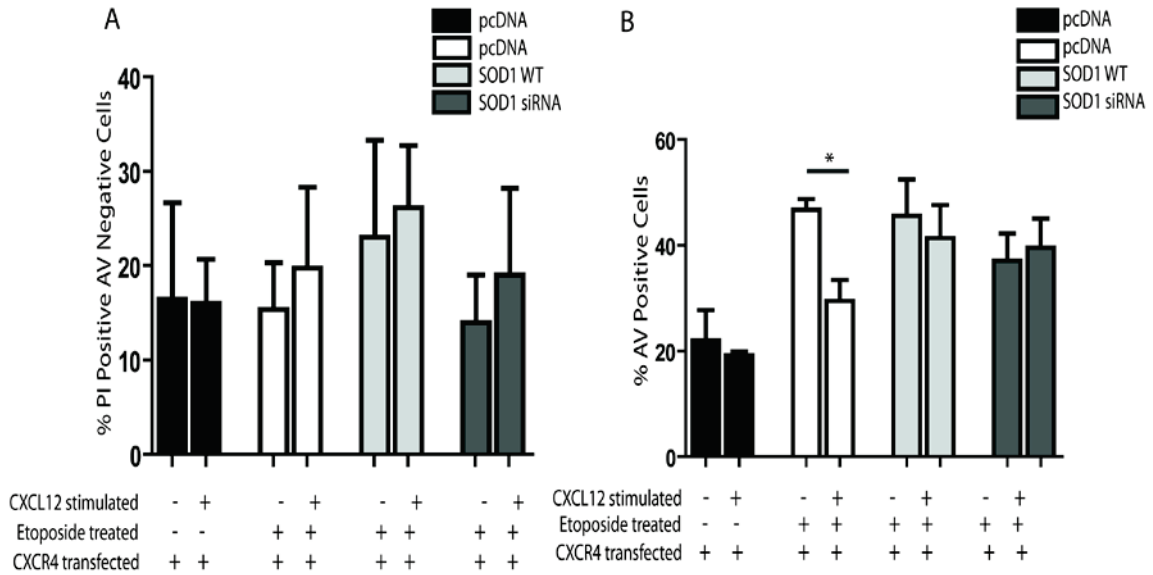


Figure 3.7 Effect of SOD1 and CXCR4 on Apoptosis Levels in PC3 Cells in Hypoxic Conditions. Results of PC3 cells transfected with CXCR4 and maintained in hypoxic conditions for 24 hr. A. Percent necrotic cells, identified as propidium iodide (PI) positive and Annexin V (AV) negative. First four bars, bars 5 and 6 and bars 7 and 8 represent results from cells co-transfected with pcDNA, SOD1 cDNA and SOD1 siRNA, respectively. The first two bars represent results from cells that were not treated with etoposide, while the remaining bars were all pre-treated with etoposide. Bars 2, 4, 6 and 8 display results of the experiment using PC3 cells that had been stimulated with 100 ng/ml CXCL12 for 18 hr. B. Percent apoptotic cells, identified as positive for AV staining. Bar layout is the same as seen in image A. Results represent the means \pm SEM of 4 independent experiments. * $p < 0.05$, using two-way ANOVA with a Bonferroni posttest.

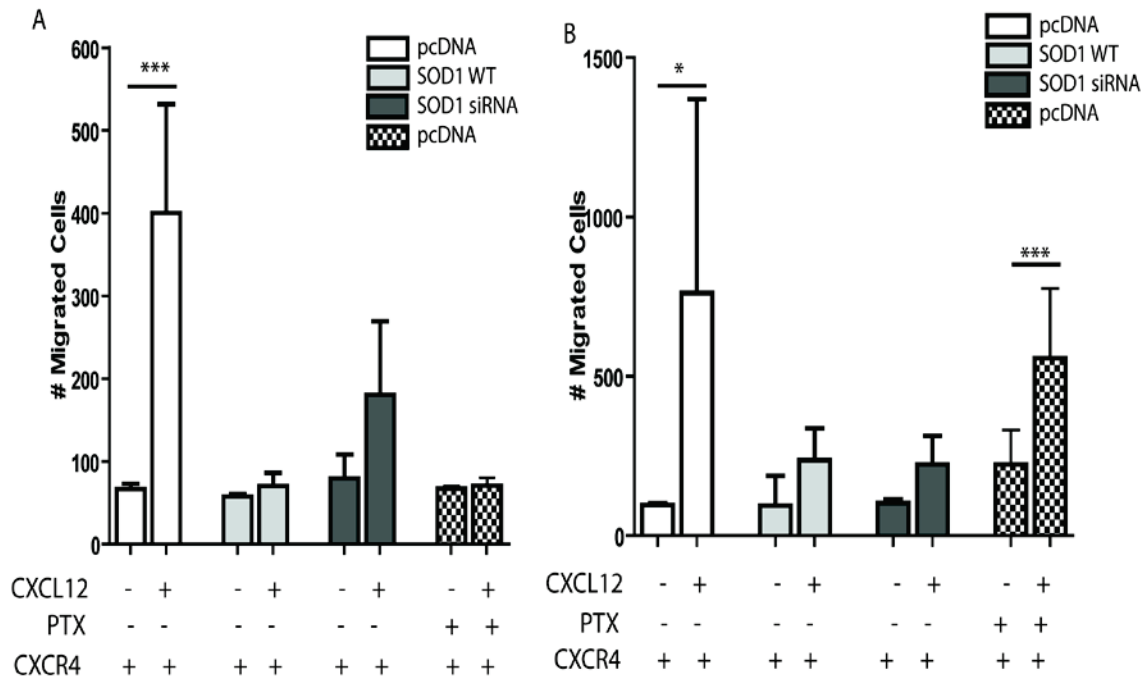


Figure 3.8 Effect of SOD1 and Pertussis Toxin (PTX) on CXCR4-Mediated Migration in Response to CXCL12 in both Normoxic and Hypoxic Conditions.

A. Histogram summarizing results of transwell migration experiments using PC3 cells transfected with CXCR4 in normoxic conditions. Columns 1, 2, 7, and 8 represent results from PC3 cells co-transfected with the pcDNA vector control. Bars 3 and 4 represent results from PC3 cells co-transfected with SOD1 cDNA. Bars 5 and 6 represent results from PC3 cells co-transfected with SOD1 small-interfering RNA (siRNA). Bars 2, 4, 6 and 8 represent results from PC3 cells treated for 24 hr with the chemoattractant CXCL12. Bars 7 and 8 represent results from PC3 cells pre-treated with the $G\alpha_i$ inhibitor PTX. B. Histogram summarizing results of transwell migration experiments using PC3 cells transfected with CXCR4 in hypoxic conditions. The layout of the bars is the same as that seen in image A. Results represent the means \pm SEM of 4 independent experiments in normoxic conditions and 3 independent experiments in hypoxic conditions. * $p < 0.05$, *** $p < 0.001$, using two-way ANOVA with a Bonferroni posttest.

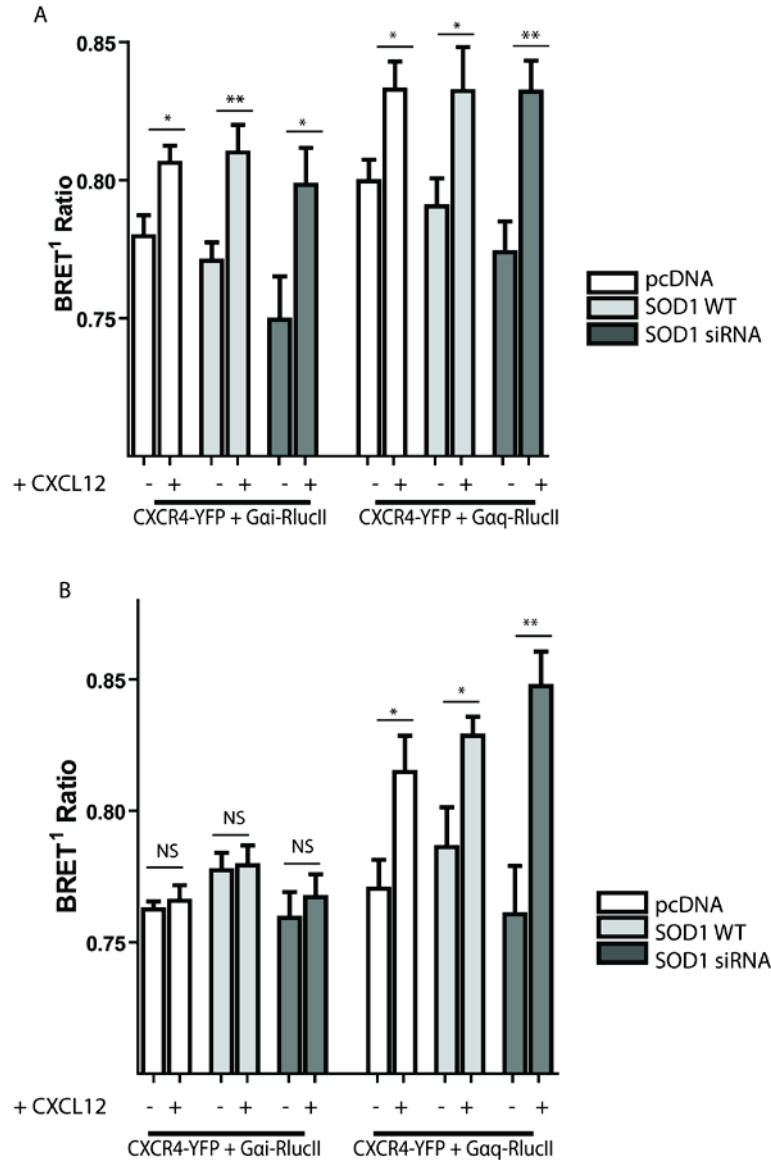


Figure 3.9 Effect of SOD1 on G Protein Coupling, Assessed Using Bioluminescence Resonance Energy Transfer (BRET), with CXCR4 in both Normoxic and Hypoxic Conditions.

A. Histogram summarizing the results of the BRET experiments in PC3 cells in maintained in normoxic conditions. The first 6 bars represent results from PC3 cells co-transfected with CXCR4-yellow fluorescent protein (YFP) and $G\alpha_i$ -Renilla luciferase (RlucII), while the last 6 bars represent results from PC3 cells co-transfected with CXCR4-YFP and $G\alpha_q$ -RlucII. B. Histogram summarizing the results of the BRET experiments in PC3 cells in maintained in hypoxic conditions. Results represent the means \pm SEM of 4 independent experiments in normoxic conditions and 4 independent experiments in hypoxic conditions. * $p < 0.05$, ** $p < 0.01$, using unpaired, two-tailed one-sample T-tests.

CHAPTER 4: DISCUSSION

4.1 Overview and Preliminary Findings

Prostate cancer is the second most commonly diagnosed cancer in males globally (Jemal et al., 2011). With an aging population and increased comorbidities such as obesity and inactivity, prostate cancer will only become more of a physical threat and financial burden to our society. Although there have been excellent attempts to encourage screening for early detection, this disease can be aggressively metastatic. The American Cancer Society suggests that as many as 1 in every 36 men in the United States will die of prostate cancer. Thus, current treatments for this disease are insufficient; more efforts need to be directed towards the understanding of aggressive and metastatic prostate cancers in order to help decrease mortality rates.

In order to discover new potential targets for the pharmaceutical treatment of prostate cancer, our lab began examining the CXCR4 receptor. There is a plethora of evidence that implicates CXCR4 in the development, progression and metastatic potential of prostate cancer (Akashi et al., 2008; Darash-Yahana et al., 2004; Domanaska et al., 2012; Fischer et al., 2008; Sun et al., 2003; Taichman et al., 2002; J. Wang et al., 2006; S. Zhang et al., 2008). Our lab performed a yeast-two hybrid screen to find proteins that interact with CXCR4 in an attempt to enhance the comprehension of the regulation of this GPCR. This screen found that CXCR4 interacted with SOD1. Due to the fact that CXCR4 levels are especially elevated in prostate cancer above other cancer types (Fischer et al., 2008), and because this type of cancer has a high probability of metastasizing, we chose to investigate this interaction in a cell model of prostate cancer.

This study used PC3 cells for several reasons. Firstly, these cells are highly metastatic in comparison with other prostate cancer cells lines (Muralikrishna et al., 2005); secondly, PC3 cells express CXCR4 protein, a finding that we confirmed in Figure 3.1A (Singh, Singh, Grizzle, & Lillard, 2004); lastly, they are from prostate cancer that has metastasized to bone and is androgen independent, suggesting an advanced disease state (Sobel & Sadar, 2005). We also found that PC3 cells, like some other cancer cell types, exhibited detectable levels of SOD1 (Figure 3.1B). Interestingly, there have been various studies that report increases and decreases in the levels of SOD1 and/or activity in prostate cancer tissue vs. normal tissue. For example, Battisti et al., 2011 examined 55 patients and 55 healthy controls and found increased levels of SOD1 activity in the patients, although no protein levels analysis was completed (Battisti et al., 2011). In contrast, Bostwick et al., 2000 showed that SOD1 is present in prostate cancer tissue, but it is found at a higher level in non-malignant tissue (Bostwick et al., 2000). While this study can confirm that SOD1 is present at endogenous and detectable levels in PC3 cells, it cannot compare these levels with healthy cells.

We also decided that examining CXCR4 and SOD1 protein level in normal vs. hypoxic conditions was an important preliminary experiment to perform. The results are shown in Figures 3.1C and 3.1D. Figure 3.1D shows that SOD1 levels increase significantly in a hypoxic environment, as was expected. Figure 3.1C shows that in contrast with the available literature (Brahimmi-Horn et al., 2007; Gupta & Massagué, 2006; Schioppa et al., 2003), the levels of CXCR4 do not change significantly following 8 hr incubation in hypoxic conditions, although there is a non-significant trend towards an increase. We believe that this apparent increase would become significant with either more experimental replicates or

longer time in hypoxic conditions; the 8 hr incubation may not be sufficient time in the hypoxic conditions for the cells to react by increasing transcription and subsequent translation of CXCR4 receptors.

Following confirmation that both CXCR4 and SOD1 are detected at endogenous levels in PC3 cells, we performed CO-IP experiments to determine whether or not the interaction seen with the yeast-two hybrid screen was also present in a cancer cell line model. As seen in Figure 3.2, CXCR4 interacts with SOD1 at an endogenous and basal level. Stimulation with CXCL12 for 15 min seemed to increase this interaction, although this was not quantified in this exploratory experiment. The specificity of this interaction was supported by the fact that knockdown of SOD1 with siRNA resulted in a decreased level of interaction. After proving that this interaction occurs at an endogenous level in PC3 cells, we chose to overexpress CXCR4 and SOD1. We confirmed the successful transient transfection of PC3 cells with both SOD1-c-myc and CXCR4-HA constructs by performing western blots against the respective tags, as seen in Figures 3.3A and 3.3B.

In order to address our hypothesis that the interaction between CXCR4 and SOD1 would decrease in hypoxic environments due to the buildup of ROS, we performed another Co-IP experiment. We cultured PC3 cells that were transfected with CXCR4 and SOD1 in either normal or hypoxic environments and performed the same experiment, immunoprecipitating CXCR4 and immunoblotting against SOD1. The representative results can be seen in Figure 3.3C. Furthermore, we attempted to quantify this data; the corresponding histogram in Figure 3.3D shows the intensity of the Co-IP band, standardized to CXCR4 input levels and normalized relative to the non-stimulated, normoxic levels of interaction. These results support our hypothesis that there is an increase in the level of

interaction following stimulation of CXCR4 by CXCL12. These results also demonstrate that in hypoxic conditions, the increase in interaction between these two proteins following stimulation is ablated. However, these results are not exactly what we expected, as there is no statistical difference between the basal level of interaction between CXCR4 and SOD1 in normoxic vs. hypoxic environments. Whether or not this lack of difference is a result of sample size is unknown at this point. Taken together, these results are partially supportive of our hypothesis, but the fact that they are not fully in line with what we had anticipated, suggest that our initial hypothesis may have been too simple and require further investigation.

Due to the role that CXCR4 and SOD1 play independently in prostate cancer incidence and metastasis, this study aimed to examine the effects of the interaction between CXCR4 and SOD1. As we were primarily interested in the metastatic process, we examined signaling pathways known to play a role in survival and proliferation, cell migration and apoptosis, all processes known to be important for cancer spread.

4.2 SOD1 May Modulate CXCR4-Induced ERK1/2 and AKT Activation

In order to more closely examine the role that the interaction between SOD1 and CXCR4 could have on CXCR4 signaling in PC3 cells, we chose to examine the activation of the ERK1/2 and AKT signaling pathways. Generally speaking, activation of these kinases leads to increased survival, migration and proliferation, and accordingly, are expected to be very active in cancer cells. Protein kinases have become one of the main subjects of interest for target-based chemotherapeutic development for several reasons. Firstly, these molecules, responsible for adding phosphate groups of other proteins, are usually an important

checkpoint in signal transduction pathways, in that their kinase activity is required for the inhibition or activation of downstream events. The importance of these molecules is emphasized by the fact that of the 518 known human kinases, over 150 have been implicated in diseases (Roberts & Der, 2007). Secondly, there are at least 10 kinase-targeted pharmaceuticals currently approved for use in humans (Roberts & Der, 2007). Mutations in these kinase signaling pathways such as the ERK1/2 and AKT, are commonly associated with cancer development, highlighting their importance (Hilger et al., 2002; Roberts & Der, 2007). Lastly, and most important for this study, both AKT and ERK1/2 can be induced by increased levels of ROS (Waris & Ahsan, 2006).

ERK molecules are mitogen activated protein kinases (MAPKs) that can be activated by several types of cell surface receptors, including EGFRs and GPCRs. The activated, phosphorylated p-ERKs will go on to activate a variety of transcription factors ultimately leading to increases in cell proliferation, survival and migration. In this particular study, we chose to examine ERK1 and ERK2 due to their implication in cell growth, movement and differentiation.

In order to determine the effects of SOD1 on CXCR4-mediated ERK1/2 activation, we transfected PC3 cells with CXCR4 and a pcDNA vector control or SOD1 WT or SOD1 siRNA. We then stimulated these cells with 100 ng/ml CXCL12 for 15 min and performed western blots against p-ERK1/2 with this cell lysate. While we were unsure of what to expect with the addition of SOD1 WT or SOD1 siRNA, we hypothesized that stimulation of CXCR4 in cells expressing the pcDNA vector control would cause an increase in ERK1/2 activation, as this has also been found in other prostate cancer studies (Gladson & Welch, 2008; J. Wang et al., 2006). Figures 3.4A and 3.4C demonstrate that in contrast with what

we had expected, there was not a significant increase in p-ERK1/2 formation following stimulation of cells expressing pcDNA. There does, however, seem to be a trend towards an increase in p-ERK1/2 formation, suggesting that more replicates may be needed. Of interest, following stimulation of CXCR4, p-ERK1/2 levels increase in cells co-transfected with CXCR4 and SOD1 WT. Cells with decreased levels of SOD1 via SOD1 siRNA transfection do not display significant ERK1/2 activation following stimulation. These findings are in line with what was found by Juarez et al., 2008, albeit in a different system. They found that SOD1 was integral for the activation of ERK1/2 in human umbilical vein endothelial cells (HUVEC) following stimulation with growth factors, as knockdown with SOD1 siRNA or inhibition with ATN-224 significantly impaired p-ERK formation (Juarez et al., 2008). In total, these results of ERK1/2 activation in normoxic conditions are similar with what we had expected, but also may suggest that the physical interaction between SOD1 and CXCR4 may be modulating CXCR4 signaling in ways we did not initially expect.

Results from the same experiment performed following 8 hrs in hypoxic conditions are shown in Figures 3.4B and 3.4D. These results show that although there seemed to be a trend towards an increase in ERK1/2 activation following stimulation of CXCR4 with CXCL12, none of these increases were significant. This ERK1/2 activation data supports our hypothesis, as we hypothesized that the effect that SOD1 would have in normoxia, here, an increase in ERK1/2 activation, would not be seen in hypoxic conditions.

Nevertheless, it is also important to note that an increase in SOD1 may not be necessarily linked with decreases in ROS. As previously mentioned, SOD1 is responsible for breaking superoxide into another ROS, H_2O_2 . Therefore, if there are insufficient enzymes available for the breakdown of H_2O_2 within the cell, overall oxidative stress may not

decrease as a result of increased SOD1 levels (Johnson & Giulivi, 2005). It has also been shown that H₂O₂ can itself activate ERK and AKT pathways (Chetram et al., 2011b; Juarez et al., 2006; Song, Lee, Jeong, Min, & Shin, 2005). Therefore, the results seen in these experiments may be convoluted by the fact that increases in p-ERK formation could be a result of increased H₂O₂ within the cells following overexpression of SOD1. In this context, more work needs to be done to separate the role of SOD1 as a CXCR4 interacting protein, an antioxidant and a producer of H₂O₂.

AKT is another kinase known to play a role in the transition to the metastatic phenotype. The PI3K/AKT pathway is closely linked to cell survival and increases in both cell size and number (Vivanco & Sawyers, 2002). Studies have demonstrated that there is an increase in active, p-AKT following stimulation with dihydrotestosterone in prostate cancer cells cultured in normal conditions (Yamasaki, Nomura, Sato, & Mimata, 2012). Furthermore, Yamasaki et al., 2012 found that chronic exposure to hypoxia caused constitutive activation of AKT. This is particularly important in the context of cancer, as AKT can prevent the induction of apoptosis. For example, AKT can activate a kinase that results in the degradation of an NF- κ B inhibitor, causing increased activity of this pro-survival transcription factor (Vivanco & Sawyers, 2002).

Similar to the ERK experiments, we transfected PC3 cells with the appropriate cDNA or siRNA, stimulated for 15 min with 100 ng/ml CXCL12 and performed a western blot against p-AKT with the lysate. Results are shown in Figures 3.5A and 3.5C for experiments carried out with normal cells and Figures 3.5B and 3.5D for experiments done with cells maintained in hypoxic conditions prior to experimentation. Results demonstrate that, as we expected, cells expressing the pcDNA vector control exhibited activation of AKT following

stimulation. This result is in support of the literature, where stimulation of CXCR4 causes p-AKT formation in a variety of cancer cell types (Scotton et al., 2002; Vivanco & Sawyers, 2002). Overexpression of SOD1 did not change this result. However, cells treated with SOD1 siRNA did not exhibit an increase in AKT activation following stimulation. Taken together, these results suggest that SOD1 may be important for the CXCR4-mediated activation of AKT in normal conditions and that the endogenous SOD1 in PC3 cells may be sufficient to allow AKT activation.

In hypoxic conditions, there was not a significant activation of AKT following stimulation, regardless of SOD1 expression levels. This suggests that the increase in p-AKT formation seen in cell transfected with either pcDNA or SOD1 occurs in normoxic, but not in hypoxic conditions. Therefore, the CXCR4-induced p-AKT formation that could lead to protection of the PC3 cells from apoptosis is no longer present in hypoxic conditions. Nevertheless, there does seem to be a trend towards an increase in AKT activation in cells maintained in hypoxic conditions that were overexpressing SOD1, suggesting that more replicates may be required. These results correlate with what was seen by Yamasaki et al., 2012, where there was no significant change in AKT activation following exposure to acute hypoxia but constitutive activation of AKT following exposure to chronic hypoxia. It could be beneficial to repeat these experiments in cells exposed to chronic hypoxia.

In summary, the results presented clearly demonstrate that SOD1 has an effect on CXCR4-mediated ERK and AKT activation. However, the multitude of signaling steps both before and after ERK/AKT activation, in addition to the multiple types of roles that SOD1 could potentially play in this system, convolute the results that we can gather from these studies. Therefore, we decided to conduct different types of experiments in order to

determine the functional result of the effects that SOD1 seems to have on CXCR4-mediated signaling.

4.3 SOD1 Protects Against Apoptosis in Normoxic, but not in Hypoxic Conditions

Apoptosis is a form of cell suicide that is ubiquitous among eukaryotes. Analyzing apoptosis levels was particularly important in this study, as cancer cells commonly bear mutations in their apoptotic machinery, which allow the tumor cells to grow and proliferate indefinitely. Also, CXCR4 and SOD1 are independently capable of modulating apoptosis levels.

In stark contrast to what the media and most of the literature leads us to believe, there is a dual role for antioxidants in cancer development and progression, largely due to their role in apoptotic processes. On one hand, oxidative stress leading to DNA damage can indeed be a contributor to cancer development; antioxidants, the reactive oxygen scavenging species, can break down the harmful ROS and potentially protect the DNA from this damage (Halliwell, 1994; Salganik, 2001). ROS have been well-established in the literature as mediators of apoptosis or cell suicide (Salganik, 2001). For instance, studies have implicated ROS as a downstream mediator of p53-mediated apoptosis (T. M. Johnson, Yu, Ferrans, Lowenstein, & Finkel, 1996; Salganik, 2001). This type of evidence was corroborated in part by a study in 2005 that displayed inhibition of PC3 prostate cancer cell growth and significant inhibition of tumor growth in mice following treatment with pomegranate (Malik et al., 2005). On the other hand, many anti-cancer therapies kill transformed cells through the increase of ROS and subsequent induction of apoptosis (Hileman et al., 2004; Juarez et al., 2006; Salganik, 2001; Watson, 2013). Consequently, while an increase in cellular

antioxidants may be beneficial for preventing initial DNA damage leading to cancer, the same reactive oxygen scavenging molecules can help protect cancer cells from apoptosis and potentially decrease the efficacy of certain chemotherapeutics. Therefore, we believed that closer examination of the effects of SOD1 on apoptosis was required.

One of the many downstream events following CXCR4 activation by CXCL12 is the prevention of apoptosis. There is a wealth of evidence available to suggest that CXCR4 stimulation decreases rates of apoptosis. In several examples, AMD3100, a selective CXCR4 inhibitor, was able to reverse the decrease in apoptosis seen with addition of CXCL12 and increase rates of apoptosis within cancer cells (Rubin et al., 2003; J. Wang et al., 2006). Other studies have used glioma cells to demonstrate that CXCL12 stimulation of CXCR4 prevented apoptosis even following serum starvation, likely through the AKT pathway (Zhou, Larsen, Hao, & Yong, 2002). Therefore, our results in normoxic conditions, found in Figure 3.6B, are similar to what was seen in the literature, as treatment of PC3 cells transfected with CXCR4 and the pcDNA vector control exhibited a significant decrease in apoptosis following 18 hr 100 ng/ml CXCL12 treatment. Neither the SOD1 WT nor the SOD1 siRNA transfected cells showed a significant difference between vehicle and CXCL12 treatment, however the SOD1 overexpressing cells seem to trend towards a decrease in apoptosis levels following stimulation. This finding is in line with what has been seen in the literature, as antioxidants in general have an anti-apoptotic effect through their ability to scavenge ROS (Salganik, 2001).

We then conducted the same experiment with PC3 cells that were maintained in hypoxic conditions for 18 hr. The results from these experiments are seen in Figure 3.7. These results show, similar to what was seen in normoxic conditions, that pcDNA vector

control transfected cells exhibit a decrease in apoptosis following CXCL12 stimulation. However, while there was a trend towards a decrease in apoptosis following stimulation of SOD1 overexpressing cells in normoxia, this was no longer apparent in hypoxic conditions. We believe that this could be for several reasons. First, the blunting of the protective effect of SOD1 on CXCR4-mediated apoptosis may be a result of increased levels of H₂O₂ within the cells causing some apoptosis (Cerella et al., 2009). Secondly, we believe that these results are in support of our hypothesis, as we believed that SOD1 would have less of an effect on CXCR4 signaling in hypoxic conditions.

Taken together, our results from the apoptosis experiments are in accordance with what is known in the literature. CXCR4 stimulation has an anti-apoptotic effect in both normoxic and hypoxic conditions. However, our study suggests that SOD1 overexpression protects cells from apoptosis in normoxic, but not necessarily in hypoxic environments. In the future, we plan to confirm these experiments with an independent marker of apoptosis, such as caspase activation. This would be advantageous, as differentiation between apoptotic vs. necrotic cells by Annexin V staining is a contentious issue. This is mostly because permeabilization of the plasma membrane can occur in necrosis and could potentially allow Annexin V labeling to occur in the absence of apoptosis. In addition, it would be advantageous to couple overexpression of SOD1 with catalase in order to determine whether or not H₂O₂ has an effect on apoptosis in our experiments.

4.4 SOD1 Inhibits Migration in Normoxic and Hypoxic Environments

We then employed transwell migration assays in order to examine the possibility that the effect of SOD1 on CXCR4-mediated ERK1/2 activation translated to a functional effect

in normal and hypoxic conditions. An overview of the technique is provided in Figure 2.2 and the results from this experiment are in Figure 3.8.

In normoxic conditions, as shown in Figure 3.8A, CXCL12 stimulation significantly increased the number of pcDNA vector-transfected control migratory cells over the same cells in absence of CXCL12. This is what was expected, as CXCR4 activation has been shown to cause cell migration (Balkwill, 2004b; Helbig et al., 2003; Kukreja et al., 2005; Müller et al., 2001; Ok et al., 2012; Scotton et al., 2002; S. Zhang et al., 2008). For example, Singh et al., 2004 found that PC3 prostate cancer cells migrated towards CXCL12 in a transwell migration assay. Also, this study showed that the CXCL12-stimulated migration was ablated by the addition of an anti-CXCR4 antibody (Singh, Singh, Grizzle, et al., 2004). However, transfection with SOD1 WT seems to have diminished the migration, as there is no longer an increase in migration following stimulation of these cells. This finding is in concert with what was seen in Chetram et al., 2011, where cells exhibited higher levels of CXCR4-mediated migration following the addition of H₂O₂, mimicking ROS accumulation. We believe that overexpression of SOD1 could decrease levels of ROS, diminishing the amount of migration. This would be similar to what is seen in other studies, where cell migration generally increases in response to oxidative stress (Brahimmi-Horn et al., 2007). However, these results are again complicated by the fact that SOD1 should decrease oxidative stress, but in theory it could be increasing levels of H₂O₂. In order to address this problem, we could add catalase to the system in order to combat the H₂O₂. Cells transfected with SOD1 siRNA also did not migrate in response to CXCL12. Interestingly, this result found in SOD1 siRNA treated cells does correspond with a study from Luo et al., 2007, where cells isolated from mice that express SOD1 G93A, a SOD1 mutant with

decreased SOD1 function, have a lower propensity to migrate towards CXCR4 following stimulation (Luo et al., 2007).

In hypoxic conditions, seen in Figure 3.8B, pcDNA vector-transfected control cells show a significant increase in migration following CXCL12 stimulation. However, in SOD1 overexpressing cells and the SOD1 siRNA treated cells do not exhibit the same increase in migration following stimulation. At first glance, these findings are not in line with what we expected to happen; if oxidative stress can cause migration, hypoxia should increase migration, as has been shown by others (Brahimmi-Horn et al., 2007; Chetram et al., 2011a). Instead, we found that there was no obvious difference between normal vs. hypoxic treatment on migration levels with variable SOD1 expression levels. However, studies by Yamasaki et al., 2011 examined the different response of prostate cancer cells to acute vs. chronic hypoxic exposure, where chronic exposure referred to cells maintained in 1% O₂ for 6 months. Their findings suggested that acute hypoxia caused a decrease in cell migration, while chronic hypoxia resulted in an increase in migration and invasion (Yamasaki et al., 2012). Therefore, more studies need to be done to determine the possible effects of SOD1 on the migration of cells maintained in chronically hypoxic conditions.

Due to the important role of CXCR4-mediated migration of cancer cells in prostate cancer metastasis, researchers have aimed to better comprehend what regulates this process. It has recently been demonstrated that G α_i signaling is important for CXCL12-mediated migration, while G α_q is involved in continuous inhibition of migration in T cells (Ngai et al., 2009). The yeast-two hybrid screen performed in our lab demonstrated an interaction between loop 1 of CXCR4 and SOD1. Previous work has shown that loop 1 of the thyrotropin receptor is an important site for interaction between the GPCR and the G proteins

(Kleinau et al., 2010). Interestingly, loop 1 of CXCR4 contains only one recognizable motif, a KKLR motif. Other studies have also demonstrated that a BBXB motif, similar to the KKLR motif (where B is a basic and X is a non-basic residue), is important for the activation of $G\alpha_i$ (Okamoto et al., 1994). Therefore, we decided to examine the possibility that SOD1 was playing a role in physically modulating G protein coupling with CXCR4, as these proteins may interact with the receptor at the same site.

Therefore, we used Pertussis toxin (PTX) to inhibit $G\alpha_i$ in order to determine whether or not the CXCR4-mediated migration of PC3 cells was dependent on $G\alpha_i$. Our results from these experiments are shown in the last two bars of Figure 3.8A and 3.8B. In normoxic conditions, PTX inhibited the CXCL12-stimulated migration of PC3 cells. This suggests that the migration seen in pcDNA vector-transfected controls following stimulation in normoxia was dependent on $G\alpha_i$. This finding is in support of other studies that have found that addition of PTX significantly impairs CXCR4-mediated migration of cancer cells (Alsayed et al., 2007; Hwang, 2003). In contrast, in hypoxic conditions, PTX treated cells had a significant increase in migration following stimulation with CXCL12. This finding suggests that the migration of PC3 cells in response to CXCL12 in hypoxic conditions is not dependent upon $G\alpha_i$. It is known that CXCR4 can couple with both $G\alpha_i$ and $G\alpha_q$. It has also been suggested that the balance between $G\alpha_i$ and $G\alpha_q$ signaling is important for the regulation of cell migration (Ngai et al., 2009). However, there are not many studies available investigating a switch in G-protein coupling; therefore, more studies need to be done in order to determine whether or not CXCR4-G protein coupling could change based on the cells environment, in this case, the presence or absence of oxygen.

4.5 G Protein Coupling with CXCR4 Appears to Change in Hypoxia

In order to more closely examine whether or not SOD1 plays a role in modulating CXCR4-G protein coupling, we performed BRET experiments. Briefly, this technique is able to determine whether or not two proteins are within 5 nm of each other. When proteins are in a close enough proximity, the BRET¹ ratio will increase, suggesting that the proteins could be interacting. We performed BRET experiments to determine the proximity of CXCR4 to both G α_i and G α_q following stimulation with CXCL12. We co-transfected the PC3 cells with SOD1 or SOD1 siRNA in order to determine if this protein-protein interaction could modulate G protein coupling with CXCR4. Results from this experiment in normoxic conditions and hypoxic conditions are shown in Figure 3.9A and Figure 3.9B, respectively.

Results demonstrated that in normoxia, regardless of SOD1 expression levels or G protein, there was a significant increase in the BRET¹ ratio. This suggested that stimulation with CXCL12 caused an increase in the proximity between CXCR4 and both G α_i and G α_q . This was expected, as it is known that CXCR4 can signal through both G proteins (Ngai et al., 2009; Shi et al., 2007). In contrast, in hypoxic conditions, results suggested that following stimulation, the proximity between CXCR4 and G α_i does not increase. In contrast, there did seem to be an increase in proximity between CXCR4 and G α_q following stimulation, as indicated by a significant increase in the BRET¹ ratio.

Taken together, these results seem to suggest that CXCR4 couples with both G proteins in normoxia, but may favour coupling with G α_q in hypoxic conditions. These BRET results support what we found in the migration assay experiment; in normoxic conditions, PTX inhibited migration of PC3 cells, while in hypoxia, the inhibition of G α_i does not effect migration. We plan to further investigate the possibility of a switch in G protein coupling in

hypoxic conditions by measuring the second messengers produced by these G proteins. Additionally, PTX has been shown to block CXCR4-mediated cell survival (Broxmeyer et al., 2003). Therefore, it would be interesting to see if PTX was able to block CXCR4-mediated anti-apoptotic activity in normoxic, but not in hypoxic environments, further supporting our hypothesis of a switch to $G\alpha_q$ mediated signaling in hypoxia.

4.6 Future Directions

While the preceding body of work was able to shed light on the effects on the interaction between CXCR4 and SOD1, further work is needed to fully comprehend the complexity of the effects of this interaction. The results of this work demonstrate that SOD1 is capable of interacting with CXCR4 in a prostate cancer cell line and that the modulation of SOD1 levels can result in differential CXCR4 signaling. In order to advance the potential of this interaction as a drug target, several additional experiments need to be done.

It would be beneficial to this study to include SOD1 activity assays in this project for several reasons. Firstly, this would allow us to verify the change in enzymatic activity following overexpression or knockdown of SOD1 protein. This would also aid in our comprehension of the potential effects of CXCR4 activation on SOD1 enzyme function. We would analyze levels of SOD1 activity with and without CXCL12 stimulation to assess this aspect of the project.

Additionally, it would be interesting to perform the same experiments we have already conducted, with PC3 cells that have been pre-treated with ATN-224, a SOD1 enzyme inhibitor. These experiments are particularly relevant, as SOD1 inhibitors are used clinically. Originally, it was discovered that some of the molecules involved in angiogenesis required

copper to function, so copper chelators became an attractive drug to test for the reduction of angiogenesis (Brewer et al., 2000; Marikovsky et al., 2002; Pan et al., 2002). Systemic administration of TM was shown to significantly reduce the number and size of blood vessels and the size of the tumors formed in mice following xenograft of breast cancer cells (Pan et al., 2002). Next, the second-generation TM drug called ATN-224 was developed. A phase II study of ATN-224 was conducted including patients who had biochemically recurrent prostate cancer with a PSA doubling time of <12 months. Results suggested that 59% of patients maintained on the low dose (30 mg daily) of ATN-224 were PSA progression free, and some patients even had a reduction in PSA levels (Lin et al., 2011). This study provided substantiation for the hypothesis that drugs targeting the interaction between SOD1 and CXCR4 could be useful for the treatment of prostate cancer. We believe that these results support our hypothesis of SOD1 acting as an important sensor of tumor cell environment. Pretreatment of PC3 cells with ATN-224 would allow us to determine whether or not the effects that we see of SOD1 levels on signal transduction, apoptosis and migration are due to the physical interaction between SOD1 and CXCR4 or whether the effects are mainly a result of the enzymatic activity of SOD1.

Next, we would like to examine the potential effects of H₂O₂ production by SOD1 in this system. As previously mentioned, increased levels of H₂O₂ can induce apoptosis in cells (Cerella et al., 2009). Therefore, it would be beneficial to add catalase, an H₂O₂-scavenging antioxidant, to the system. This would allow us to tease apart the effects of SOD1 interaction with CXCR4 from the effects of overproduction of H₂O₂ by exogenous SOD1 expression on apoptosis levels seen in this system.

Lastly, we would like to use different experimental techniques to confirm the possibility of the switch between CXCR4-G α_i /G α_q signaling in normoxia and CXCR4- G α_q signaling in hypoxia. In order to assess this, we need to employ different techniques, as there is no known specific inhibitor of G α_q that is analogous to PTX for G α_i . Therefore, we plan to use second messenger reporter assays to measure levels of IP₃ for G α_q activation and cAMP for G α_i activation in normoxic and hypoxic conditions. If our preliminary results are correct, there should be higher rates of IP₃ production (signifying G α_q activation) in hypoxic conditions than in normoxic conditions. Additionally, G α_i should be more effective at inhibiting cAMP production in the presence of forskolin, an adenylyl cyclase activator, in normoxic conditions than in hypoxic conditions. This would provide additional evidence that O₂ levels can influence CXCR4-G protein coupling, ultimately modulating metastasis-linked cellular effects.

Following completion of the above-mentioned future work, we should have a more comprehensive understanding of the effects of the interaction between SOD1 and CXCR4. However, given the complexity of this project, there are multiple avenues this work could expand. We hope to move what is found in the PC3 cell line into an animal model. We would create a cross between the transgene adenocarcinoma mouse prostate (TRAMP) transgenic mouse that spontaneously develops metastasizing prostate cancer and a SOD1 -/- mouse. This would specifically allow us to analyze the effects of the interaction between CXCR4 and SOD1 in an *in vivo* model.

CHAPTER 5: CONCLUSION

Prostate cancer is a diagnosis that is becoming increasingly common with an aging population. Although there are several effective treatments available for localized disease, metastatic prostate cancer remains a dangerous and deadly disease. The lack of effective treatment for late-stage prostate cancer necessitates the continued research and investigation into why and how cancer cells metastasize, in addition to the discovery of novel drug targets to prevent prostate cancer deaths.

In order to advance the comprehension of cancer spread, we chose to investigate the regulation of the chemokine receptor CXCR4, a receptor that is known to be involved in cancer cell growth, motility and survival (Taichman et al., 2002; J. Wang, Loberg, & Taichman, 2006; Balkwill, 2004b; Ganju et al., 1998). Our lab discovered a protein-protein interaction between CXCR4 and superoxide dismutase, an antioxidant molecule. In addition to what is known about the role of antioxidants in cancer, SOD1 has also been examined independently of CXCR4 as a potential biomarker, a drug target, and a potential site of DNA mutations in relation to prostate cancer (Abe et al., 2011; Bostwick et al., 2000; Estrada-carrasco et al., 2010; Juarez et al., 2006). Due to the vital role that each of these molecules play individually in metastasis, we examined the effects of SOD1 on CXCR4-mediated signaling in PC3 prostate cancer cells.

Results from this study indicate that SOD1 interacts at a basal level with CXCR4 in PC3 cells in both normal and hypoxic conditions. We hypothesized that the interaction would decrease in hypoxic conditions, because SOD1 would dissociate from CXCR4 to combat the accumulation of ROS within the cell. Our hypothesis was partially correct. We found that stimulation of CXCR4 caused an increase in the interaction between CXCR4 and

SOD1 in normoxic, but not in hypoxic conditions. Additional results from this study support this finding, as SOD1-transfected cells exhibit increased ERK activation in normoxic, but not hypoxic conditions. Also, SOD1-transfected cells were protected from etoposide-induced apoptosis following stimulation of CXCR4 by CXCL12 in normoxic, but not in hypoxic conditions.

However, certain results in this study suggest that our initial hypothesis was too simple. We determined through BRET experiments that there may be a shift in CXCR4-G protein coupling in hypoxia, whereby CXCR4 couples to both $G\alpha_i$ and $G\alpha_q$ in normoxic conditions, but preferentially couples with $G\alpha_q$ in hypoxic conditions. This potential shift in G protein coupling would have extensive implications, as the balance between $G\alpha_i$ and $G\alpha_q$ signaling has been implicated in modulating cell migration, an aspect important for the metastatic transition (Ngai et al., 2009). This indication allows us to modify our hypothesis slightly; the updated hypothesis can be found in Figure 5.1, below.

SOD1 and CXCR4 have individually been targeted for the treatment of prostate cancer drug (ATN-224 and AMD3100, respectively). However, neither of these targets are currently used clinically due to either potential adverse effects or to ineffectiveness. We believe that the interaction that we discovered is thus representative of a novel potential drug target. While further elucidation of the effects and potential outcomes of blocking the interaction of CXCR4 and SOD1 is necessary, we believe that this protein-protein interaction represents a potentially valuable and unique target for the treatment of not only prostate cancer, but potentially other cancer types that express both CXCR4 and SOD1.

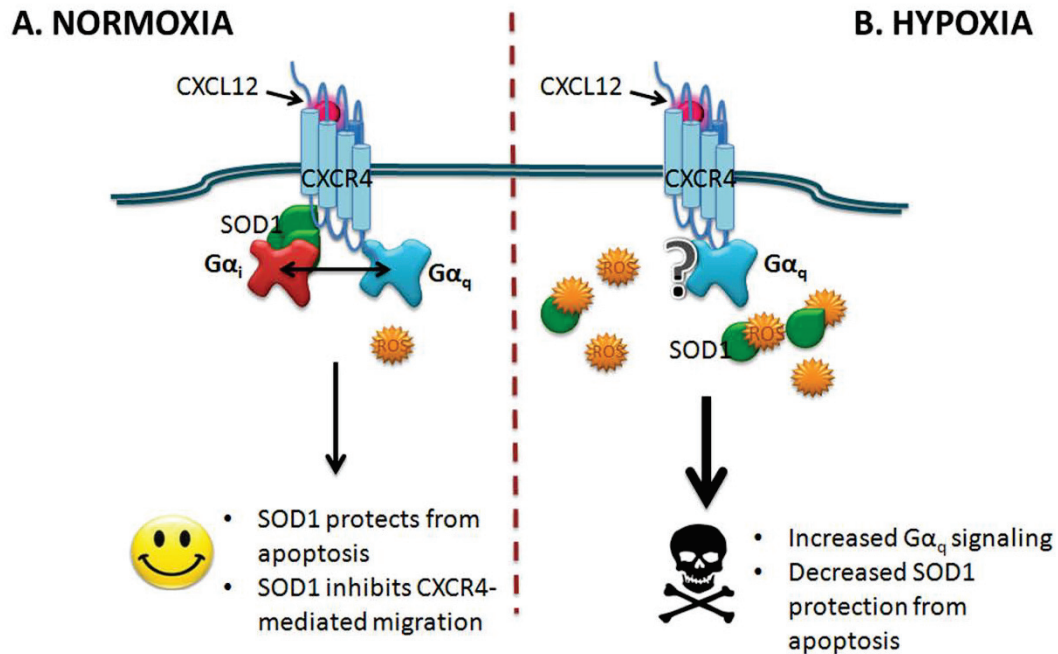


Figure 5.1 Updated Hypothesis

Same image as seen in Figure 1.8, modified to incorporate new findings. The schematic of our new hypothesis is in two parts, with the cartoon cell in normoxic conditions in Figure 5.1A and hypoxic conditions in Figure 5.1B. A. CXCL12 will bind to CXCR4 and initiate signaling. We found that SOD1 interacts with CXCR4 at a basal level, and that this interaction increases following stimulation with CXCL12. In normal conditions, CXCR4 couples to both $G\alpha_i$ and $G\alpha_q$. This results in a basal level of CXCR4 signaling. Some effects mentioned in this figure are SOD1's ability to protect the cell from apoptosis and reduce CXCL12-stimulated chemotaxis. B. In hypoxic conditions, CXCR4 and SOD1 interact at a basal level; however, there is no longer an increase in the interaction between these two molecules following CXCL12 stimulation. We found that in hypoxic conditions, CXCR4 seems to couple preferentially with $G\alpha_q$, which could help to explain the modulation of signaling that we see in hypoxia. Some of the results we found are represented in this figure and include decreased $G\alpha_i$ coupling and a reduction in the SOD1-mediated protection from apoptosis.

REFERENCES

- Abe, M., Xie, W., Regan, M. M., King, I. B., Stampfer, M. J., Kantoff, P. W., Oh, W. K., et al. (2011). Single-nucleotide polymorphisms within the antioxidant defence system and associations with aggressive prostate cancer. *BJU International*, 107(1):126–34.
- Akashi, T., Koizumi, K., Tsuneyama, K., Saiki, I., Takano, Y., & Fuse, H. (2008). Chemokine receptor CXCR4 expression and prognosis in patients with metastatic prostate cancer. *Cancer Science*, 99(3):539–42.
- Alsayed, Y., Ngo, H., Runnels, J., Leleu, X., Singha, U. K., Pitsillides, C. M., Spencer, J. a, et al. (2007). Mechanisms of regulation of CXCR4/SDF-1 (CXCL12)-dependent migration and homing in multiple myeloma. *Blood*, 109(7):2708–17.
- Balk, S. P., Ko, Y.-J., & Bubley, G. J. (2003). Biology of Prostate-Specific Antigen. *Journal of Clinical Oncology*, 21(2):383–391.
- Balkwill, F. (2004a). Cancer and the chemokine network. *Nature Reviews. Cancer*, 4(7):540–50.
- Balkwill, F. (2004b). The significance of cancer cell expression of the chemokine receptor CXCR4. *Seminars in Cancer Biology*, 14(3):171–9.
- Barbero, S., Bonavia, R., Bajetto, A., Porcile, C., Pirani, P., Ravetti, J. L., Zona, G. L., et al. (2003). Stromal Cell-derived Factor 1 α Stimulates Human Glioblastoma Cell Growth through the Activation of Both Extracellular Signal-regulated Kinases 1 / 2 and Akt Stromal Cell-derived Factor 1 α Stimulates Human Glioblastoma Cell Growth. *Cancer Research*, 63:1969-1974.
- Battisti, V., Maders, L. D. K., Bagatini, M. D., Reetz, L. G. B., Chiesa, J., Battisti, I. E., Gonçalves, J. F., et al. (2011). Oxidative stress and antioxidant status in prostate cancer patients: relation to Gleason score, treatment and bone metastasis. *Biomedicine Pharmacotherapy Biomédecine Pharmacothérapie*, 65(7):516–24.
- Berridge, M., Lipp, P., & Bootman, M. (2000). The versatility and universality of calcium signalling. *Nature Reviews Molecular cell biology*, 1:11-21.
- Bostwick, D. G., Alexander, E. E., Singh, R., Shan, a, Qian, J., Santella, R. M., Oberley, L. W., et al. (2000). Antioxidant enzyme expression and reactive oxygen species damage in prostatic intraepithelial neoplasia and cancer. *Cancer*, 89(1):123–34.
- Brahimmi-Horn, M. C., Chiche, J., & Pouyssegur, J. (2007). Hypoxia and cancer. *Journal of Molecular Medicine*, 85(12):1301–1307.

- Brewer, G. J., Dick, R. D., Grover, D. K., Leclaire, V., Tseng, M., Wicha, M., Pienta, K., et al. (2000). Treatment of Metastatic Cancer with Tetrathiomolybdate, an Anticopper, Antiangiogenic Agent : Phase I Study. *Clinical Cancer Research*, 1:1–10.
- Broxmeyer, H. E., Cooper, S., Kohli, L., Hangoc, G., Lee, Y., Mantel, C., Clapp, D. W., et al. (2003). Transgenic expression of stromal cell-derived factor-1/CXC chemokine ligand 12 enhances myeloid progenitor cell survival/antiapoptosis in vitro in response to growth factor withdrawal and enhances myelopoiesis in vivo. *The Journal of Immunology*, 170:421–429.
- Cerella, C., Coppola, S., Maresca, V., De Nicola, M., Radogna, F., & Ghibelli, L. (2009). Multiple mechanisms for hydrogen peroxide-induced apoptosis. *Annals of the New York Academy of Sciences*, 1171: 559–63.
- Chetram, M. a, Don-Salu-Hewage, A. S., & Hinton, C. V. (2011a). ROS enhances CXCR4-mediated functions through inactivation of PTEN in prostate cancer cells. *Biochemical and Biophysical Research Communications*, 410(2):195–200.
- Coghlin, C., & Murray, G. I. (2010). Current and emerging concepts in tumour metastasis. *The Journal of Pathology*, 222(1):1–15.
- Cooner, W. H., Mosley, B. R., Rutherford, C. L., Beard, J. H., Pond, H. S., Terry, W. J., Igel, T. C., et al. (2002). Prostate cancer detection in a clinical urological practice by ultrasonography, digital rectal examination and prostate specific antigen. *The Journal of Urology*, 167:966–73.
- Croce, C. M. (2008). Oncogenes and cancer. *The New England Journal of Medicine*, 358(5):502–11.
- Darash-Yahana, M., Pikarsky, E., Abramovitch, R., Zeira, E., Pal, B., Karplus, R., Beider, K., et al. (2004). Role of high expression levels of CXCR4 in tumor growth, vascularization, and metastasis. *FASEB journal*, 18(11):1240–2.
- Dewan, M. Z., Ahmed, S., Iwasaki, Y., Ohba, K., Toi, M., & Yamamoto, N. (2006). Stromal cell-derived factor-1 and CXCR4 receptor interaction in tumor growth and metastasis of breast cancer. *Biomedicine & Pharmacotherapy*, 60(6):273–6.
- Domanaska, U., Timmer-Bosscha, H., Nagengast, W. B., Munnink, T. H. O., Kliphuis, N. M., & Huls, G. (2012). CXCR4 Inhibition with AMD3100 Sensitizes Prostate Cancer to docetaxel chemotherapy. *Neoplasia*, 14(8):709–718.
- Dupré, D. J., Robitaille, M., Rebois, R. V., & Hébert, T. E. (2009). The role of Gβγ subunits in the organization, assembly, and function of GPCR signaling complexes. *Annual Review of Pharmacology and Toxicology*, 49:31–56.

- Estrada-Carrasco, C., Flores-Terrazas, J., López-Silvestre, J., Campos-Salcedo, J.G., Zapata-Villalba, M., & Mendoza-álvarez, L. (2010). Regulation of antioxidant enzymes as prostate tumor markers. *Revista Mexicana de Urologia*, 70(3):157–163.
- Filmore, D. (2004). It's a GPCR World. *Moden Drug Discovery*, 24–27.
- Fischer, T., Nagel, F., Jacobs, S., Stumm, R., & Schulz, S. (2008). Reassessment of CXCR4 chemokine receptor expression in human normal and neoplastic tissues using the novel rabbit monoclonal antibody UMB-2. *PLoS One*, 3(12):e4069.
- Fowler, F., McNaughton Collins, M., Albertsen, P. C., Zietman, A., Elliott, D., & Barry, M. (2001). Comparison of recommendations by urologists and radiation oncologists for treatment of clinically localized prostate cancer. *The Journal of Urology*, 165(2):731–2.
- Fredriksson, R., Lagerström, M. C., Lundin, L.G., & Schiöth, H. B. (2003). The G-protein-coupled receptors in the human genome form five main families. Phylogenetic analysis, paralogon groups, and fingerprints. *Molecular Pharmacology*, 63(6):1256–72.
- Freedland, S. J. (2011). Screening, risk assessment, and the approach to therapy in patients with prostate cancer. *Cancer*, 117(6):1123–35.
- Ganju, R., Brubaker, S, Meyer, J., Dutt, P., Yang, Y., Qin, S., Newman, W., et al. (1998). The α -Chemokine, Stromal Cell-Derived Factor-1 α , Binds to the Transmembrane G-protein-coupled CXCR-4 Receptor and Activates Multiple Signal Transduction Pathways, *The Journal of Biological Chemistry*, 273(36):23169–23175.
- Gibbs, M., Stanford, J., Jarvik, G., Janer, M., Badzioch, M., Peters, M. a, Goode, E., et al. (2000). A genomic scan of families with prostate cancer identifies multiple regions of interest. *American Journal of Human Genetics*, 67(1):100–9.
- Gilman, A. (1995). G Proteins and Regulation of Adenylyl Cyclase. *Bioscience Reports*, 15(2):65-97.
- Gladson, C., & Welch, D. (2008). New insights into the role of CXCR4 in prostate cancer metastasis. *Cancer Biology & Therapy*, 7(11):1849–1851.
- Gloriam, D., Fredriksson, R., & Schiöth, H. (2007). The G protein-coupled receptor subset of the rat genome. *BMC Genomics*, 8:338.
- Gupta, G., & Massagué, J. (2006). Cancer metastasis: building a framework. *Cell*, 127(4): 679–95.
- Gurevich, V., & Gurevich, E. (2009). GPCR monomers and oligomers: it takes all kinds. *Trends in Neuroscience*, 31(2), 74–81.

- Halliwell, B. (1994). Free radicals, antioxidants, and human disease: curiosity, cause, or consequence? *The Lancet*, 344(8924):721–724.
- Hargrave, P., McDowell, H., Curtis, D., Wang, J., Juszczak, E., Fong, S., Rao, J., et al. (1983). The Structure of Bovine Rhodopsin. *Biophysics of Structure & Mechanism*, 9:235–244.
- Hauser, A., Debes, G., Arce, S., Cassese, G., Hamann, A., Radbruch, A., & Manz, R. (2002). Chemotactic responsiveness toward ligands for CXCR3 and CXCR4 is regulated on plasma blasts during the time course of a memory immune response. *Journal of Immunology*, 169(3):1277–82.
- Helbig, G., Christopherson, K., Bhat-Nakshatri, P., Kumar, S., Kishimoto, H., Miller, K., Broxmeyer, H., et al. (2003). NF- κ B promotes breast cancer cell migration and metastasis by inducing the expression of the chemokine receptor CXCR4. *The Journal of Biological Chemistry*, 278(24):21631–8.
- Hileman, E., Liu, J., Albitar, M., Keating, M., & Huang, P. (2004). Intrinsic oxidative stress in cancer cells: a biochemical basis for therapeutic selectivity. *Cancer Chemotherapy and Pharmacology*, 53(3):209–19.
- Hilger, R., Scheulen, M., & Strumberg, D. (2002). The Ras-Raf-MEK-ERK pathway in the treatment of cancer. *Onkologie*, 25(6):511–8.
- Hirota, K., & Semenza, G. (2006). Regulation of angiogenesis by hypoxia-inducible factor 1. *Critical Reviews in Oncology/Hematology*, 59(1):15–26.
- Hopkins, A., & Groom, C. (2002). The druggable genome. *Nature Reviews Drug Discovery*, 1(9):727–30.
- Hwang, J., Hwang, J., Chung, H., Kim, D., Hwang, E., Suh, J., Kim, H., et al. (2003). CXC Chemokine Receptor 4 Expression and Function in Human Anaplastic Thyroid Cancer Cells. *Journal of Clinical Endocrinology & Metabolism*, 88(1):408–416.
- Jemal, A., Bray, F., & Ferlay, J. (2011). Global Cancer Statistics. *CA: A Cancer Journal for Clinicians*, 61(2):69–90.
- Jensen, A., Guarnieri, F., Rasmussen, S., Asmar, F., Ballesteros, J., & Gether, U. (2001). Agonist-induced conformational changes at the cytoplasmic side of transmembrane segment 6 in the β 2 adrenergic receptor mapped by site-selective fluorescent labeling. *The Journal of Biological Chemistry*, 276(12):9279–90.
- Johnson, F., & Giulivi, C. (2005). Superoxide dismutases and their impact upon human health. *Molecular Aspects of Medicine*, 26(4-5):340–52.

- Johnson, T., Yu, Z., Ferrans, V., Lowenstein, R., & Finkel, T. (1996). Reactive oxygen species are downstream mediators of p53-dependent apoptosis. *Proceedings of the National Academy of Sciences of the United States of America*, 93(21):11848–52.
- Juarez, J., Betancourt, O., Pirie-Shepherd, S., Guan, X., Price, M., Shaw, D., Mazar, A., et al. (2006). Copper binding by tetrathiomolybdate attenuates angiogenesis and tumor cell proliferation through the inhibition of superoxide dismutase 1. *Clinical Cancer Research*, 12(16), 4974–82.
- Juarez, J., Manuia, M., Burnett, M., Betancourt, O., Boivin, B., Shaw, D., Tonks, N., et al. (2008). Superoxide dismutase 1 (SOD1) is essential for H₂O₂-mediated oxidation and inactivation of phosphatases in growth factor signaling. *Proceedings of the National Academy of Sciences of the United States of America*, 105(20):7147–52.
- Kimbro, K., & Simons, J. (2006). Hypoxia-inducible factor-1 in human breast and prostate cancer. *Endocrine-Related Cancer*, 13(3):739–49. doi:10.1677/erc.1.00728
- Kleinau, G., Jaeschke, H., Worth, C., Mueller, S., Gonzalez, J., Paschke, R., & Krause, G. (2010). Principles and determinants of G-protein coupling by the rhodopsin-like thyrotropin receptor. *PloS One*, 5(3):e9745. doi:10.1371/journal.pone.0009745
- Knaut, H., Werz, C., Geisler, R., & Nüsslein-Volhard, C. (2003). A zebrafish homologue of the chemokine receptor CXCR4 is a germ-cell guidance receptor. *Nature*, 421(6920): 279–82.
- Kobilka, B. (2007). G protein coupled receptor structure and activation. *Biochimica et Biophysica Acta*, 1768(4):794–807.
- Kochetkova, M., Kumar, S., & McColl, S. (2009). Chemokine receptors CXCR4 and CCR7 promote metastasis by preventing anoikis in cancer cells. *Cell Death and Differentiation*, 16(5):664–73.
- Kristiansen, K. (2004). Molecular mechanisms of ligand binding, signaling, and regulation within the superfamily of G-protein-coupled receptors: molecular modeling and mutagenesis approaches to receptor structure and function. *Pharmacology & Therapeutics*, 103(1):21–80.
- Kukreja, P., Abdel-Mageed, A., Mondal, D., Liu, K., & Agrawal, K. (2005). Up-regulation of CXCR4 expression in PC-3 cells by stromal-derived factor-1 α (CXCL12) increases endothelial adhesion and transendothelial migration: role of MEK/ERK signaling pathway-dependent NF- κ B activation. *Cancer Research*, 65(21):9891–8.
- Lagerström, M., & Schiöth, H. (2008). Structural diversity of G protein-coupled receptors and significance for drug discovery. *Nature Reviews Drug Discovery*, 7(4):339–57.

- Lin, J., Zahurak, M., Beer, T., Ryan, C., Wilding, G., Mathew, P., Morris, M., et al. (2011). A non-comparative randomized phase II study of 2 doses of ATN-224, a copper/zinc superoxide dismutase inhibitor, in patients with biochemically recurrent hormone-naïve prostate cancer. *Urologic Oncology*, 31(5):581-588.
- Wei, J., Calhoun, E., & Jacobsen, S. Benign Prostatic Hyperplasia. In: Litwin M., Saigal C., editors. *Urologic Diseases in America*. US Department of Health and Human Services, Public Health Service, National Institutes of Health, National Institute of Diabetes and Digestive and Kidney Diseases. Washington, DC: US Government Publishing Office, 2004; NIH Publication No. 04-5512 [pp. 43-71].
- Luo, Y., Xue, H., Pardo, A., Mattson, M., Rao, M., & Maragakis, N. (2007). Impaired SDF1/CXCR4 Signaling in Glial Progenitors Derived From SOD1 G93A Mice. *Journal of Neuroscience Research*, 85:2422–2432.
- Malik, A., Afaq, F., Sarfaraz, S., Adhami, V., Syed, D., & Mukhtar, H. (2005). Pomegranate fruit juice for chemoprevention and chemotherapy of prostate cancer. *Proceedings of the National Academy of Sciences of the United States of America*, 102(41):14813–8.
- Marikovsky, M., Nevo, N., Vadai, E., & Harris-Cerruti, C. (2002). Cu/Zn superoxide dismutase plays a role in angiogenesis. *International Journal of Cancer*, 97(1):34–41.
- Mashino, K., Sadanaga, N., & Yamaguchi, H. (2002). Expression of Chemokine Receptor CCR7 Is Associated with Lymph Node Metastasis of Gastric Carcinoma. *Cancer Research*, 62:2937–2941.
- Matthys, P., Hatse, S., Vermeire, K., Wuyts, A., Bridger, G., Henson, G., Clercq, E. De, et al. (2001). AMD3100, a potent and specific antagonist of the stromal cell-derived factor-1 chemokine receptor CXCR4, inhibits autoimmune joint inflammation in IFN- γ receptor-deficient mice. *The Journal of Immunology*, 167:4686–4692.
- Miller, D., Zheng, S., Dunn, R., Sarma, A., Montie, J., Lange, E., Meyers, D., et al. (2003). Germ-line Mutations of the Macrophage Scavenger Receptor 1 Gene: Association with Prostate Cancer Risk in African-American Men. *Cancer Research*, 63(13):3486–3489.
- Müller, A., Homey, B., Soto, H., Ge, N., Catron, D., Buchanan, M., McClanahan, T., et al. (2001). Involvement of chemokine receptors in breast cancer metastasis. *Nature*, 410(6824):50–6.
- Muralikrishna, P., Gondi, C., Lakka, S., Julta, A., Gujrati, M., & Rao, J. (2005). RNA Interference-Directed Knockdown of Urokinase Plasminogen Activator and Urokinase Plasminogen Activator Receptor Inhibits Prostate Cancer Cell Invasion, Survival and Tumorigenicity In vivo. *Journal of Biological Chemistry*, 280(43):36529–36540.
- Nagasawa, T., Hirota, S., Tachibana, K., Takakura, N., Nishikawa, S., Kitamura, Y., Yoshida, N., Kikutani, H., & Kishimoto, T. (1996). Defects of B-cell lymphopoiesis and

- bone-marrow myelopoiesis in mice lacking the CXC chemokine PBSF/SDF-1. *Nature*, 382:635-638.
- Nathans, J., & Hogness, D. (1984). Isolation and nucleotide sequence of the gene encoding human rhodopsin. *Proceedings of the National Academy of Sciences of the United States of America*, 81(15):4851-5.
- Ngai, J., Inngjerdigen, M., Berge, T., & Taskén, K. (2009). Interplay between the heterotrimeric G-protein subunits Galphaq and Galphai2 sets the threshold for chemotaxis and TCR activation. *BMC Immunology*, 10(27).
- O'Hara, B., & Olson, W. (2002). HIV entry inhibitors in clinical development. *Current Opinion in Pharmacology*, 2(5):523-8.
- Ok, S., Kim, S., Kim, C., Nam, D., Shim, B. S., Kim, S., Ahn, K. (2012). Emodin inhibits invasion and migration of prostate and lung cancer cells by downregulating the expression of chemokine receptor CXCR4. *Immunopharmacology and Immunotoxicology*, 34(5):768-78.
- Okamoto, T., Murayama, Y., Strittmatter, S. M., Katada, T., Asano, S., Ogata, E., & Nishimoto, I. (1994). An Intrinsic Guanine Nucleotide Exchange Inhibitor in Gi2α. *The Journal of Biological Chemistry*, 269:13756-13759.
- Oldham, W., & Hamm, H. (2008). Heterotrimeric G protein activation by G-protein-coupled receptors. *Nature Reviews Molecular Cell Biology*, 9(1):60-71.
- Overington, J., Al-Lazikani, B., & Hopkins, A. (2006). How many drug targets are there? *Nature Reviews Drug Discovery*, 5(12):993-6.
- Pan, Q., Kleer, C., van Golen, K., Irani, J., Bottema, K., Bias, C., de Carvalho, M., et al. (2002). Copper Deficiency Induced by Tetrathiomolybdate Suppresses Tumor Growth and Angiogenesis Advances in Brief Copper Deficiency Induced by Tetrathiomolybdate Suppresses Tumor Growth. *Cancer Research*, 62:4854-4859.
- Pierson, T., & Doms, R. (2003). HIV-1 entry inhibitors: new targets, novel therapies. *Immunology Letters*, 85(2):113-8.
- Rall, T., Sutherland, E., & Berther, J. (1957). The relationship of epinephrine and glucagon to liver phosphorylase. IV. Effect of epinephrine and glucagon on the reactivation of phosphorylase in liver homogenates. *The Journal of Biological Chemistry*, 224:463-475.
- Roberts, P., & Der, C. (2007). Targeting the Raf-MEK-ERK mitogen-activated protein kinase cascade for the treatment of cancer. *Oncogene*, 26(22):3291-310.

- Rodbell, M., Birnbaumer, L., & Pohl, S. (1970). Adenyl cyclase in fat cells. III. Stimulation by secretin and the effects of trypsin on the receptors for lipolytic hormones. *The Journal of Biological Chemistry*, 245(4):718–722.
- Rossi, D., & Zlotnik, A. (2000). The biology of chemokines and their receptors. *Annual Review of Immunology*, 18(6):217–42.
- Rubin, J., Kung, A., Klein, R., Chan, J., Sun, Y., Schmidt, K., Kieran, M., et al. (2003). A small-molecule antagonist of CXCR4 inhibits intracranial growth of primary brain tumors. *Proceedings of the National Academy of Sciences of the United States of America*, 100(23):13513–8.
- Salganik, R. (2001). The benefits and hazards of antioxidants: controlling apoptosis and other protective mechanisms in cancer patients and the human population. *Journal of the American College of Nutrition*, 20(5):464–472.
- Schioppa, T., Uranchimeg, B., Saccani, A., Biswas, S., Doni, A., Rapisarda, A., Bernasconi, S., et al. (2003). Regulation of the chemokine receptor CXCR4 by hypoxia. *The Journal of Experimental Medicine*, 198(9):1391–402.
- Scotton, C., Wilson, J., Scott, K., Stamp, G., Wilbanks, G., Fricker, S., Bridger, G., et al. (2002). Multiple Actions of the Chemokine CXCL12 on Epithelial Tumor Cells in Human Ovarian Cancer Multiple Actions of the Chemokine CXCL12 on Epithelial Tumor Cells in Human Ovarian Cancer. *Cancer Research*, 62:5930–5938.
- Shi, G., Partida-Sánchez, S., Misra, R., Tighe, M., Borchers, M., Lee, J., Simon, M., et al. (2007). Identification of an alternative Gαq-dependent chemokine receptor signal transduction pathway in dendritic cells and granulocytes. *The Journal of Experimental Medicine*, 204(11):2705–18.
- Singh, S., Singh, U., Grizzle, W., & Lillard, J. (2004). CXCL12-CXCR4 interactions modulate prostate cancer cell migration, metalloproteinase expression and invasion. *Laboratory Investigation*, 84(12):1666–76.
- Singh, S., Singh, U., Stiles, J., Grizzle, W., & Lillard, J. (2004). Expression and functional role of CCR9 in prostate cancer cell migration and invasion. *Clinical cancer research*, 10(24):8743–50.
- Sobel, R., & Sadar, M. (2005). Cell lines used in prostate cancer research: a compendium of old and new lines-part 1. *The Journal of Urology*, 173(2):342–59.
- Song, H., Lee, T., Jeong, J., Min, Y., & Shin, C. (2005). Hydrogen Peroxide-Induced Extracellular Signal-Regulated Kinase Activation in Cultured Feline Ileal Smooth Muscle Cells. *The Journal of Pharmacology and Experimental Therapeutics*, 312(1):391–398.

- Sullivan, R., Chateaufneuf, A., Coulombe, N., Kolakowski, L., Johnson, M., Hebert, T., Ethier, N., et al. (2000). Coexpression of full-length γ -aminobutyric acid_B (GABA_B) receptors with truncated receptors and metabotropic glutamate receptor 4 supports the GABA_B heterodimer as the functional receptor. *The Journal of Pharmacology and Experimental Therapeutics*, 293(2):460–7.
- Sun, Y., Wang, J., Shelburne, C., Lopatin, D., Chinnaiyan, A., Rubin, M., Pienta, K., et al. (2003). Expression of CXCR4 and CXCL12 (SDF-1) in human prostate cancers (PCa) in vivo. *Journal of Cellular Biochemistry*, 89(3):462–73.
- Sutherland, E., & Rall, T. (1957). Fractionation and characterization of a cyclic adenine ribonucleotide formed by tissue particles. *The Journal of Biological Chemistry*, 232(2):1077–1091.
- Suzuki, H., Tomida, A., & Tsuruo, T. (2001). Dephosphorylated hypoxia-inducible factor 1 α as a mediator of p53-dependent apoptosis during hypoxia. *Oncogene*, 20(41):5779–88.
- Taichman, R., Cooper, C., Keller, E., Pienta, K., Taichman, N., & Mccauley, L. (2002). Use of the Stromal Cell-derived Factor-1/CXCR4 Pathway in Prostate Cancer Metastasis to Bone Metastasis to Bone. *Cancer Research*, 62:1832–1837.
- Thompson, I., Pauler, D., Goodman, P., Tangen, C., Lucia, M., Parnes, H., Minasian, L., et al. (2004). Prevalence of prostate cancer among men with a prostate-specific antigen level \leq 4.0 ng per milliliter. *The New England Journal of Medicine*, 350(22):2239–2246.
- Tosoian, J., Trock, B., Landis, P., Feng, Z., Epstein, J., Partin, A., Walsh, P., et al. (2011). Active surveillance program for prostate cancer: an update of the Johns Hopkins experience. *Journal of Clinical Oncology*, 29(16):2185–90.
- Vaupel, P., Kelleher, D., & Hockel, M. (2001). Oxygenation status of malignant tumors: Pathogenesis of hypoxia and significance for tumor therapy. *Seminars in Oncology*, 28(2):29–35.
- Vivanco, I., & Sawyers, C. (2002). The phosphatidylinositol 3-Kinase AKT pathway in human cancer. *Nature Reviews. Cancer*, 2(7):489–501.
- Vonk, W., Wijmenga, C., Berger, R., Van de Sluis, B., & Klomp, L. (2010). Cu,Zn superoxide dismutase maturation and activity are regulated by COMMD1. *The Journal of Biological Chemistry*, 285(37):28991–9000.
- Wang, G., Jiang, B., Rue, E., & Semenza, G. (1995). Hypoxia-inducible factor 1 is a basic-helix-loop-helix-PAS heterodimer regulated by cellular O₂ tension. *Proceedings of the National Academy of Sciences of the United States of America*, 92(12):5510–4.

- Wang, J., Loberg, R., & Taichman, R. (2006). The pivotal role of CXCL12 (SDF-1)/CXCR4 axis in bone metastasis. *Cancer Metastasis Reviews*, 25(4):573–87.
- Waris, G., & Ahsan, H. (2006). Reactive oxygen species: role in the development of cancer and various chronic conditions. *Journal of Carcinogenesis*, 5(14).
- Watson, J. (2013). Oxidants, antioxidants and the current incurability of metastatic cancers. *Open Biology*, 3:120144.
- Wong, D., & Korz, W. (2008). Translating an Antagonist of Chemokine Receptor CXCR4: from bench to bedside. *Clinical Cancer Research*, 14(24):7975–80.
- Xing, Y., Liu, M., Du, Y., Qu, F., Li, Y., Zhang, Q., Xiao, Y., et al. (2008). Tumor cell-specific blockade of CXCR4/SDF-1 interactions in prostate cancer cells by hTERT promoter induced CXCR4 knockdown. *Cancer Biology and Therapy*, 7(11):1839–1848.
- Yamasaki, M., Nomura, T., Sato, F., & Mimata, H. (2012). Chronic hypoxia induces androgen-independent and invasive behavior in LNCaP human prostate cancer cells. *Urologic Oncology*. In press.
- Yousef, G., & Diamandis, E. (2001). The new human tissue kallikrein gene family: structure, function, and association to disease. *Endocrine Reviews*, 22(2):184–204.
- Zhang, K., Salzman, S., Reding, D., Suarez, B., Catalona, W., & Burmester, J. (2003). Genetics of Prostate Cancer. *Clinical Medicine & Research*, 1(1), 21–28.
- Zhang, S., Qi, L., Li, M., Zhang, D., Xu, S., Wang, N., & Sun, B. (2008). Chemokine CXCL12 and its receptor CXCR4 expression are associated with perineural invasion of prostate cancer. *Journal of Experimental & Clinical Cancer Research*, 27(62).
- Zhong, H., Agani, F., Baccala, A., Laughner, E., Rioseco-camacho, N., Simons, J., Semenza, G., et al. (1998). Increased Expression of Hypoxia Inducible Factor-1 α in Rat and Human Prostate Cancer. *Cancer Research*, 58:5280–5284.
- Zhou, Y., Larsen, P., Hao, C., & Yong, V. (2002). CXCR4 is a major chemokine receptor on glioma cells and mediates their survival. *The Journal of Biological Chemistry*, 277(51):49481–7.
- Zou, Y., Kottmann, A., Kuroda, M., Taniuchi, I., & Littman, D. (1998). Function of the chemokine receptor CXCR4 in haematopoiesis and in cerebellar development. *Nature*, 393(6685):595–9.

Appendix i: American Joint Committee on Cancer Prostate Cancer Staging

American Joint Committee on Cancer Prostate Cancer Staging 7th EDITION



Figure A. T4 tumor invading adjacent structures other than seminal vesicles, such as bladder, rectum, levator muscles, and/or pelvic wall.

ANATOMIC STAGE/PROGNOSTIC GROUPS ⁴						
Group	T	N	M	PSA	Gleason	
I	T1a-c	NO	MO	PSA <10	Gleason ≤6	
	T2a	NO	MO	PSA <10	Gleason ≤6	
	T1-2a	NO	MO	PSA X	Gleason X	
IIA	T1a-c	NO	MO	PSA <20	Gleason 7	
	T1a-c	NO	MO	PSA ≥10 <20	Gleason ≤6	
	T2a	NO	MO	PSA ≥10 <20	Gleason ≤6	
	T2a	NO	MO	PSA <20	Gleason 7	
	T2b	NO	MO	PSA <20	Gleason ≤7	
	T2b	NO	MO	PSA X	Gleason X	
IIB	T2c	NO	MO	Any PSA	Any Gleason	
	T1-2	NO	MO	PSA ≥20	Any Gleason	
	T1-2	NO	MO	Any PSA	Gleason ≥8	
III	T3a-b	NO	MO	Any PSA	Any Gleason	
IV	T4	NO	MO	Any PSA	Any Gleason	
	Any T	N1	MO	Any PSA	Any Gleason	
	Any T	Any N	M1	Any PSA	Any Gleason	

Definitions

Primary Tumor (T)

CLINICAL

- TX** Primary tumor cannot be assessed
- T0** No evidence of primary tumor
- T1** Clinically inapparent tumor neither palpable nor visible by imaging
- T1a** Tumor incidental histologic finding in 5% or less of tissue resected
- T1b** Tumor incidental histologic finding in more than 5% of tissue resected
- T1c** Tumor identified by needle biopsy (for example, because of elevated PSA)
- T2** Tumor confined within prostate¹
- T2a** Tumor involves one-half of one lobe or less
- T2b** Tumor involves more than one-half of one lobe but not both lobes
- T2c** Tumor involves both lobes
- T3** Tumor extends through the prostate capsule²
- T3a** Extracapsular extension (unilateral or bilateral)
- T3b** Tumor invades seminal vesicle(s)
- T4** Tumor is fixed or invades adjacent structures other than seminal vesicles, such as external sphincter, rectum, bladder, levator muscles, and/or pelvic wall (Figure A)

Pathologic (pT)³

CLINICAL

- pT2** Organ confined
- pT2a** Unilateral, one-half of one side or less
- pT2b** Unilateral, involving more than one-half of side but not both sides
- pT2c** Bilateral disease
- pT3** Extraprostatic extension
- pT3a** Extraprostatic extension or microscopic invasion of bladder neck⁴
- pT3b** Seminal vesicle invasion
- pT4** Invasion of rectum, levator muscles, and/or pelvic wall

Regional Lymph Nodes (N)

CLINICAL

- NX** Regional lymph nodes were not assessed
- N0** No regional lymph node metastasis
- N1** Metastasis in regional lymph node(s)

PATHOLOGIC

- pNX** Regional nodes not sampled
- pN0** No positive regional nodes
- pN1** Metastases in regional node(s)

Distant Metastasis (M)⁵

- M0** No distant metastasis
- M1** Distant metastasis
- M1a** Nonregional lymph node(s)
- M1b** Bone(s)
- M1c** Other site(s) with or without bone disease

Notes

- ¹ Tumor found in one or both lobes by needle biopsy, but not palpable or reliably visible by imaging, is classified as T1c.
- ² Invasion into the prostatic apex or into (but not beyond) the prostatic capsule is classified not as T3 but as T2.
- ³ There is no pathologic T1 classification.
- ⁴ Positive surgical margin should be indicated by an R1 descriptor (residual microscopic disease).
- ⁵ When more than one site of metastasis is present, the most advanced category is used. pM1c is most advanced.
- ⁶ When either PSA or Gleason is not available, grouping should be determined by T stage and/or either PSA or Gleason as available.



Financial support for AJCC
7th Edition Staging Posters
provided by the American Cancer Society



Appendix ii: License for Figure 1.2

RightsLink - Your Account

<https://s100.copyright.com/MyAccount/viewPrintableLicenseDetails?..>

NATURE PUBLISHING GROUP LICENSE TERMS AND CONDITIONS

Jun 27, 2013

This is a License Agreement between James Werhman ("You") and Nature Publishing Group ("Nature Publishing Group") provided by Copyright Clearance Center ("CCC"). The license consists of your order details, the terms and conditions provided by Nature Publishing Group, and the payment terms and conditions.

All payments must be made in full to CCC. For payment instructions, please see information listed at the bottom of this form.

License Number	3176740325498
License date	Jun 26, 2013
Licensed content publisher	Nature Publishing Group
Licensed content subdivision	Nature Reviews Molecular Cell Biology
Licensed content title	Heterotrimeric G protein activation by G-protein-coupled receptors
Licensed content author	William M. Cushman and Heidi E. Hamm
Licensed content date	Jan 1, 2006
Volume number	9
Issue number	1
Type of Use	reuse in a thesis/dissertation
Requestor type	academic/educational
Format	print and electronic
Position	figures/tables/illustrations
Number of figures/tables/illustrations	1
High-res required	no
Figures	Fig. 1 reproduced in original form as Fig. 2. in my thesis
Author of the NPG article	None
Your reference number	None
Title of your thesis / dissertation	An examination of the possible role of superoxide dismutase on CXCR4-mediated signal transduction in prostate cancer cells
Expertise number/date	Jul 2013
Estimated size (number of pages)	100
Total	0.00 USD
Terms and Conditions	Terms and Conditions for Permissions

Nature Publishing Group hereby grants you a non-exclusive license to reproduce this material for this purpose, and for no other use, subject to the conditions below.

1. NPG warrants that it has, to the best of its knowledge, the rights to license reuse of this material. However, you should ensure that the material you are requesting is original to Nature Publishing Group and does not carry the copyright of another entity (as credited in the published version). If the credit line on any part of the material you have requested indicates that it was reprinted or adapted by NPG with permission from another source, then you should also seek permission from that source to reuse the material.

2. Permission granted free of charge for material in print is also usually granted for any electronic version of that work, provided that the material is incidental to the work as a whole and that the electronic version is essentially equivalent to, or substitutes for, the print version. Where print permission has been granted for a fee, separate permission must be obtained for any additional, electronic re-use (unless, as in the case of a full paper, this has already been accounted for during your initial request in the calculation of a print run). NB: In all cases, web-based use of full-text articles must be authorized separately through the 'Use on a Web Site' option when requesting permission.

3. Permission granted for a first edition does not apply to second and subsequent editions and for editions in other languages (except for signatories to the STM Permissions Guidelines, or where the first edition permission was granted for free).

4. Nature Publishing Group's permission must be acknowledged next to the figure, table or abstract in print. In electronic form, this acknowledgement must be visible at the same time as the figure/table/abstract, and must be hyperlinked to the journal's homepage.

5. The credit line should read:
Reprinted by permission from Macmillan Publishers Ltd. [JOURNAL NAME] (reference citation), copyright (year of publication)

For AOP papers, the credit line should read:

Reprinted by permission from Macmillan Publishers Ltd. [JOURNAL NAME], advance online publication, day month year (doi: 10.1038/nj [JOURNAL ACRONYM] XXXXX)

Note: For republication from the British Journal of Cancer, the following credit lines apply.

Reprinted by permission from Macmillan Publishers Ltd on behalf of Cancer Research UK. [JOURNAL NAME] (reference citation), copyright (year of publication) (For AOP papers, the credit line should read:

Reprinted by permission from Macmillan Publishers Ltd on behalf of Cancer Research UK. [JOURNAL NAME], advance online publication, day month year (doi: 10.1038/nj [JOURNAL ACRONYM] XXXXX)

6. Adaptations of single figures do not require NPG approval. However, the adaptation should be credited as follows:

Adapted by permission from Macmillan Publishers Ltd. [JOURNAL NAME] (reference citation), copyright (year of publication)

Note: For adaptation from the British Journal of Cancer, the following credit line applies.

Adapted by permission from Macmillan Publishers Ltd on behalf of Cancer Research UK. [JOURNAL NAME] (reference citation), copyright (year of publication)

7. Translations of 401 words up to a whole article require NPG approval. Please visit <http://www.nature.com/naturepublications/permissions> for more information. Translations of up to a 400 words do not require NPG approval. The translation should be credited as follows:

Translated by permission from Macmillan Publishers Ltd. [JOURNAL NAME] (reference citation), copyright (year of publication)

Note: For translation from the British Journal of Cancer, the following credit line applies.

Translated by permission from Macmillan Publishers Ltd on behalf of Cancer Research UK. [JOURNAL NAME] (reference citation), copyright (year of publication)

We are certain that all parties will benefit from this agreement and wish you the best in the use of this material. Thank you.

Special Terms:

v1.1

If you would like to pay for this license now, please remit this license along with your payment made payable to "COPYRIGHT CLEARANCE CENTER" otherwise you will be invoiced within 48 hours of the license date. Payment should be in the form of a check or money order referencing your account number and this invoice number RLK50105537. Once you receive your invoice for this order, you may pay your invoice by credit card. Please follow instructions provided at that time.

Make Payment To:
Copyright Clearance Center
Dept 001
P.O. Box 843006
Boston, MA 02284-3006

For suggestions or comments regarding this order, contact RightsLink Customer Support: customerservice@copyright.com or +1-877-822-5543 (toll free in the US) or +1-978-646-2777.

Gratis licenses (referencing \$0 in the Total field) are free. Please retain this printable license for your reference. No payment is required.

Appendix iii: License for Table 1.1

RightsLink - Your Account

<https://s100.copyright.com/MyAccount/viewPrintableLicenseDetails?...>

NATURE PUBLISHING GROUP LICENSE TERMS AND CONDITIONS

Jun 27, 2013

This is a License Agreement between Jaime Wirtman ("You") and Nature Publishing Group ("Nature Publishing Group") provided by Copyright Clearance Center ("CCC"). The license consists of your order details, the terms and conditions provided by Nature Publishing Group, and the payment terms and conditions.

All payments must be made in full to CCC. For payment instructions, please see information listed at the bottom of this form.

License Number	3176151355683
License date	Jun 25, 2013
Licensed content publisher	Nature Publishing Group
Licensed content subpublisher	Nature Reviews Cancer
Licensed content title	Cancer and the chemokine network
Licensed content author	Fran Balkwill
Licensed content date	Jul 1, 2004
Volume number	4
Issue number	7
Type of Use	reuse in a thesis/dissertation
Requester type	academic/educational
Format	print and electronic
Position	figures/tables/illustrations
Number of figures/tables/illustrations	1
High-res required	no
Figures	Table 1 in the original text, reproduced with minor changes as Table 1 in my thesis.
Author of the NPG article	no
Your reference number	None
Title of your thesis/dissertation	An examination of the possible role of superoxide dismutase on CXCR4-mediated signal transduction in prostate cancer cells
Expected completion date	Jul 2013
Estimated size (number of pages)	100
Total	0.00 USD

Terms and Conditions

Terms and Conditions for Permissions

Nature Publishing Group hereby grants you a non-exclusive license to reproduce this material for this purpose, and for no other use, subject to the conditions below.

- NPG warrants that it has, to the best of its knowledge, the rights to license reuse of this material. However, you should ensure that the material you are requesting is original to Nature Publishing Group and does not carry the copyright of another entity (as credited in the published version). If the credit line on any part of the material you have requested indicates that it was reprinted or adapted by NPG with permission from another source, then you should also seek permission from that source to reuse the material.
- Permission granted free of charge for material in print is also usually granted for any electronic version of that work, provided that the material is incidental to the work as a whole and that the electronic version is essentially equivalent to, or substitutes for, the print version. Where print permission has been granted for a fee, separate permission must be obtained for any additional, electronic re-use (unless, as in the case of a full paper, this has already been accounted for during your initial request in the calculation of a print run) NB: in all cases, web-based use of full-text articles must be authorized separately through the 'Use on a Web Site' option when requesting permission.
- Permission granted for a first edition does not apply to second and subsequent editions and for editions in other languages (except for signatories to the STM Permissions Guidelines, or where the first edition permission was granted for free).
- Nature Publishing Group's permission must be acknowledged next to the figure, table or abstract in print. In electronic form, this acknowledgement must be visible at the same time as the figure/table/abstract, and must be hyperlinked to the journal's homepage.

5. The credit line should read

Reprinted by permission from Macmillan Publishers Ltd [JOURNAL NAME] (reference citation), copyright (year of publication)

For AOP papers, the credit line should read

Reprinted by permission from Macmillan Publishers Ltd [JOURNAL NAME], advance online publication, day month year (doi: 10.1038/[JOURNAL ACRONYM]XXXXX)

Note: For republication from the British Journal of Cancer, the following credit lines apply.

Reprinted by permission from Macmillan Publishers Ltd on behalf of Cancer Research UK [JOURNAL NAME] (reference citation), copyright (year of publication) For AOP papers, the credit line should read

Reprinted by permission from Macmillan Publishers Ltd on behalf of Cancer Research UK [JOURNAL NAME], advance online publication, day month year (doi: 10.1038/[JOURNAL ACRONYM]XXXXX)

6. Adaptations of single figures do not require NPG approval. However, the adaptation should be credited as follows:

Adapted by permission from Macmillan Publishers Ltd [JOURNAL NAME] (reference citation), copyright (year of publication)

Note: For adaptation from the British Journal of Cancer, the following credit line applies.

Adapted by permission from Macmillan Publishers Ltd on behalf of Cancer Research UK [JOURNAL NAME] (reference citation), copyright (year of publication)

7. Translations of 401 words up to a whole article require NPG approval. Please visit <http://www.macmillanmedicalandnursingcare.com> for more information. Translations of up to a 400 words do not require NPG approval. The translation should be credited as follows:

Translated by permission from Macmillan Publishers Ltd [JOURNAL NAME] (reference citation), copyright (year of publication)

Note: For translation from the British Journal of Cancer, the following credit line applies.

Translated by permission from Macmillan Publishers Ltd on behalf of Cancer Research UK [JOURNAL NAME] (reference citation), copyright (year of publication)

We are certain that all parties will benefit from this agreement and wish you the best in the use of this material. Thank you.

Special Terms

v1.1

If you would like to pay for this license now, please remit this license along with your payment made payable to "COPYRIGHT CLEARANCE CENTER" otherwise you will be invoiced within 48 hours of the license date. Payment should be in the form of a check or money order referencing your account number and this invoice number RLNR501051429.

Once you receive your invoice for this order, you may pay your invoice by credit card. Please follow instructions provided at that time.

Make Payment To:

Copyright Clearance Center

Dept 001

P.O. Box 643006

Boston, MA 02284-3006

For suggestions or comments regarding this order, contact RightsLink Customer Support: customerscare@copyright.com or +1-877-422-5543 (toll free in the US) or +1-978-646-2777.

Gratis licenses (referencing \$0 in the Total field) are free. Please retain this printable license for your reference. No payment is required.

Appendix iv: License for Figure 1.3A

Rightslink Printable License

https://s100.copyright.com/App/PrintableLicenseFrame.jsp?publishe...

NATURE PUBLISHING GROUP LICENSE TERMS AND CONDITIONS

Jun 29, 2013

This is a License Agreement between Jaime Wertman ("You") and Nature Publishing Group ("Nature Publishing Group") provided by Copyright Clearance Center ("CCC"). The license consists of your order details, the terms and conditions provided by Nature Publishing Group, and the payment terms and conditions.

All payments must be made in full to CCC. For payment instructions, please see information listed at the bottom of this form.

License Number	317831069021
License date	Jun 29, 2013
Licensed content publisher	Nature Publishing Group
Licensed content publication	Nature Reviews Drug Discovery
Licensed content title	The bicyclam AMD3100 story
Licensed content author	Erik De Clercq
Licensed content date	Jul 1, 2003
Volume number	2
Issue number	7
Type of Use	reuse in a thesis/dissertation
Requestor type	academic/educational
Format	print and electronic
Portion	figures/tables/illustrations
Number of figures/tables /illustrations	1
High-res required	no
Figures	Figure 6 reproduced as Figure 1.3 in my thesis.
Author of this NPG article	no
Your reference number	
Title of your thesis / dissertation	An examination of the possible role of superoxide dismutase on CXCR4-mediated signal transduction in prostate cancer cells
Expected completion date	Jul 2013
Estimated size (number of pages)	100
Total	0.00 USD
Terms and Conditions	

Terms and Conditions for Permissions

Nature Publishing Group hereby grants you a non-exclusive license to reproduce this material for this purpose, and for no other use, subject to the conditions below:

1. NPG warrants that it has, to the best of its knowledge, the rights to license reuse of this material. However, you should ensure that the material you are requesting is original to Nature Publishing Group and does not carry the copyright of another entity (as credited in the published version). If the credit line on any part of the material you have requested indicates that it was reprinted or adapted by NPG with permission from another source, then you should also seek permission from that source to reuse the material.
2. Permission granted free of charge for material in print is also usually granted for any electronic version of that work, provided that the material is incidental to the work as a whole and that the electronic version is essentially equivalent to, or substitutes for, the print version. Where print permission has been granted for a fee, separate permission must be obtained for any additional, electronic re-use (unless, as in the case of a full paper, this has already been accounted for during your initial request in the calculation of a print run). NB. In all cases, web-based use of full-text articles must be authorized separately through the 'Use on a Web Site' option when requesting permission.
3. Permission granted for a first edition does not apply to second and subsequent editions and for editions in other languages (except for signatories to the STM Permissions Guidelines, or where the first edition permission was granted for free).
4. Nature Publishing Group's permission must be acknowledged next to the figure, table or abstract in print. In electronic form, this acknowledgement must be visible at the same time as the figure/table/abstract, and must be hyperlinked to the journal's homepage.
5. The credit line should read:
Reprinted by permission from Macmillan Publishers Ltd. [JOURNAL NAME]
(reference citation), copyright (year of publication)
For AOP papers, the credit line should read:
Reprinted by permission from Macmillan Publishers Ltd. [JOURNAL NAME],
advance online publication, day month year (doi: 10.1038/sj [JOURNAL
ACRONYM] XXXXX)
Note: For republication from the British Journal of Cancer, the following credit lines apply.
Reprinted by permission from Macmillan Publishers Ltd on behalf of Cancer Research UK. [JOURNAL NAME] (reference citation), copyright (year of publication) For AOP papers, the credit line should read:
Reprinted by permission from Macmillan Publishers Ltd on behalf of Cancer Research UK. [JOURNAL NAME], advance online publication, day month year (doi: 10.1038/sj [JOURNAL ACRONYM] XXXXX)
6. Adaptations of single figures do not require NPG approval. However, the adaptation

Appendix v: License for Figure 1.3B

Rightslink Printable License

<https://s100.copyright.com/App/PrintableLicenseFrame.jsp?publishe...>

THE AMERICAN ASSOCIATION FOR THE ADVANCEMENT OF SCIENCE LICENSE TERMS AND CONDITIONS

Jun 29, 2013

This is a License Agreement between Jaime Wertman ("You") and The American Association for the Advancement of Science ("The American Association for the Advancement of Science") provided by Copyright Clearance Center ("CCC"). The license consists of your order details, the terms and conditions provided by The American Association for the Advancement of Science, and the payment terms and conditions.

All payments must be made in full to CCC. For payment instructions, please see information listed at the bottom of this form.

License Number	3178330296437
License date	Jun 29, 2013
Licensed content publisher	The American Association for the Advancement of Science
Licensed content publication	Science
Licensed content title	Structures of the CXCR4 Chemokine GPCR with Small-Molecule and Cyclic Peptide Antagonists
Licensed content author	Beili Wu, Ellen Y. T. Chien, Clifford D. Mol, Gustavo Fenalti, Wei Liu, Vsevolod Katrich, Ruben Abagyan, Alexei Brooun, Peter Wells, F. Christopher Yu, Damon J. Hamel, Peter Kuhn, Tracy M. Handel, Vadim Cherezov, Raymond C. Stevens
Licensed content date	Nov 19, 2010
Volume number	330
Issue number	6007
Type of Use	Thesis / Dissertation
Requester type	Scientist/individual at a research institution
Format	Print and electronic
Portion	Figure
Number of figures/tables	1
Order reference number	
Title of your thesis / dissertation	An examination of the possible role of superoxide dismutase on CXCR4-mediated signal transduction in prostate cancer cells
Expected completion date	Jul 2013
Estimated size (pages)	100
Total	0.00 USD
Terms and Conditions	

American Association for the Advancement of Science TERMS AND CONDITIONS

Regarding your request, we are pleased to grant you non-exclusive, non-transferable permission, to republish the AAAS material identified above in your work identified above, subject to the terms and conditions herein. We must be contacted for permission for any uses other than those specifically identified in your request above.

The following credit line must be printed along with the AAAS material: "From [Full Reference Citation]. Reprinted with permission from AAAS."

All required credit lines and notices must be visible any time a user accesses any part of the AAAS material and must appear on any printed copies and authorized user might make.

This permission does not apply to figures / photos / artwork or any other content or materials included in your work that are credited to non-AAAS sources. If the requested material is sourced to or references non-AAAS sources, you must obtain authorization from that source as well before using that material. You agree to hold harmless and indemnify AAAS against any claims arising from your use of any content in your work that is credited to non-AAAS sources.

If the AAAS material covered by this permission was published in Science during the years 1974 - 1994, you must also obtain permission from the author, who may grant or withhold permission, and who may or may not charge a fee if permission is granted. See original article for author's address. This condition does not apply to news articles.

The AAAS material may not be modified or altered except that figures and tables may be modified with permission from the author. Author permission for any such changes must be secured prior to your use.

Whenever possible, we ask that electronic uses of the AAAS material permitted herein include a hyperlink to the original work on AAAS's website (hyperlink may be embedded in the reference citation).

AAAS material reproduced in your work identified herein must not account for more than 30% of the total contents of that work.

AAAS must publish the full paper prior to use of any text.

AAAS material must not imply any endorsement by the American Association for the Advancement of Science.

This permission is not valid for the use of the AAAS and/or Science logos.

AAAS makes no representations or warranties as to the accuracy of any information contained in the AAAS material covered by this permission, including any warranties of merchantability or fitness for a particular purpose.

If permission fees for this use are waived, please note that AAAS reserves the right to charge for reproduction of this material in the future.

Permission is not valid unless payment is received within sixty (60) days of the issuance of this permission. If payment is not received within this time period then all rights granted herein shall be revoked and this permission will be considered null and void.

Appendix vi: License for Figure 1.5

Rightslink Printable License

<https://s100.copyright.com/CustomerAdmin/PLF.jsp?ref=26bedd27-...>

NATURE PUBLISHING GROUP LICENSE TERMS AND CONDITIONS

Jun 27, 2013

This is a License Agreement between Jaime Wertman ("You") and Nature Publishing Group ("Nature Publishing Group") provided by Copyright Clearance Center ("CCC"). The license consists of your order details, the terms and conditions provided by Nature Publishing Group, and the payment terms and conditions.

All payments must be made in full to CCC. For payment instructions, please see information listed at the bottom of this form.

License Number	3177211043386
License date	Jun 27, 2013
Licensed content publisher	Nature Publishing Group
Licensed content publication	Nature
Licensed content title	Angiogenesis in cancer and other diseases
Licensed content author	Peter Carmeliet and Rakesh K. Jain
Licensed content date	Sep 14, 2000
Volume number	407
Issue number	6801
Type of Use	reuse in a thesis/dissertation
Requestor type	academic/educational
Format	print and electronic
Portion	figures/tables/illustrations
Number of figures/tables /illustrations	1
Figures	Figure 2 will be reproduced in my thesis without alteration.
Author of this NPG article	no
Your reference number	
Title of your thesis / dissertation	An examination of the possible role of superoxide dismutase on CXCR4-mediated signal transduction in prostate cancer cells
Expected completion date	Jul 2013
Estimated size (number of pages)	100
Total	0.00 USD
Terms and Conditions	

Terms and Conditions for Permissions

Nature Publishing Group hereby grants you a non-exclusive license to reproduce this material for this purpose, and for no other use, subject to the conditions below:

1. NPG warrants that it has, to the best of its knowledge, the rights to license reuse of this material. However, you should ensure that the material you are requesting is original to Nature Publishing Group and does not carry the copyright of another entity (as credited in the published version). If the credit line on any part of the material you have requested indicates that it was reprinted or adapted by NPG with permission from another source, then you should also seek permission from that source to reuse the material.
2. Permission granted free of charge for material in print is also usually granted for any electronic version of that work, provided that the material is incidental to the work as a whole and that the electronic version is essentially equivalent to, or substitutes for, the print version. Where print permission has been granted for a fee, separate permission must be obtained for any additional, electronic re-use (unless, as in the case of a full paper, this has already been accounted for during your initial request in the calculation of a print run). NB: In all cases, web-based use of full-text articles must be authorized separately through the 'Use on a Web Site' option when requesting permission.
3. Permission granted for a first edition does not apply to second and subsequent editions and for editions in other languages (except for signatories to the STM Permissions Guidelines, or where the first edition permission was granted for free).
4. Nature Publishing Group's permission must be acknowledged next to the figure, table or abstract in print. In electronic form, this acknowledgement must be visible at the same time as the figure/table/abstract, and must be hyperlinked to the journal's homepage.
5. The credit line should read:
Reprinted by permission from Macmillan Publishers Ltd. [JOURNAL NAME] (reference citation), copyright (year of publication)
For AOP papers, the credit line should read:
Reprinted by permission from Macmillan Publishers Ltd. [JOURNAL NAME], advance online publication, day month year (doi: 10.1038/sj [JOURNAL ACRONYM] XXXXX)

Note: For republication from the *British Journal of Cancer*, the following credit lines apply.

Reprinted by permission from Macmillan Publishers Ltd on behalf of Cancer Research UK. [JOURNAL NAME] (reference citation), copyright (year of publication) For AOP papers, the credit line should read:
Reprinted by permission from Macmillan Publishers Ltd on behalf of Cancer Research UK. [JOURNAL NAME], advance online publication, day month year (doi: 10.1038/sj [JOURNAL ACRONYM] XXXXX)

6. Adaptations of single figures do not require NPG approval. However, the adaptation should be credited as follows:

Appendix vii: License for Figure 1.6

Rightslink Printable License

<https://s100.copyright.com/App/PrintableLicenseFrame.jsp?publishe...>

NATURE PUBLISHING GROUP LICENSE TERMS AND CONDITIONS

Jul 01, 2013

This is a License Agreement between Jaime Wertman ("You") and Nature Publishing Group ("Nature Publishing Group") provided by Copyright Clearance Center ("CCC"). The license consists of your order details, the terms and conditions provided by Nature Publishing Group, and the payment terms and conditions.

All payments must be made in full to CCC. For payment instructions, please see information listed at the bottom of this form.

License Number	3180300526746
License date	Jul 01, 2013
Licensed content publisher	Nature Publishing Group
Licensed content publication	Nature Neuroscience
Licensed content title	Wild-type and mutant SOD1 share an aberrant conformation and a common pathogenic pathway in ALS
Licensed content author	Daryl A Bosco, Gerardo Morfini, N Murat Karabacak, Yuyu Song, Francois Gros-Louis, Piera Pasinelli
Licensed content date	Oct 17, 2010
Volume number	13
Issue number	11
Type of Use	reuse in a thesis/dissertation
Requestor type	academic/educational
Format	print and electronic
Portion	figures/tables/illustrations
Number of figures/tables/illustrations	1
High-res required	no
Figures	Figure 2 will be reused as Figure 1.6 in my thesis.
Author of this NPG article	no
Your reference number	
Title of your thesis / dissertation	An examination of the possible role of superoxide dismutase on CXCR4-mediated signal transduction in prostate cancer cells
Expected completion date	Jul 2013
Estimated size (number of pages)	100
Total	0.00 USD
Terms and Conditions	

Terms and Conditions for Permissions

Nature Publishing Group hereby grants you a non-exclusive license to reproduce this material for this purpose, and for no other use, subject to the conditions below.

1. NPG warrants that it has, to the best of its knowledge, the rights to license reuse of this material. However, you should ensure that the material you are requesting is original to Nature Publishing Group and does not carry the copyright of another entity (as credited in the published version). If the credit line on any part of the material you have requested indicates that it was reprinted or adapted by NPG with permission from another source, then you should also seek permission from that source to reuse the material.
2. Permission granted free of charge for material in print is also usually granted for any electronic version of that work, provided that the material is incidental to the work as a whole and that the electronic version is essentially equivalent to, or substitutes for, the print version. Where print permission has been granted for a fee, separate permission must be obtained for any additional, electronic re-use (unless, as in the case of a full paper, this has already been accounted for during your initial request in the calculation of a print run). NB: In all cases, web-based use of full-text articles must be authorized separately through the 'Use on a Web Site' option when requesting permission.
3. Permission granted for a first edition does not apply to second and subsequent editions and for editions in other languages (except for signatories to the STM Permissions Guidelines, or where the first edition permission was granted for free).
4. Nature Publishing Group's permission must be acknowledged next to the figure, table or abstract in print. In electronic form, this acknowledgement must be visible at the same time as the figure/table/abstract, and must be hyperlinked to the journal's homepage.
5. The credit line should read:
Reprinted by permission from Macmillan Publishers Ltd. [JOURNAL NAME] (reference citation), copyright (year of publication)
For AOP papers, the credit line should read:
Reprinted by permission from Macmillan Publishers Ltd. [JOURNAL NAME], advance online publication, day month year (doi: 10.1038/sj [JOURNAL ACRONYM].XXXXX)

Note: For republication from the *British Journal of Cancer*, the following credit lines apply.

Reprinted by permission from Macmillan Publishers Ltd on behalf of Cancer Research UK. [JOURNAL NAME] (reference citation), copyright (year of publication) For AOP papers, the credit line should read:
Reprinted by permission from Macmillan Publishers Ltd on behalf of Cancer Research UK. [JOURNAL NAME], advance online publication, day month year (doi: 10.1038/sj [JOURNAL ACRONYM].XXXXX)

Appendix viii: SOD1 siRNA-Mediated Knockdown

